THE UNIVERSITY OF MICHIGAN

INDUSTRY PROGRAM OF THE COLLEGE OF ENGINEERING

LOW-TEMPERATURE VAPOR-LIQUID EQUILIBRIA IN TERNARY AND QUATERNARY SYSTEMS CONTAINING HYDROGEN, NITROGEN, METHANE AND ETHANE

Harry F. Cosway

A dissertation submitted in partial fulfillment
of the requirements for the degree of
Doctor of Philosophy in the
University of Michigan
1958

June, 1958

IP-300

en ? ✓

UMR 4665

ACKNOWLEDGMENT

I wish to express my gratitude to all those who have assisted and encouraged me in my graduate work. In particular I wish to thank the following:

The chairman of my doctoral committee, Dr. Donald L. Katz, without whose aid and encouragement this work could never have been completed.

The other members of my committee, namely Drs. G. Brymer Williams, Julius T. Banchero, Lee O. Case, and Kenneth F. Gordon, for their advice and help so willingly given.

David Brown for his invaluable aid and suggestions concerning the analytical procedure using the mass spectrometer.

The staff of the Department of Chemical and Metallurgical Engineering at the University of Michigan for their assistance in obtaining materials and repairing equipment.

The Phillips Petroleum Company for the pure hydrocarbons donated for use in this work.

The Shell Oil Company for the fellowship funds during two years of my graduate work.

Keki Gharda and Ben Bray for their forbearance as laboratory partners.

The Industry Program at the University of Michigan for the assistance in the reproduction of this thesis.

TABLE OF CONTENTS

LIST OF TABLES

LIST OF FIGURES

LIST OF FIGURES CONT'D

LIST OF FIGURES CONT'D

LIST OF FIGURES CONT'D

LIST OF FIGURES CONT'D

LIST OF APPENDICES

INTRODUCTION

The increasing importance of low-temperature processes, as exemplified by the recent work of Napier [52] and Palazzo, Schreiner, and Skaperdas [58], has emphasized the need for more data on phase behavior in the low-temperature region.

Napier [52] discusses the purification of hydrogen from coke-oven gas for use in ammonia synthesis. Several plants have been erected in Europe using this process and one plant is in operation in this country. The coke-oven feed gas for the plant being operated in the United States has a composition of approximately 53 percent hydrogen, 27 percent methane, and smaller percentages of carbon monoxide, nitrogen, ethylene, ethane and carbon dioxide[52].

Palazzo, Schreiner, and Skaperdas [58] discuss the low-temperature recovery of high purity hydrogen from refinery gases for use in hydrogenation or ammonia synthesis. The feed gas used in their design is typical of platinum reformer off-gases and consists of approximately 85 percent hydrogen, 8.5 percent methane, 4.4 percent ethane, and smaller amounts of the other light hydrocarbons.

The equilibrium ratios for the constituents in the hydrogen-methane-ethane ternary system, the hydrogen-nitrogen-methane ternary system, and the hydrogen-nitrogen-methane-ethane quaternary system will play increasingly more important roles in future low-temperature separation and purification processes.

Also, in the liquefaction and storage of natural gases containing significant quantities of nitrogen, the equilibrium ratios in the nitrogen-methane-ethane ternary system would be useful for the proper design of the liquefaction, handling, and storage facilities. Therefore, this dissertation was undertaken to obtain a further insight into the vapor-liquid equilibria at low temperatures and high pressures for light hydrocarbon systems containing hydrogen and nitrogen.

Several studies of the vapor-liquid equilibria in systems containing hydrogen, nitrogen, and the light hydrocarbons have been made, as shown in Table I. However, most of these investigations have been concerned with only the binary systems, and very little ternary or multicomponent data are available. While the equilibrium ratios in the binary systems are invaluable aids in estimating the ratios in ternary or multicomponent systems, more ternary and multicomponent data are required if accurate predictions of the equilibrium ratios in multicomponent systems are to be made.

Many approaches have been tried in correlating vapor-liquid equilibria. A review of such work, normally given in a thesis at this point, has been placed in Appendix A because of its length. It provides background for the correlations carried out in this research.

TABLE I

SOURCES OF VAPOR-LIQUID EQUILIBRIUM DATA FOR LIGHT HYDROCARBON SYSTEMS CONTAINING HYDROGEN AND NITROGEN

SYSTEM	AUTHOR AND REFERENCE NO.	APPROX. TEMP. RANGE °F	APPROX. PRESS. RANGE PSIA
HYDROGEN-METHANE	LEVITSKAYA[44,45]	-175 to -120	440 to 1175
HYDROGEN-METHANE	FASTOWSKY AND GONIKBERG[28]	-298 to -230	2650 to 3400
HYDROGEN-METHANE	FREETH AND VERSCHOYLE[29]	-310 to -295	250 to 3000
HYDROGEN-METHANE	STECKEL AND ZINN[68]	-298 to -266	150 to 1500
HYDROGEN-METHANE	BENHAM AND KATZ[14]	-250 to -150	500 to 4000
HYDROGEN-ETHYLENE	LIKHTER AND TIKHONOVICH[46]	-175 to -120	440 to 1175
HYDROGEN-ETHYLENE	WILLIAMS AND KATZ[79]	-250 to 0	250 to 8000
HYDROGEN-ETHANE	LEVITSKAYA[44,45]	-175 to -120	440 to 1175
HYDROGEN-ETHANE	WILLIAMS AND KATZ[79]	-275 to +50	250 to 8000
HYDROGEN-PROPYLENE	WILLIAMS AND KATZ[79]	-250 to +75	250 to 8000
HYDROGEN-PROPANE	WILLIAMS AND KATZ[79]	-300 to +75	250 to 10,000
HYDROGEN-PROPANE	BURRIS, HSU, REAMER AND SAGE[21]	+40 to +190	500 to 8000
HYDROGEN-ISOBUTANE	DEAN AND TOOKE[25]	+100 to +250	500 to 3000
HYDROGEN-n-BUTANE	AROYAN AND KATZ[5]	-200 to +75	300 to 8000
HYDROGEN-n-BUTANE	NELSON AND BONNELL[54]	+75 to +240	325 to 1550
HYDROGEN-n-HEXANE	NICHOLS, REAMER AND SAGE[55]	+40 to +460	10 to 10,000
HYDROGEN-METHANE-ETHYLENE	LIKHTER AND TIKHONOVICH[46]	-175 to -120	440 to 1175
HYDROGEN-METHANE-ETHANE	LEVITSKAYA[44]	-175 to -120	440 to 1175
HYDROGEN-METHANE-PROPYLENE	BENHAM AND KATZ[14,15]	-100	500
HYDROGEN-METHANE-PROPANE	BENHAM AND KATZ[14,15]	-200 to 0	500 and 1000
HYDROGEN-NITROGEN-METHANE	STECKEL AND ZINN[68]	-298 to -266	150 to 1500
HYDROGEN-ETHYLENE-ETHANE HYDROGEN-PROPYLENE-PROPANE HYDROGEN-ETHYLENE-PROPYLENE	WILLIAMS AND KATZ[79] (TWO DATA POINTS IN EACH SYSTEM)	-100	1000 and 8000
HYDROGEN-METHANE-ETHYLENE-ETHANE-PROPYLENE-PROPANE	BENHAM AND KATZ[14] (FIVE DATA POINTS)	-100 and 0	500 and 1000
NITROGEN-METHANE	TOROCHESHNIKOV AND LEVIUS[74]	-298 to -220	15 to 150
NITROGEN-METHANE	CINES, ROACH, HOGAN AND ROLAND[23]	-280 to -150	15 to 650
NITROGEN-METHANE	BLOOMER AND PARENT[17]	-295 to -117	15 to 735
NITROGEN-METHANE	MC TAGGART AND EDWARDS[51]	-298 to -259	14.7
NITROGEN-ETHYLENE	TSIKLIS[75]	32	15,000 to 100,000
NITROGEN-n-BUTANE	AKERS, ATTWELL AND ROBINSON[1]	+100 to +300	500 to 4200
NITROGEN-n-HEPTANE	AKERS, KEHN AND KILGORE[2]	+90 to +360	1000 to 10,000
NITROGEN-n-HEPTANE	BOOMER, JOHNSON AND PIERCEY[20]	+77 to +239	1483
NITROGEN-METHANE-n-PENTANE	BOOMER, JOHNSON AND PIERCEY[18]	+77 to +185	51.5 to 275
NITROGEN-METHANE-MIXED-PENTANES	BOOMER, JOHNSON AND PIERCEY[18]	+77	100 to 200
NITROGEN-METHANE-n-HEXANE	BOOMER AND JOHNSON[19]	+77 to +185	50 to 340
NITROGEN-METHANE-MIXED-HEXANES	BOOMER AND JOHNSON[19]	+77	50 to 300
NITROGEN-METHANE-n-HEPTANE	BOOMER, JOHNSON AND PIERCEY[20]	+77 to +185	50 to 370
NITROGEN-HELIUM-METHANE-ETHANE-PROPANE-BUTANE	STUTZMAN AND BROWN[71]	-238 to -130	100

EXPERIMENTAL PROGRAM

The existing binary and ternary system data listed in Table I were examined and evaluated. It was found that the existing data for the hydrogen-methane-ethane ternary system were internally inconsistent, and it was decided that this system should be given further experimental study. The intention was to obtain more accurate data over a wider temperature range than has been reported in the literature, and to add to our knowledge of ternary light hydrocarbon systems containing hydrogen.

While excellent binary system data are available in the literature on the systems nitrogen-methane and methane-ethane, no data are available on the ternary system nitrogen-methane-ethane. It was decided that data on this system would be helpful as a guide to an understanding of the behavior of nitrogen in complex systems containing hydrogen, nitrogen, and the light hydrocarbons.

Published data are available on the hydrogen-nitrogen-methane ternary system at temperatures approaching the freezing point of methane. It was decided that data at a somewhat higher temperature would be helpful in completing our knowledge of this ternary system.

As a check on the use of any correlation which might be obtained for the behavior of complex systems containing hydrogen, nitrogen, and the light hydrocarbons, it was decided that data on the quaternary system hydrogen-nitrogen-methane-ethane should be obtained.

The experimental conditions chosen for study are given in Table II.

TABLE II

EXPERIMENTAL CONDITIONS CHOSEN FOR STUDY

System	Pressures (psia)	Temperatures (°F)
hydrogen-methane-ethane	500 and 1000	-100 and -200
hydrogen-nitrogen-methane	500 and 1000	-200
nitrogen-methane-ethane	500 and 1000	-100 and -200
hydrogen-nitrogen-methane-ethane	1000	-100
hydrogen-nitrogen-methane-ethane	500	-200

The purity of the materials used in this investigation will now be discussed and the equipment used to obtain the samples of the equilibrium liquid and vapor phases will be described. The experimental data will then be presented.

Purity of Materials

The pure grade hydrocarbons which were used were obtained from the Phillips Petroleum Company, and were specified as 99 mole percent pure. The hydrogen and nitrogen used in these investigations were water-pumped. The materials used, and the impurities detected in them by mass spectrometer analysis, are listed in Table III. The impurities listed in Table III were removed in a dessicator train (B in Figure 2) before the materials were used in these investigations.

TABLE III

PURITY OF MATERIALS

Component	Minimum Purity (mole % as rec'd)	Impurities
hydrogen	99.5	H_2O, N_2
nitrogen	99.5	H_2O, Argon
methane	99.0	C_2H_6, N_2
ethane	99.0	CH_4, C_3H_8

Description of Equipment

The equipment used to obtain the vapor-liquid equilibrium data for this thesis is of the vapor-recirculation type. It was built by Aroyan[4] for equilibrium investigations at pressures up to 10,000 psi and at temperatures from room temperature to -300°F.

A schematic diagram of the equipment is shown in Figure 2. The system is essentially composed of three main sections:

1.) Gas inlet and pressure generation section

2.) Equilibrium cell, cooling and circulation system

3.) Sampling section

Since the equipment is designed to operate at pressures well above the normal gas cylinder pressure, some means has to be employed to compress the cylinder gases to the pressures desired in the equilibrium cell. This is accomplished in the pressure generation section. This section provides the required high pressure gases and also the high pressure mercury for use in the equilibrium cell and circulation system.

Referring to Figure 2, A represents the cylinders of pure gases used in these experiments. The gases are passed through a dessicator train, B, composed of silica gel, ascarite, and activated charcoal to remove trace amounts of water, carbon dioxide, and the heavier hydrocarbons which may be present in the charge gases. The charge gases are passed from the dessicator train to the compression cylinder, C. Compression of the gas to the desired operating pressure is accomplished here. A gear pump, E,

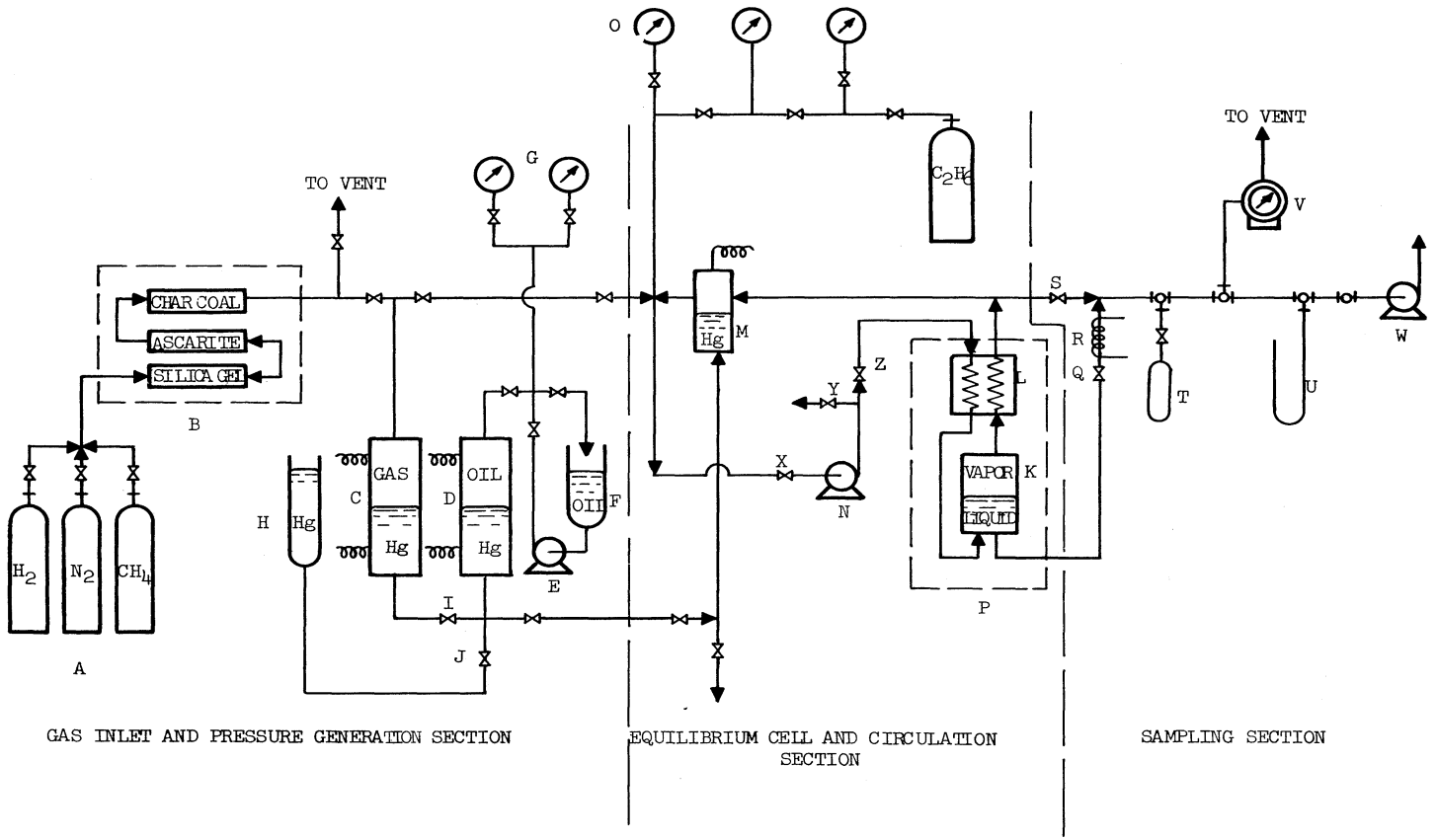

A	GAS CYLINDERS	I	VALVE IN HIGH PRESSURE MERCURY LINE	Q	LIQUID PHASE SAMPLE VALVE
B	DESSICATOR TRAIN	J	VALVE FOR ADMITTING MERCURY TO	R	ELECTRIC HEATER
C	HIGH PRESSURE GAS COMPRESSION CYLINDER		COMPRESSION CYLINDER	S	VAPOR PHASE SAMPLE VALVE
D	HIGH PRESSURE COMPRESSION CYLINDER	K	VAPOR-LIQUID EQUILIBRIUM CELL	T	SAMPLE BULB FOR MASS SPECTROMETER
E	HIGH PRESSURE OIL PUMP	L	COUNTER-CURRENT HEAT EXCHANGER	U	MERCURY MANOMETER
F	OIL RESERVOIR	M	VARIABLE-VOLUME HIGH PRESSURE	V	WET TEST METER
G	PRESSURE GAGES IN PRESSURE GENERATION		MERCURY RESERVOIR	W	VACUUM PUMP
	SECTION	N	HIGH PRESSURE MAGNETIC PUMP	X,Y	HIGH PRESSURE VALVES
H	MERCURY RESERVOIR	O	PRESSURE GAGES IN CIRCULATION SECTION	AND Z	
		P	CONSTANT TEMPERATURE AIR BATH		

Figure 2. Schematic Diagram of Apparatus Used to Obtain Vapor-Liquid Equilibrium Data

pumps oil from a reservoir, F, into a compression cylinder, D. The compression of the mercury in the cylinder causes mercury to flow through valve I to the second compression cylinder, C, where the mercury compresses the gas which has been charged into it without contamination of the gas with hydrocarbons from the oil. Pressure gages, G, on the oil lines determine the pressure of the gas in cylinder C. Electrical probes are located in the top and bottom of cylinders C and D to indicate when the level of the mercury interface in either cylinder becomes too high or too low. This prevents mercury from entering the equilibrium cell and circulation system which happens if the mercury level rises too high in cylinder C, and also prevents the oil or gas from contaminating the mercury lines if the mercury level falls too low in either cylinder. The probe on the top of cylinder D helps to prevent mercury contamination of the high pressure oil pump, E, as well as contamination of the oil reservoir F and the lines leading to the pressure gages. The system is so designed that the power to the oil pump is immediately cut off if the level of the mercury becomes too high or too low in either cylinder. When cylinder D is at atmospheric pressure, the level of the mercury can be adjusted by adding more mercury to the cylinder from the mercury reservoir, H, through valve J. When cylinder D is under pressure with valve I open, both high pressure gas and high pressure mercury can be obtained from the pressure generation section.

The equilibrium cell, K, together with the circulation system and the cooling system, forms the main section of the apparatus. Basically this section consists of the equilibrium cell and accompanying heat exchange equipment surrounded by a heavily insulated air bath, plus a variable-volume high-pressure cell and a magnetically-operated pump located outside of the cold bath for the circulation of the vapor phase through the stationary liquid phase. This section also includes the cooling system and temperature controller for providing the desired temperature during the runs.

The equilibrium cell, which was built by Aroyan [4] and has been described in detail by Williams [78] and Aroyan [4] [5], is constructed of two machined halves of 304 stainless steel welded together. It has an internal diameter of 2 inches and an external diameter of 4 inches. The overall length of the cell is 9-3/4 inches and the internal volume of the cell has been estimated as approximately 300 cubic centimeters. The cell is equipped with a thermowell and holds a three junction thermopile for indicating the temperature in the cell. The cell also contains two horizontal baffles to facilitate contacting of the vapor and liquid phases in the cell.

The vapor phase circulation system operates in the following manner. Vapor from the equilibrium cell is first passed through a counter-current heat exchanger, L, inside the cooled air bath, and part of the heat of the vapor stream returning to the bottom of the cell is absorbed by the outgoing vapor. It then

passes through the variable-volume high-pressure cell, M, which contains mercury from the pressure generation system. This reservoir of mercury is used to maintain constant pressure in the system when a vapor or liquid sample is being withdrawn. This is accomplished by injecting high pressure mercury into the reservoir to decrease the total volume of the system at constant pressure by an amount equivalent to the volume occupied by the particular phase being sampled.

From the reservoir, M, the vapor is passed to a plunger-type, magnetically-operated pump, N, which has been described by Williams [78] and Aroyan [4] [5]. It consists of a magnetic plunger inside a nonmagnetic cylinder. The plunger is raised by a solenoid around the cylinder and is returned by gravity and a spring when the solenoid is de-energized. An electronic timer is used to apply the electric current to the solenoid at various time intervals and thereby produce the pumping action. A most important property of this type of pump is that the operation of the pump makes no change in the total volume of the system.

The valves X, Y, and Z are located in the vapor circulation section so that the magnetic pump can be removed from the system for cleaning purposes and be replaced without necessitating the venting of the contents of the equilibrium cell. After completing a run, the valves X and Z are closed and the contents of the system between the two valves are vented through valve Y. After the pump has been removed and serviced, it is returned to its position and the system between valves X and Z is evacuated through valve Y

by means of the vacuum pump, W. The pressure in the remainder of the system is increased by addition of more gas from the pressure generation system; valve Y is then closed and valves X and Z are opened. At this point the magnetic pump is in good operating order and the system is ready for a new run with a minimum of disturbance to the contents of the equilibrium cell.

From the magnetic pump, N, the vapor is returned to the air bath and passed through the counter-current heat exchanger, L, where some of its heat is absorbed by the vapor being withdrawn from the equilibrium cell by the magnetic pump. This heat exchanger consists of two five-foot lengths of 1/4 inch O. D. high pressure tubing wound parallel and spirally around a six-inch mandrel and soldered together for most of their length. The warm circulating vapor passes through this exchanger counter-current to the cold vapor leaving the cell and, after leaving the exchanger, passes through another six feet of tubing in the air bath before returning to the bottom of the cell where it is bubbled through the liquid phase. The addition of this second heat exchanger greatly reduces the change in the equilibrium cell temperature when the magnetic pump is operated.

The pressure gages, O, are used to measure the pressure of the equilibrium system. Three gages are used for this purpose depending upon the operating pressure. One gage has a range of 0-800 psi with graduations of 10 psi, the second has a range of 0-3000 psi with graduations of 25 psi, and the third has a range of 0-10,000 psi with 50 psi graduations.

All tubing used in the equipment is 1/4 inch O. D. stainless steel high pressure tubing and all valves are of high pressure construction.

The air bath, P, containing the equilibrium cell and heat exchange equipment is insulated with two inches of rock cork insulation over the sides and bottom and six inches across the top. The sides and bottom are further insulated with six inches of loose Santocell insulation. The internal dimensions of the air bath are 6 x 12 x 18 inches with the depth being 18 inches.

Copper-Constantan thermocouples are used to measure the temperatures in the bath and in the cell. A Leeds and Northrup portable precision potentiometer is used to measure the emf developed by the various thermocouples. A total of seven thermocouples are used. They are located in the following positions:

Thermocouple Number	Location
1	Gas return line to bottom of cell
2	At side of cell three inches from bottom
3	Inside counter-current heat exchanger two inches from the cold end
4	In the air bath two inches above the top of the cell
5	In the air bath two inches below the bottom of the cell

6	Three junction thermopile in the thermowell of the equilibrium cell
7	Eight junction thermopile used for temperature control and fastened to the side of the equilibrium cell three inches from the bottom

The temperature is controlled by a Brown potentiometric recorder-controller of the self-balancing galvanometer type. It was designed for use with a single iron-constantan thermocouple and for temperatures up to 2000°F. It is used in conjunction with the eight junction thermopile of couple No. 7 and gives nearly full scale reading on the recorder at temperatures of approximately -250°F.

The cooling system for the air bath depends upon the temperature desired. For investigations at -100°F the cooling is provided by crushed dry ice introduced into the bath. A fan inside the bath circulates the air and carbon dioxide vapors over the equilibrium cell and related heat exchangers. Since the sublimation temperature of the dry ice (about -110°F) is only slightly lower than the desired temperature of -100°F, the forced circulation system employing the fan inside the bath is required to reach and maintain the operating temperature. The temperature controller is used in this case to actuate a small electric heater inside the bath. When the bath temperature falls below -100°F, the heater adds heat to the bath and thereby brings the bath back to the desired temperature. Enough dry ice is supplied to the air bath to maintain the temperature below -100°F and the temperature is controlled by frequent additions of small amounts of heat.

The -200°F temperatures are obtained by the use of liquid nitrogen as the coolant. No heat is supplied to the bath as the heat leak from the surroundings is sufficient for proper control. A low pressure air system is employed to force liquid nitrogen into the bath. The temperature controller actuates a solenoid valve in the low pressure air line and the coolant is forced into the bath whenever the control temperature rises above the desired operating temperature.

The third section of the equipment consists of the apparatus required for obtaining a representative sample of the liquid and vapor phases. The liquid samples pass from the bottom of the cell to a valve, Q, around which is wrapped an electric heater, R, to prevent the valve from getting too cold during the low temperature investigations. The vapor sample is taken from a line immediately above the cell and passed through a valve, S, to the evacuated sample bulbs. Both sample lines are 1/4 O. D. x 3/32 I. D. stainless steel tubing with 14 gage Chromel A wire inside to reduce the holdup. This procedure is recommended by Dodge and Dunbar [27]. Both the liquids and vapors of all systems studied exist in the gaseous state at room temperature and atmospheric pressure, so that their treatment after passing through their respective sample valves (Q and S) is identical.

As shown in Figure 2, the sampling section contains a sample bulb for mass spectrometer analysis, T, a mercury manometer, U, a wet test meter, V, and a vacuum pump, W.

The vacuum pump is used to evacuate the sample bulbs and the sample lines up to the sample valves prior to obtaining phase samples.

The wet test meter is used to determine the proper amount of material to be bled off before taking a sample in order to insure complete removal of the holdup in the sample lines from the previous sampling operation.

The sample bulbs used for obtaining phase samples for mass spectrometer analyses have a volume of approximately 25 cubic centimeters and are closed by an evacuated, hollow-core stopcock carrying a 10/30 ground-glass, tapered joint.

A Consolidated Engineering Corporation Model 21-103B analytical mass spectrometer was used to analyze all of the samples taken for this work. This instrument and the method of analysis is described in greater detail in Appendix D.

Experimental Data

The experimental data for the hydrogen-methane-ethane system are given in Table IV and the smoothed data for this ternary system are listed in Table V. The isothermal and isobaric phase diagrams for this system are shown in Figures 3 through 6.

Figure 3 is a conventional triangular composition diagram for the hydrogen-methane-ethane system at -100°F and 500 psia. Both the hydrogen-ethane and methane-ethane binaries exist at these conditions. The amount of ethane in the vapor phase is relatively constant, varying from 7.0 percent in the

TABLE IV

EXPERIMENTAL DATA FOR THE HYDROGEN-METHANE-ETHANE SYSTEM INCLUDING BINARY SYSTEM DATA FROM THE LITERATURE

Run No. or Reference	Liquid Phase Composition			Vapor Phase Composition		
	Mole % H_2	Mole % CH_4	Mole % C_2H_6	Mole % H_2	Mole % CH_4	Mole % C_2H_6
			Pressure = 500 psia Temperature = -100°F			
(78)(79)*	1.87	0.00	98.13	91.66	0.00	8.34
15	1.33	29.42	69.25	46.23	45.86	7.91
14	1.34	32.55	66.11	39.40	52.30	8.30
17	1.20	38.59	60.21	30.62	61.53	7.86
16	1.01	43,25	55.75	23.08	69.13	7.79
(16)*	0.00	66.00	34.00	0.00	93.00	7.00
			Pressure = 1000 psia Temperature = -100°F			
(78)(79)*	3.90	0.00	96.10	94.76	0.00	5.24
29	3.82	0.00	96.18	94.83	0.00	5.17
10	3.51	4.41	92.08	93.25	3.24	3.51
11	4.00	11.53	84.47	83.72	11.02	5.26
12	3.76	49.57	46.67	45.79	48.62	5.59
13	4.01	60.48	35.51	- -	- -	- -
27	4.40	73.96	21.64	- -	- -	- -
			Pressure = 500 psia Temperature = -200°F			
(78)(79)*	1.20	0.00	98.80	99.69	0.00	0.31
24	1.67	52.24	46.09	81.54	18.19	0.272
25	1.81	74.60	23.59	- -	- -	- -
26	1.75	76.08	22.17	74.12	25.72	0.164
22	3.27	92.03	4.70	69.15	30.80	0.051
(13)(14)*	3.43	96.57	0.00	63.92	36.08	0.00
			Pressure = 1000 psia Temperature = -200°F			
(78)(79)*	2.25	0.00	97.75	99.74	0.00	0.26
18	2.42	11.15	86.43	97.10	2.66	0.231
19	2.96	35.04	62.00	91.15	8.56	0.290
20	3.13	40.81	56.07	90.09	9.68	0.230
23	4.87	75.71	19.42	82.33	17.54	0.136
21	6.43	87.32	6.25	79.29	20.65	0.061
30	8.32	91.68	0.00	76.01	23.99	0.00
(13)(14)*	7.81	92.19	0.00	76.18	23.82	0.00

* Data from literature.

TABLE V

SMOOTHED DATA FOR THE HYDROGEN-METHANE-ETHANE SYSTEM

Liquid Phase Composition mole %			Vapor Phase Composition mole %			Equilibrium Ratio K = y/x		
H_2	CH_4	C_2H_6	H_2	CH_4	C_2H_6	H_2	CH_4	C_2H_6
Pressure = 500 psia					Temperature = -100°F			
1.87	0.00	98.13	91.66	0.00	8.34	49.0	- -	0.0850
1.80	10.0	88.2	76.5	15.2	8.27	42.5	1.52	0.0937
1.66	20.0	78.3	60.7	31.1	8.17	36.6	1.56	0.104
1.43	30.0	68.6	44.5	47.5	8.03	31.1	1.58	0.117
1.12	40.0	58.9	28.6	63.6	7.84	25.6	1.59	0.133
0.73	50.0	49.3	14.7	77.7	7.59	20.1	1.55	0.154
0.28	60.0	39.7	4.10	88.6	7.26	14.6	1.48	0.183
0.00	66.0	34.0	0.00	93.0	7.00	- -	1.41	0.206
Pressure = 1000 psia					Temperature = -100°F			
3.82	0 00	96 18	94.83	0.00	5.17	24.8	- -	0.0537
3.83	10 0	86.2	85.1	9.63	5.25	22.2	0.963	0.0609
3.84	20.0	76.2	75.3	19.36	5.33	19.6	0.968	0.0699
3.85	30.0	66.1	65.4	29.2	5.42	17.0	0.973	0.0820
3.87	40.0	56.1	55.4	39.1	5.51	14.3	0.978	0.0981
3.92	50.0	46.1	45.2	49.2	5.60	11.5	0.983	0.121
4.02	60.0	36.0	35.0	59.3	5.69	8.70	0.988	0.158
4.24	70.0	25.8	24.7	69.5	5.79	5.82	0.993	0.224
5.30	80.0	14.7	13.5	79.8	6.70	2.55	0.998	0.455
Pressure = 500 psia					Temperature = -200°F			
1.20	0.00	98.80	99.69	0.00	0.310	83.1	- -	0.00314
1.24	10.0	88.8	96.3	3.40	0.309	77.6	0.340	0.00348
1.28	20.0	78.7	92.9	6.80	0.307	72.5	0.340	0.00390
1.33	30.0	68.7	89.5	10.2	0.302	67.3	0.340	0.00440
1.39	40.0	58.6	86.1	13.6	0.293	62.0	0.340	0.00500
1.46	50.0	48.5	82.7	17.0	0.277	56.6	0.340	0.00571
1.55	60 0	38.4	79.4	20.4	0.247	51.2	0.340	0.00643
1.67	70.0	28.3	76.0	23.8	0.202	45.5	0.340	0.00714
1.89	80.0	18.1	72.7	27.2	0.141	38.5	0.340	0.00779
2.34	90.0	7.66	69.2	30.7	0.063	29.6	0.341	0.00821
3.43	96.57	0.00	63.92	36.08	0.00	18.6	0.374	- -
Pressure = 1000 psia					Temperature = -200°F			
2.25	0.0	97.75	99.74	0.00	0.260	44.3	- -	0.00266
2.42	10.0	87.6	97.4	2.38	0.256	40.2	0.238	0.00292
2.60	20.0	77.4	95.0	4.76	0.250	36.6	0.238	0.00323
2.81	30.0	67.2	92.6	7.14	0.242	33.0	0.238	0.00360
3.07	40.0	56.9	90.3	9.52	0.231	29.4	0.238	0.00406
3.41	50.0	46.6	87.9	11.9	0.216	25.8	0.238	0.00463
3.86	60.0	36.1	85.5	14.3	0.194	22.2	0.238	0.00537
4.46	70.0	25.5	83.1	16.7	0.162	18.6	0.238	0.00635
5.39	80.0	14.6	80.8	19.1	0.113	15.0	0.239	0.00774
7.40	90.0	2.60	78.2	21.8	0.030	10.6	0.242	0.0115
8.32	91.68	0.00	76.01	23.99	0.000	9.13	0.262	- -

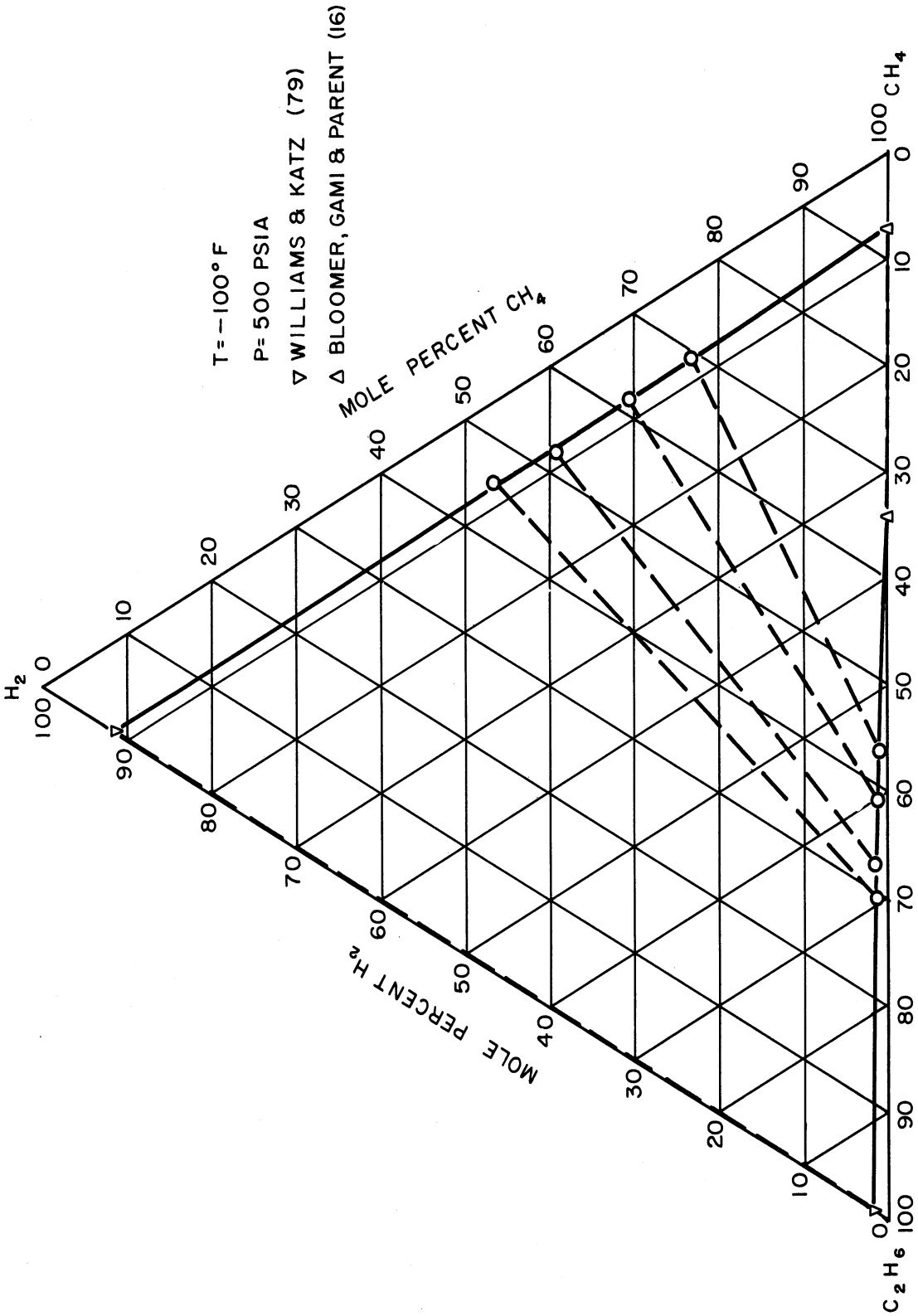

Figure 3. Triangular Composition Diagram for the Hydrogen-Methane-Ethane System at -100°F and 500 psia

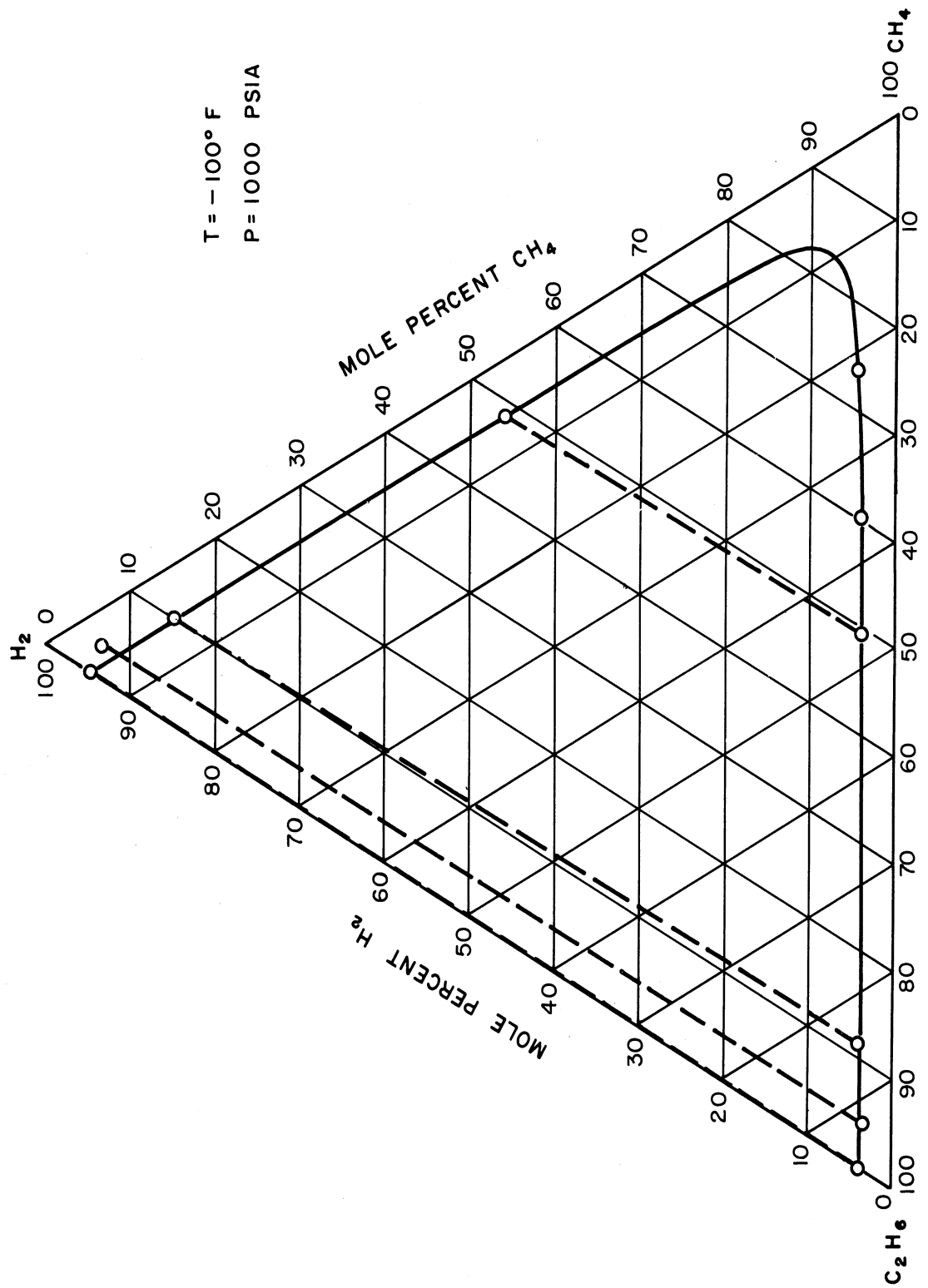

Figure 4. Triangular Composition Diagram for the Hydrogen-Methane-Ethane System at -100°F and 1000 psia

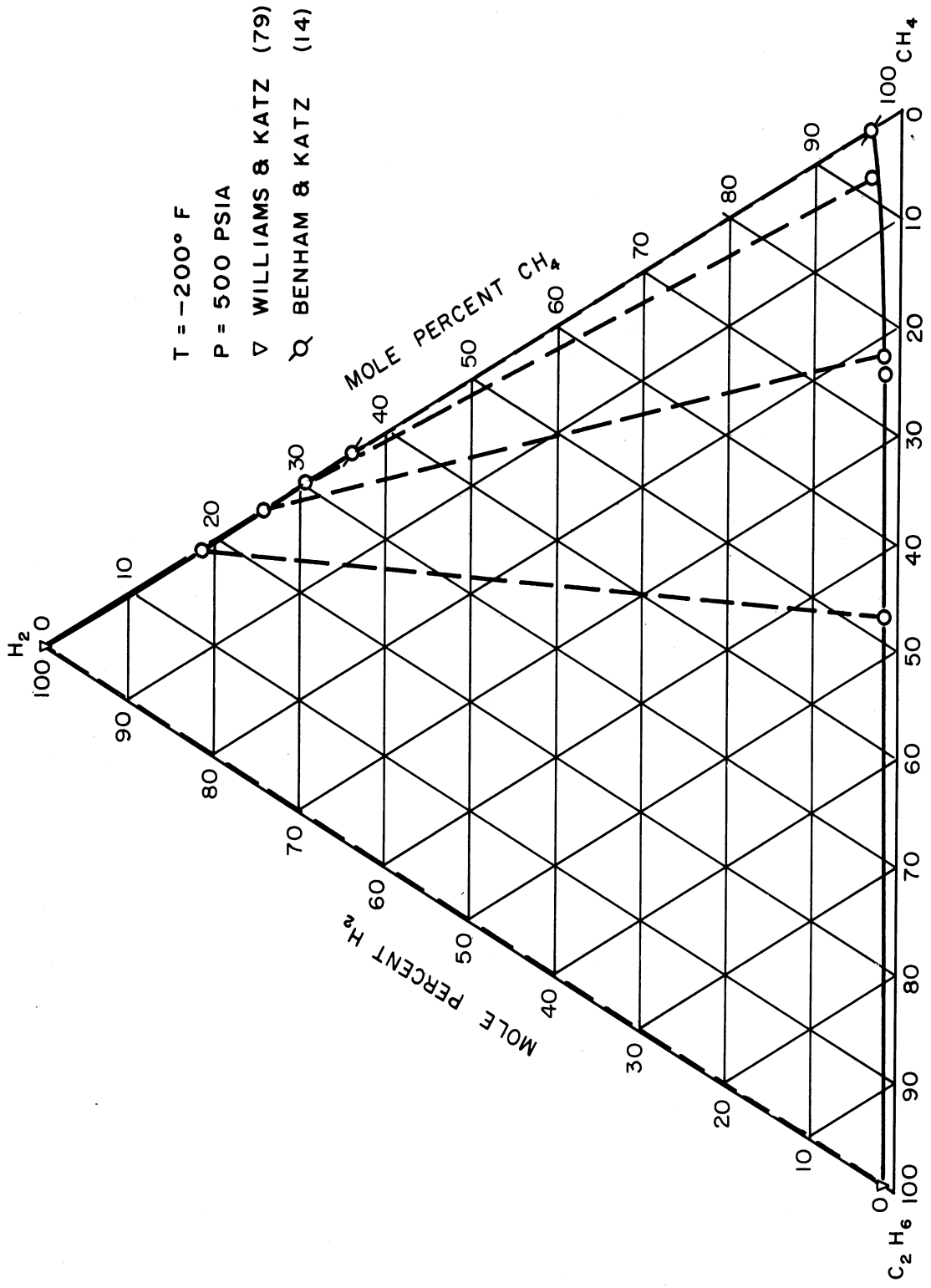

Figure 5. Triangular Composition Diagram for the Hydrogen-Methane-Ethane System at -200°F and 500 psia

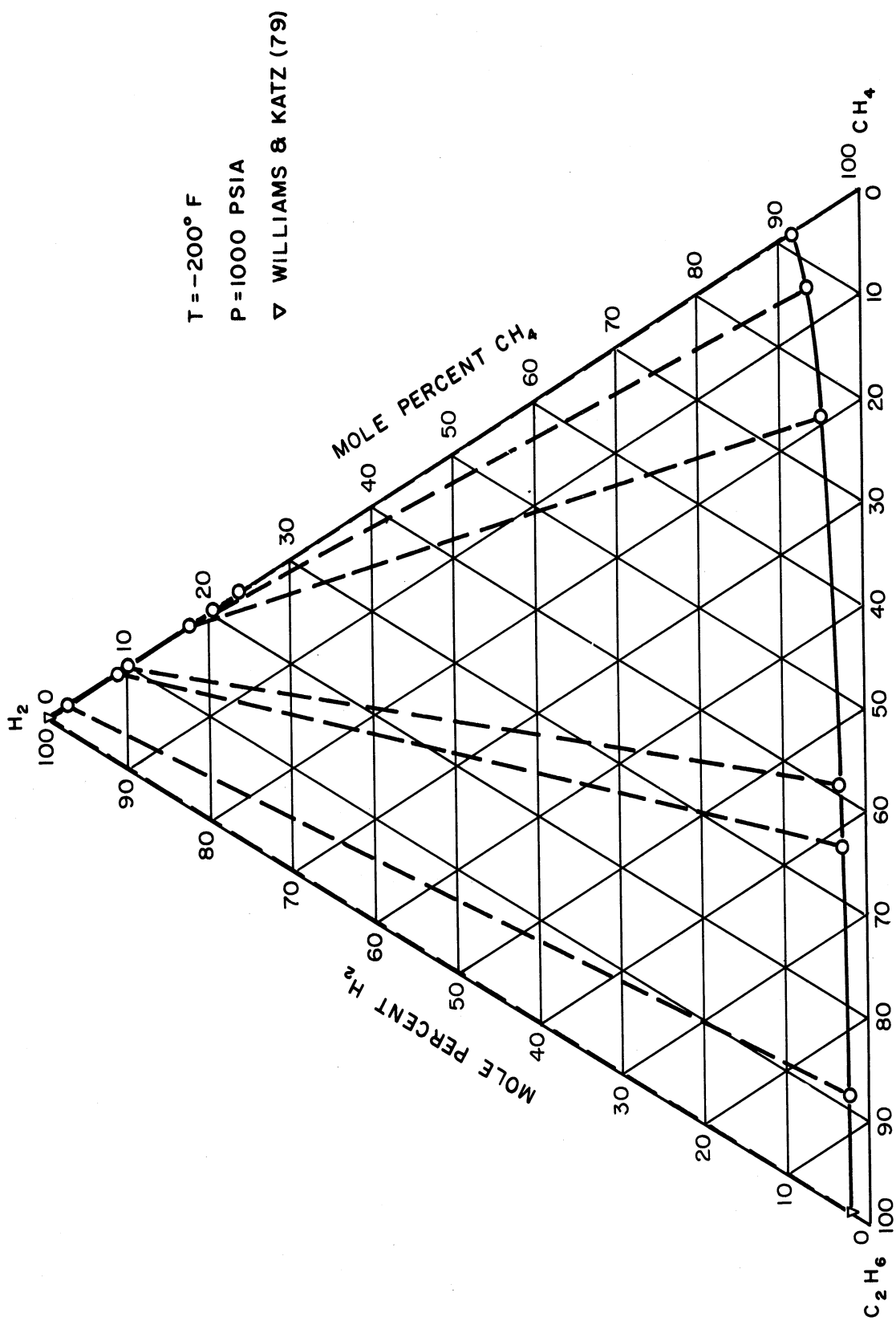

Figure 6. Triangular Composition Diagram for the Hydrogen-Methane-Ethane System at -200°F and 1000 psia

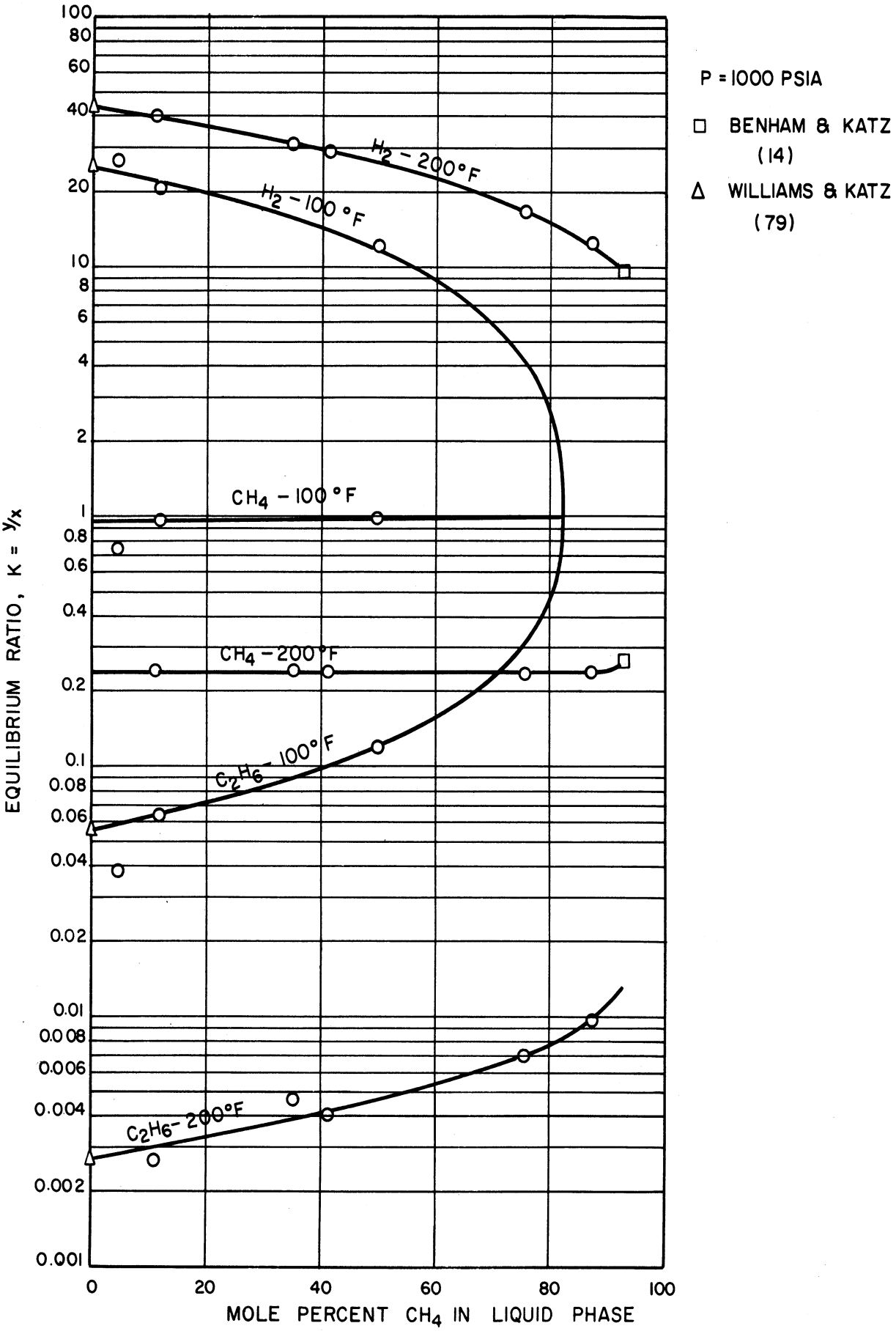

Figure 7. Equilibrium Ratios for Constituents in the Hydrogen-Methane-Ethane System at 1000 psia as a Function of the Mole Percent Methane in the Liquid Phase

methane-ethane binary to 8.34 percent in the hydrogen-ethane binary system. The solubility of hydrogen in the liquid phase decreases as the quantity of methane in the ternary system increases.

A critical point exists in the hydrogen-methane-ethane system at 1000 psia and -100°F as shown in Figure 4. Only the hydrogen-ethane binary system exists at these conditions, and a critical composition of approximately 83 percent methane, 8 percent hydrogen, and 9 percent ethane appears to be indicated. The variations in the amounts of hydrogen in the liquid phase and ethane in the vapor phase are small as the quantity of methane in the system is increased until the critical point is approached.

At very low temperatures the quantity of ethane in the vapor phase is extremely small. This can be seen in Figure 5 and Figure 6. Figure 5 shows the phase diagram at -200°F and 500 psia. The binary systems of hydrogen with methane and ethane exist at these conditions. The maximum amount of ethane in the vapor phase is found to be 0.31 percent--the amount existing in the vapor phase of the hydrogen-ethane binary system.

Figure 6 also shows that almost no ethane is present in the vapor phase at -200°F and 1000 psia. Again, the binaries of hydrogen with methane and ethane exist at this temperature and pressure. The maximum amount of ethane in the vapor phase at -200°F and 1000 psia is 0.26 percent, which is the amount in the vapor of the hydrogen-ethane binary system. The increase in pressure from 500 to 1000 psia more than doubles the solubility of hydrogen in the liquid phase over most ranges of composition.

Figure 5 and Figure 6 show that the amount of ethane in the vapor phase is negligible at temperatures of -200°F or lower and for pressures greater than a few hundred pounds.

The binary points for the hydrogen-ethane system shown in Figure 3, Figure 5, and Figure 6 were obtained from the work of Williams and Katz (78) (79), while the binary point for the methane-ethane system shown in Figure 3, was obtained from the work of Bloomer, Gami, and Parent (16). The binary point shown in Figure 5 for the hydrogen-methane system was obtained from the data of Benham and Katz (13) (14).

Equilibrium ratios for the components in the hydrogen-methane-ethane ternary system at 1000 psia have been plotted as a function of the mole percent methane in the liquid phase. It may be seen from Figure 7 that the equilibrium ratios, particularly those of hydrogen and ethane, are definitely functions of composition as well as functions of temperature and pressure. The effect of composition becomes especially important when the system is near its critical point.

The experimental data for the nitrogen-methane-ethane system are given in Table VI and the smoothed data for this ternary system are listed in Table VII. The isothermal and isobaric phase diagrams for this system are shown in Figures 8 through 10.

Figure 8 shows the ternary phase diagram at -100°F and 500 psia. Both the nitrogen-ethane and methane-ethane binaries exist at this temperature and pressure. The methane-ethane

TABLE VI

EXPERIMENTAL DATA FOR THE NITROGEN-METHANE-ETHANE SYSTEM
INCLUDING BINARY SYSTEM DATA FROM THE LITERATURE

Run No. or Reference	Liquid Phase Composition			Vapor Phase Composition		
	Mole % N_2	Mole % CH_4	Mole % C_2H_6	Mole % N_2	Mole % CH_4	Mole % C_2H_6
			Pressure = 500 psia Temperature = -100°F			
50	9.56	0.00	90.44	89.22	0.00	10.78
51	7.15	19.89	72.96	60.29	29.79	9.92
(16)*	0.00	66.00	34.00	0.00	93.00	7.00
			Pressure = 1000 psia Temperature = -100°F			
31	21.29	0.00	78.71	90.55	0.00	9.45
35	20.64	15.64	63.72	74.60	16.42	8.98
38	17.52	56.12	26.36	34.35	56.08	9.57
			Pressure = 500 psia Temperature = -200°F			
32	18.26	0.00	81.74	99.23	0.00	0.766
33	24.03	25.25	50.72	88.10	11.31	0.593
34	35.06	44.99	19.95	79.75	19.79	0.463
(17)*	49.00	51.00	0.00	73.00	27.00	0.00
(23)*	50.90	49.10	0.00	75.20	24.80	0.00

* Data from literature.

TABLE VII

SMOOTHED DATA FOR THE NITROGEN-METHANE-ETHANE SYSTEM

Liquid Phase Composition mole %			Vapor Phase Composition mole %			Equilibrium Ratio K = y/x		
N_2	CH_4	C_2H_6	N_2	CH_4	C_2H_6	N_2	CH_4	C_2H_6
Pressure = 500 psia					Temperature = -100°F			
9.56	0.00	90.44	89.22	0.00	10.78	9.33	- -	0.119
8.35	10.0	81.6	74.4	15.2	10.4	8.90	1.52	0.127
7.14	20.0	72.9	60.0	30.0	9.95	8.40	1.50	0.137
5.93	30.0	64.1	46.2	44.4	9.42	7.79	1.48	0.147
4.60	40.0	55.4	32.8	58.4	8.82	7.13	1.46	0.159
3.07	50.0	46.9	19.8	72.0	8.16	6.44	1.44	0.174
1.29	60.0	38.7	7.35	85.2	7.45	5.70	1.42	0.193
0.00	66.0	34.0	0.00	93.0	7.00	- -	1.41	0.206
Pressure = 1000 psia					Temperature = -100°F			
21.29	0.00	78.71	90.55	0.00	9.45	4.25	- -	0.120
20.6	10.0	69.4	80.0	10.5	9.47	3.88	1.05	0.137
19.9	20.0	60.1	69.7	20.8	9.49	3.50	1.04	0.158
19.2	30.0	50.8	59.6	30.9	9.51	3.11	1.03	0.187
18.5	40.0	41.5	49.7	40.8	9.53	2.69	1.02	0.230
17.8	50.0	32.2	39.9	50.5	9.55	2.24	1.01	0.296
17.1	60.0	22.9	30.4	60.0	9.57	1.78	1.00	0.418
Pressure = 500 psia					Temperature = -200°F			
18.26	0.00	81.74	99.23	0.00	0.766	5.44	- -	0.00937
20.1	10.0	69.9	94.9	4.40	0.698	4.72	0.440	0.00999
22.6	20.0	57.4	90.6	8.80	0.630	4.01	0.440	0.0110
26.0	30.0	44.0	86.2	13.2	0.562	3.32	0.440	0.0128
31.0	40.0	29.0	81.9	17.6	0.494	2.64	0.440	0.0170
45.0	50.0	5.0	76.0	23.6	0.350	1.69	0.472	0.070
49.0	51.0	0.00	73.0	27.0	0.00	1.49	0.530	- -

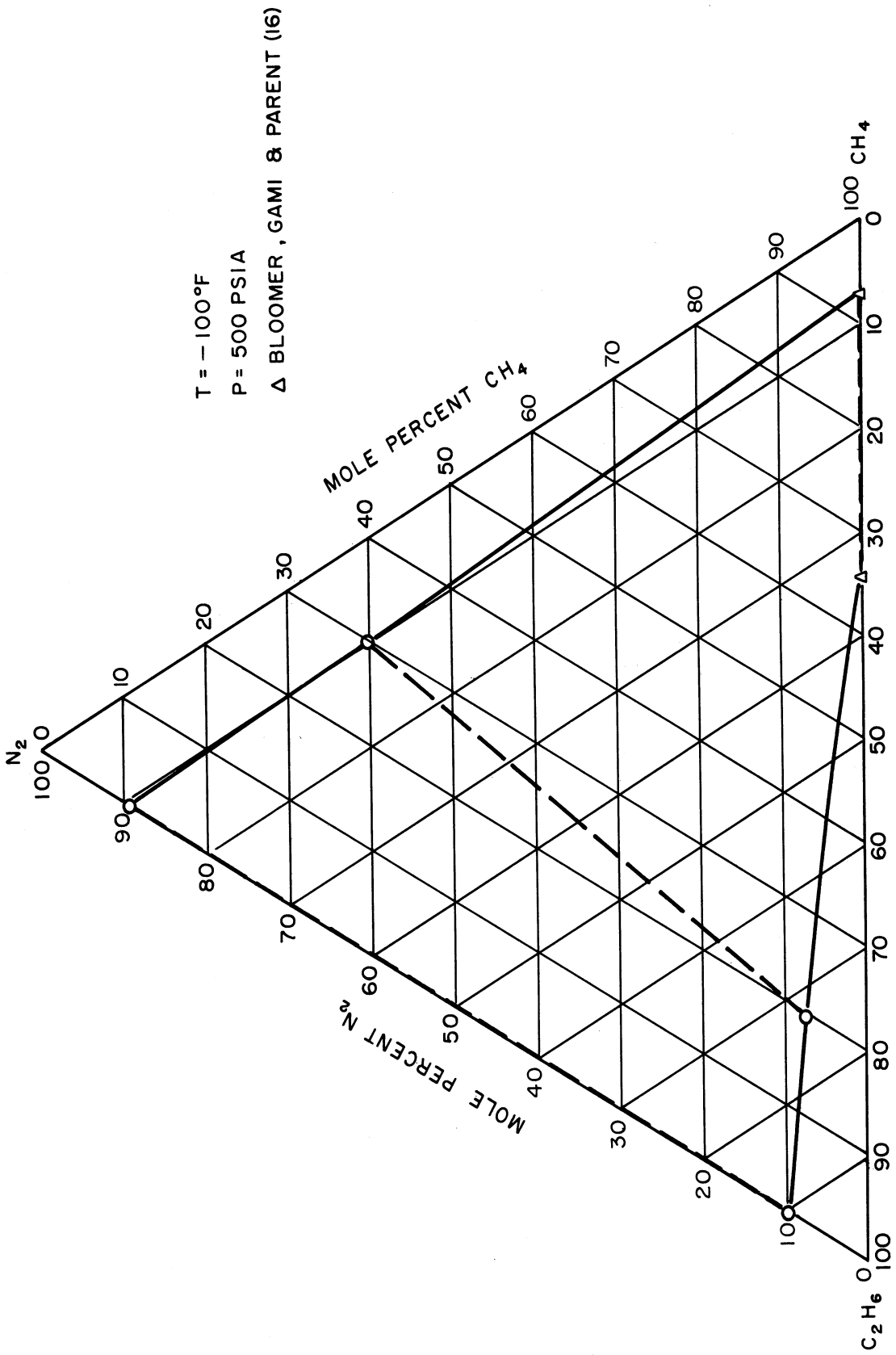

Figure 8. Triangular Composition Diagram for the Nitrogen-Methane-Ethane System at -100°F and 500 psia

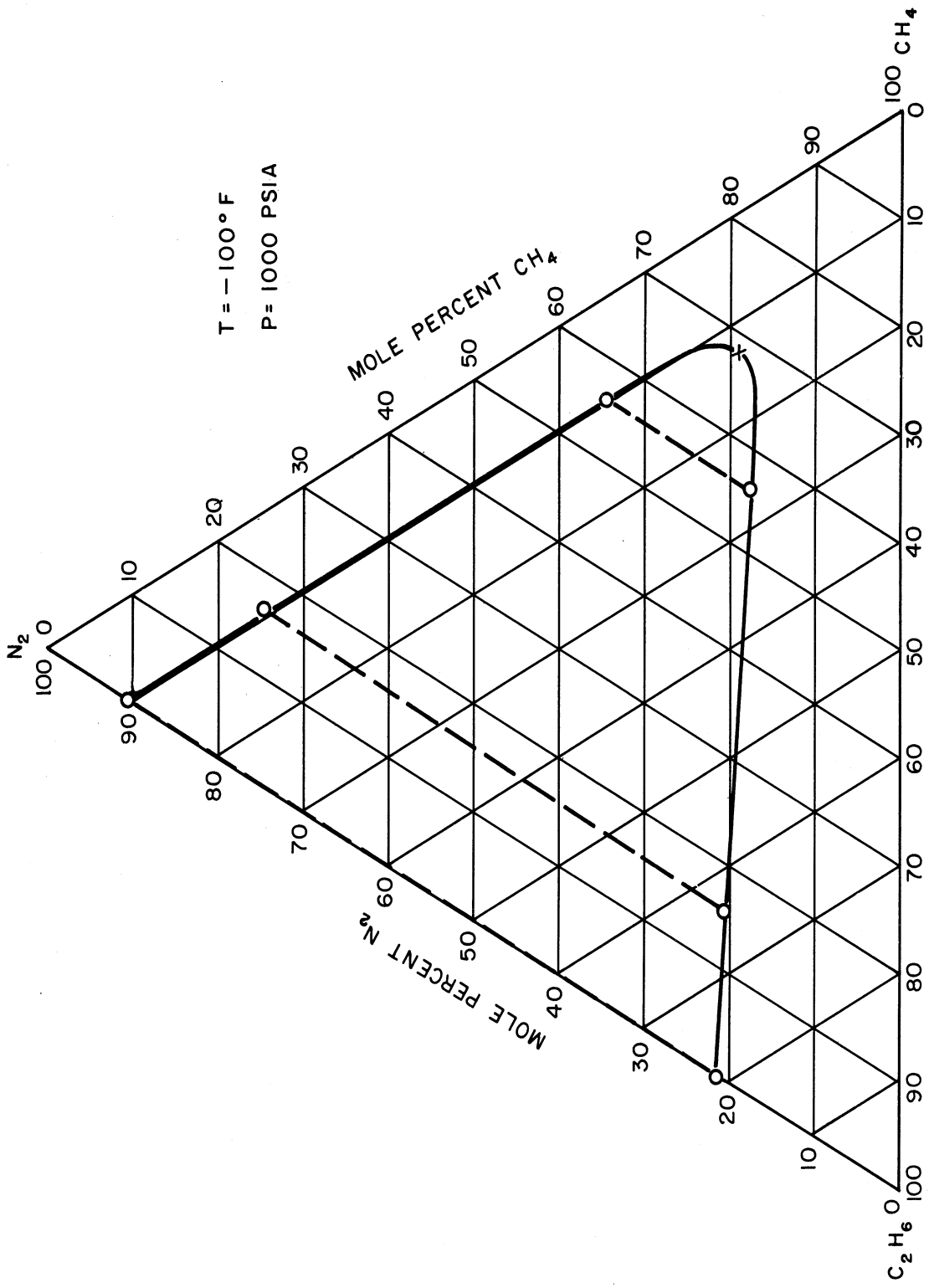

Figure 9. Triangular Composition Diagram for the Nitrogen-Methane-Ethane System at -100°F and 1000 psia

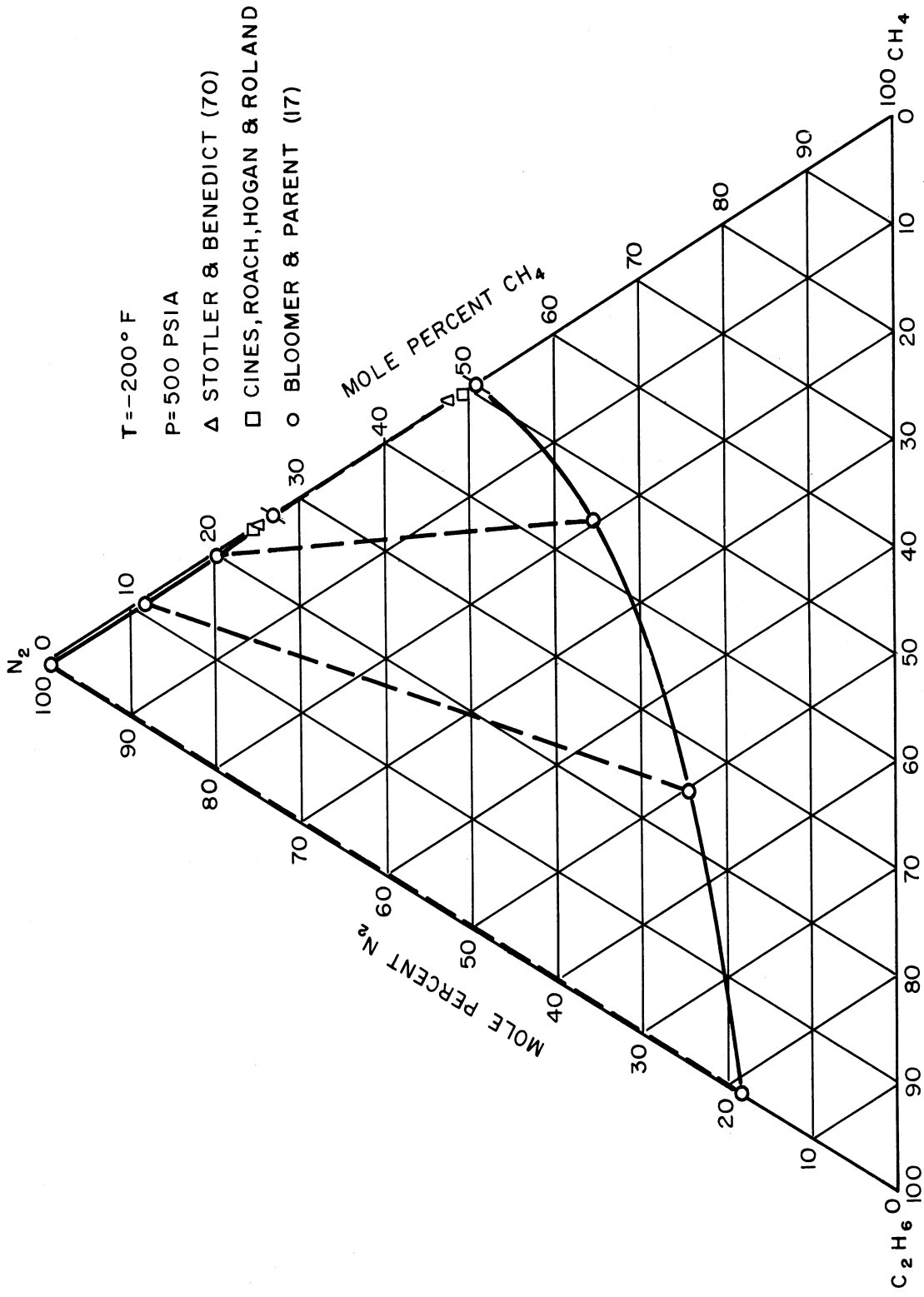

Figure 10. Triangular Composition Diagram for the Nitrogen-Methane-Ethane System at -200°F and 500 psia

binary point shown on this phase diagram was taken from the data of Bloomer, Gami, and Parent [16]. It may be noted that the vapor phase contains considerable quantities of ethane over the entire range of liquid phase compositions. The solubility of nitrogen in ethane is almost 10 percent at these conditions, but it decreases as the amount of methane in the system increases.

The phase diagram at -100°F and 1000 psia is shown in Figure 9. Since the nitrogen-ethane binary is the only binary system which can exist at these conditions, a critical point must be found in the ternary system at this temperature and pressure. The composition at the critical point may be estimated from Figure 9 to be approximately 68 percent methane, 19 percent nitrogen, and 13 percent ethane. As may be noted in the smoothed data of Table VII, the amount of ethane in the vapor phase varies only 0.1 percent for all liquid phase compositions until the critical point is approached.

The ternary phase diagram at -200°F and 500 psia is given in Figure 10. The data for the nitrogen-methane binary system were obtained from the works of Bloomer and Parent [17], Cines and co-workers [23], and from the Stotler and Benedict [70] correlation of the data taken by Cines et. al. The solubility of nitrogen in the liquid phase of the ternary system varies considerably with composition -- increasing as the amount of methane in the system increases. The amount of ethane in the vapor phase is slight, but it is, in most cases, greater than the

amount of ethane in the vapor phase of the hydrogen-methane-ethane ternary system at the same conditions of temperature and pressure.

Since no data for the nitrogen-ethane binary system could be found in the literature, the binary data required to complete the ternary phase diagrams were also obtained in this work. Pressure-composition diagrams for the nitrogen-ethane binary system at -100 and -200°F are shown in Figure 11. The critical regions of the envelopes have been dashed.

Figure 12 shows the critical loci of the binary systems nitrogen-methane, methane-ethane, and nitrogen-ethane, and portions of the critical loci of the binary systems hydrogen-nitrogen, hydrogen-methane, and hydrogen-ethane. The critical loci for the nitrogen-methane and methane-ethane systems are based on the data of Bloomer and co-workers (16) (17). The critical locus for the nitrogen-ethane system has been estimated from data taken in this work. The critical locus for the hydrogen-nitrogen system is based on the data of Verschoyle (77), Ruhemann and Zinn (63), Gonikberg, Fastowsky, and Gurwitsch (32), and Steckel and Zinn (68). The critical locus for the hydrogen-methane system is based on the data of Benham and Katz (14), and the critical locus for the hydrogen-ethane system is based on the data of Williams and Katz (79).

The equilibrium ratios for the constituents in the nitrogen-methane-ethane ternary system at -100°F were plotted as a function of the mole percent methane in the liquid phase. The equilibrium ratios shown in Figure 13 were calculated from the

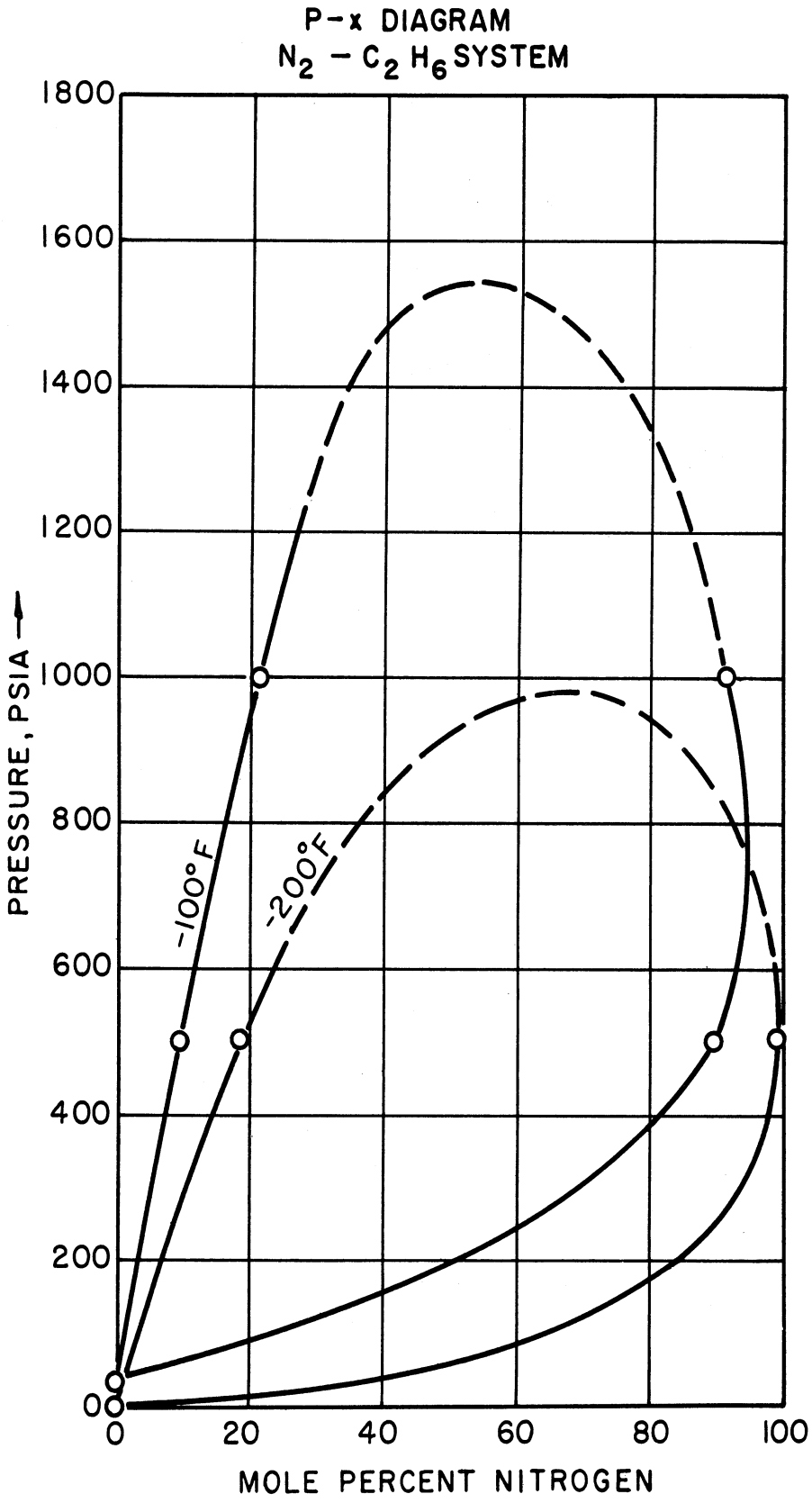

Figure 11. Pressure-Composition Diagram for the Nitrogen-Ethane Binary System

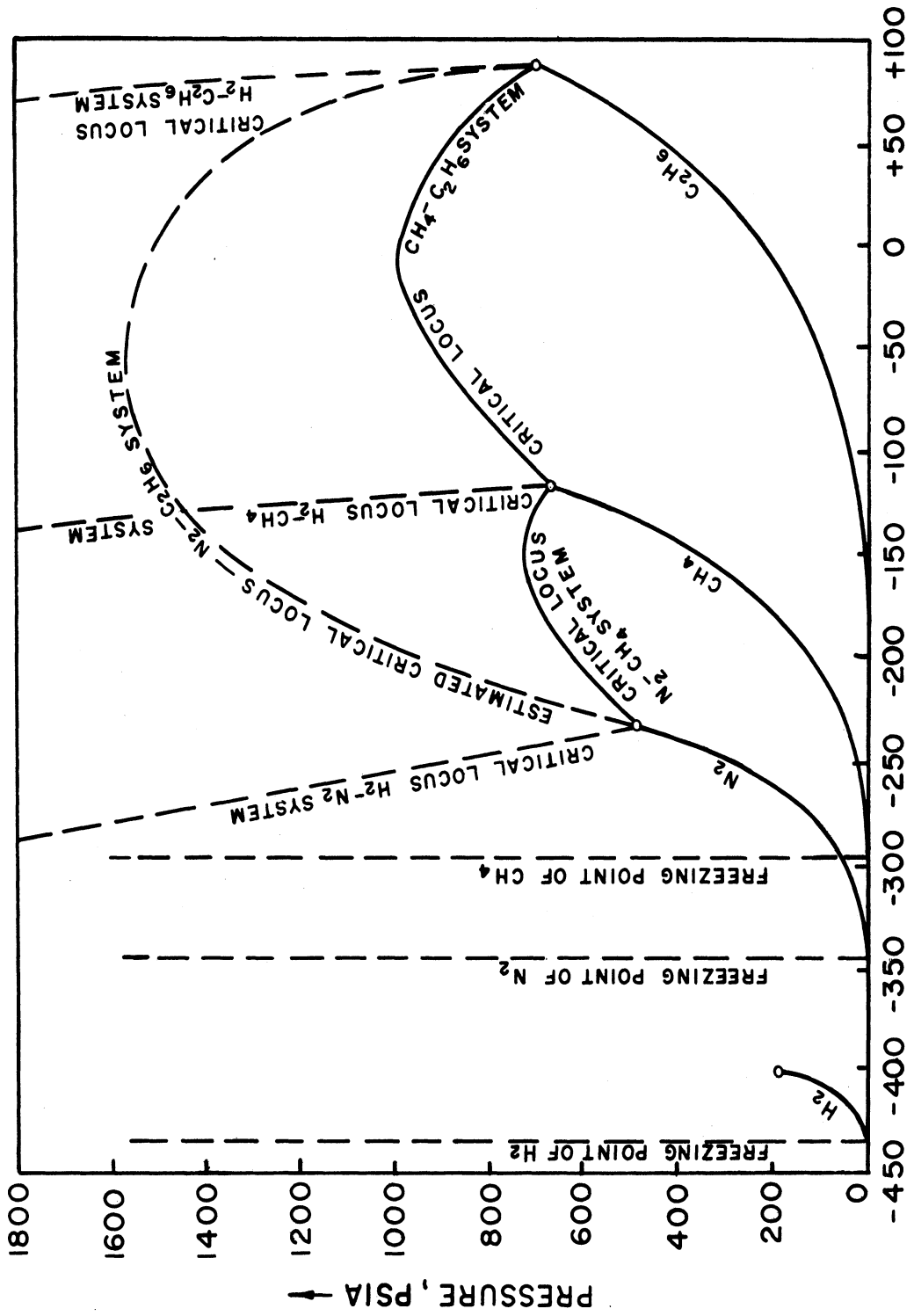

Figure 12. Critical Loci for Binary Systems Containing Hydrogen, Nitrogen, Methane, and Ethane

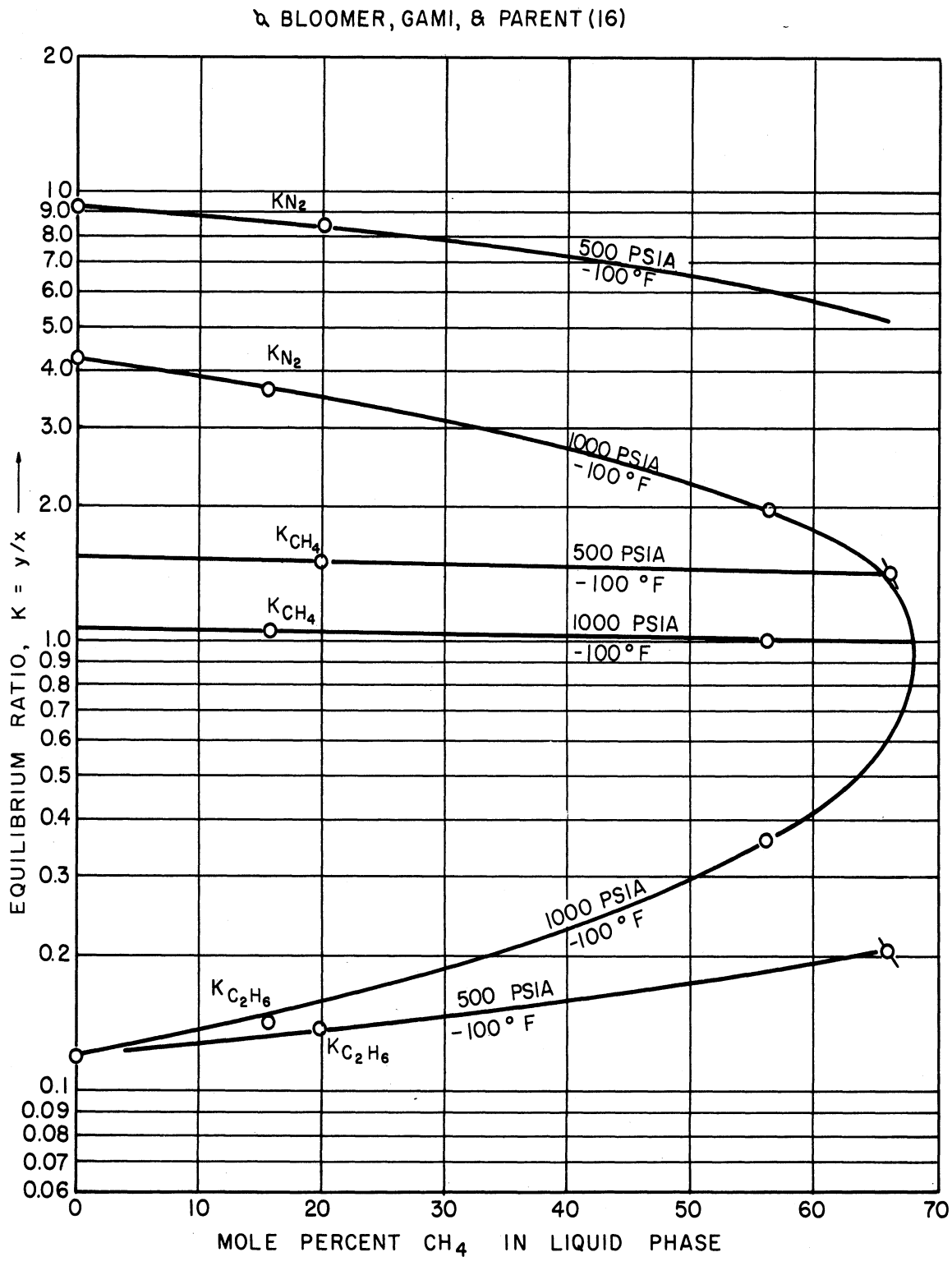

Figure 13. Equilibrium Ratios for Constituents in the Nitrogen-Methane-Ethane System at -100°F as a Function of the Mole Percent Methane in the Liquid Phase

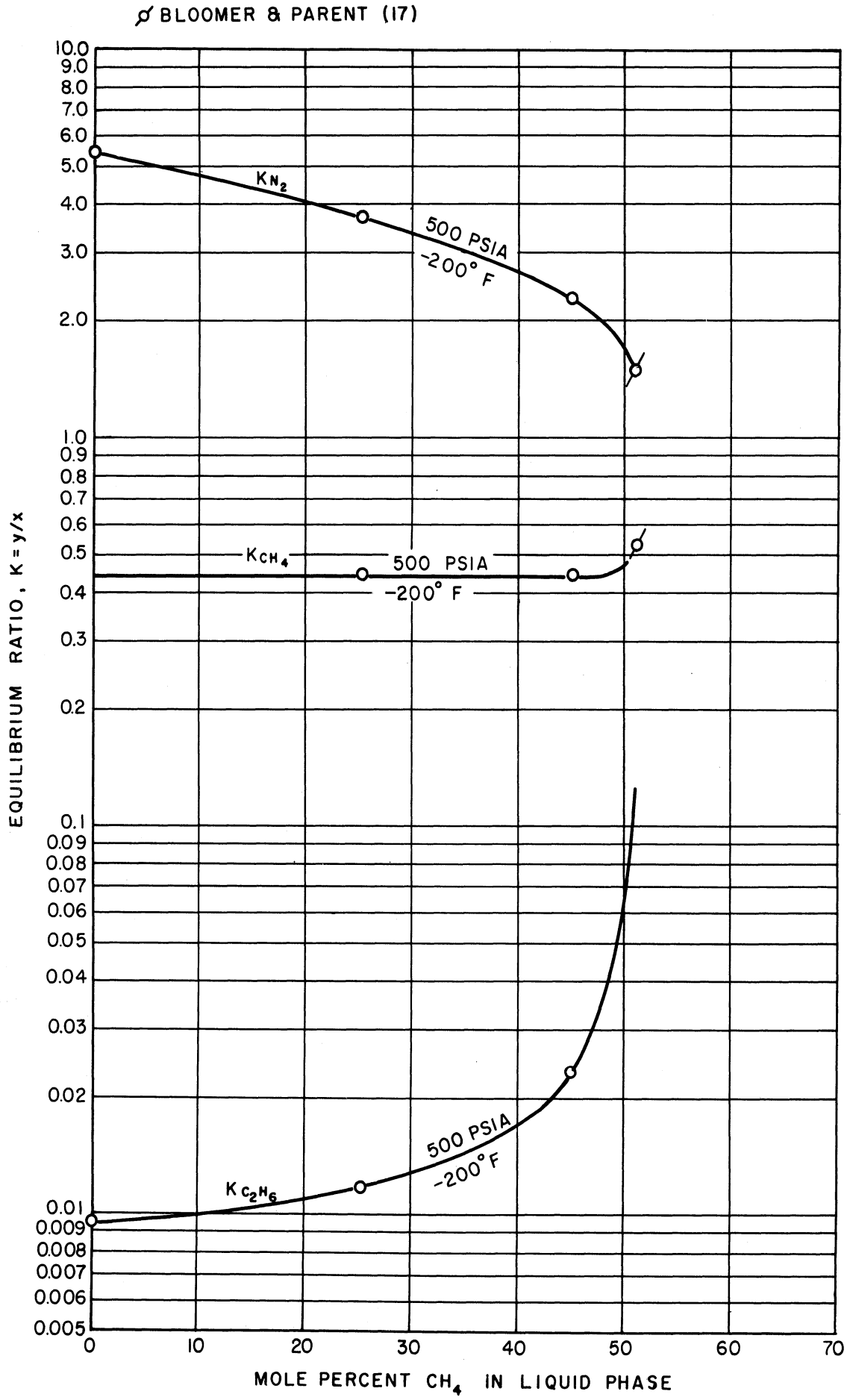

Figure 14. Equilibrium Ratios for Constituents in the Nitrogen-Methane-Ethane System at -200°F as a Function of the Mole Percent Methane in the Liquid Phase

smoothed data given in Table VII, and the actual data points were included to illustrate the agreement between the original data and the smoothed values.

Figure 14 is a similar plot of the equilibrium ratios at -200°F and 500 psia as a function of the mole percent methane in the liquid phase. The equilibrium ratios for this plot were also calculated from the smoothed data. The effect of composition on the equilibrium ratios is clearly illustrated.

The experimental data for the hydrogen-nitrogen-methane ternary system are given in Table VIII. Smoothed data are given in Table IX. The corresponding phase diagrams are shown in Figure 15 and Figure 16.

Figure 15 is the ternary phase diagram at -200°F and 500 psia. The hydrogen-methane binary point on this diagram was obtained from the work of Benham and Katz [14], while the nitrogen-methane binary point was obtained, as before, from the work of Bloomer and Parent [17], Cines and co-workers [23], and Stotler and Benedict [70]. At this temperature and pressure the vapor phase contains large quantities of the heavy component (methane). The amount of methane in the vapor phase ranges between 27 and 36 percent. The solubility of hydrogen in the liquid phase decreases as the amount of nitrogen in the liquid phase increases.

At -200°F and 1000 psia the ternary phase diagram shows a critical point at approximately 31 percent methane, 55.5 percent nitrogen, and 13.5 percent hydrogen. Figure 16 shows the phase diagram for these conditions of temperature and pressure. The vapor

TABLE VIII

EXPERIMENTAL DATA FOR THE HYDROGEN-NITROGEN-METHANE SYSTEM INCLUDING BINARY SYSTEM DATA FROM THE LITERATURE

Run No. or Reference	Liquid Phase Composition			Vapor Phase Composition		
	Mole % H_2	Mole % N_2	Mole % CH_4	Mole % H_2	Mole % N_2	Mole % CH_4
			Pressure = 500 psia Temperature = -200°F			
(13)(14)*	3.43	0.00	96.57	63.92	0.00	36.08
37	2.86	9.98	87.16	43.37	21.91	34.72
40	2.08	21.76	76.15	- -	- -	- -
42	1.55	27.39	71.06	16.77	50.80	32.43
45	0.302	41.76	57.94	2.36	67.93	29.71
(17)*	0.00	49.00	51.00	0.00	73.00	27.00
(23)*	0.00	50.90	49.10	0.00	75.20	24.80
			Pressure = 1000 psia Temperature = -200°F			
(13)(14)*	7.81	0.00	92.19	76.18	0.00	23.82
30	8.32	0.00	91.68	76.01	0.00	23.99
47	8.26	6.17	85.57	67.35	8.38	24.27
43	8.49	17.91	73.60	50.02	23.77	26.21
46	9.15	37.33	53.52	31.30	42.91	25.79
44	9.32	39.12	51.56	30.05	44.13	25.82
49	9.26	41.37	49.37	27.58	46.37	26.05
48	11.57	53.54	34.89	- -	- -	- -

* Data from literature.

TABLE IX

SMOOTHED DATA FOR THE HYDROGEN-NITROGEN-METHANE SYSTEM

Liquid Phase Composition mole %			Vapor Phase Composition mole %			Equilibrium Ratio K = y/x		
H_2	N_2	CH_4	H_2	N_2	CH_4	H_2	N_2	CH_4
Pressure = 500 psia					Temperature = -200°F			
3.43	0.00	96.57	63.92	0.00	36.08	18.6	- -	0.374
3.16	5.00	91.8	53.0	11.5	35.5	16.8	2.30	0.387
2.86	10.0	87.1	43.1	21.9	35.0	15.1	2.19	0.402
2.53	15.0	82.5	34.2	31.4	34.4	13.5	2.09	0.417
2.17	20.0	77.8	26.5	39.8	33.7	12.2	1.99	0.433
1.81	25.0	73.2	19.8	47.3	32.9	10.9	1.89	0.449
1.44	30.0	68.6	14.0	54.0	32.0	9.73	1.80	0.466
1.06	35.0	63.9	9.10	59.9	31.0	8.58	1.71	0.485
0.67	40.0	59.3	5.06	64.8	30.1	7.55	1.62	0.507
0.28	45.0	54.7	2.00	69.0	29.0	7.15	1.53	0.530
0.00	49.0	51.0	0.00	73.0	27.0	- -	1.49	0.530
Pressure = 1000 psia					Temperature = -200°F			
8.18	0.00	91.68	76.01	0.00	23.99	9.30	- -	0.262
8.32	5.00	86.7	68.8	6.95	24.3	8.26	1.39	0.280
8.46	10.0	81.5	62.0	13.4	24.6	7.32	1.34	0.302
8.60	15.0	76.4	55.6	19.5	24.9	6.46	1.30	0.326
8.74	20.0	71.3	49.7	25.2	25.1	5.69	1.26	0.352
8.88	25.0	66.1	44.2	30.5	25.3	4.98	1.22	0.382
9.02	30.0	61.0	39.0	35.4	25.6	4.32	1.18	0.420
9.16	35.0	55.8	33.9	40.2	25.9	3.70	1.15	0.465
9.30	40.0	50.7	29.4	44.4	26.2	3.16	1.11	0.516
9.74	45.0	45.3	25.1	48.5	26.4	2.58	1.08	0.582
10.5	50.0	39.5	20.5	52.0	27.5	1.95	1.04	0.696
12.4	55.0	32.6	15.0	55.5	29.5	1.21	1.01	0.909

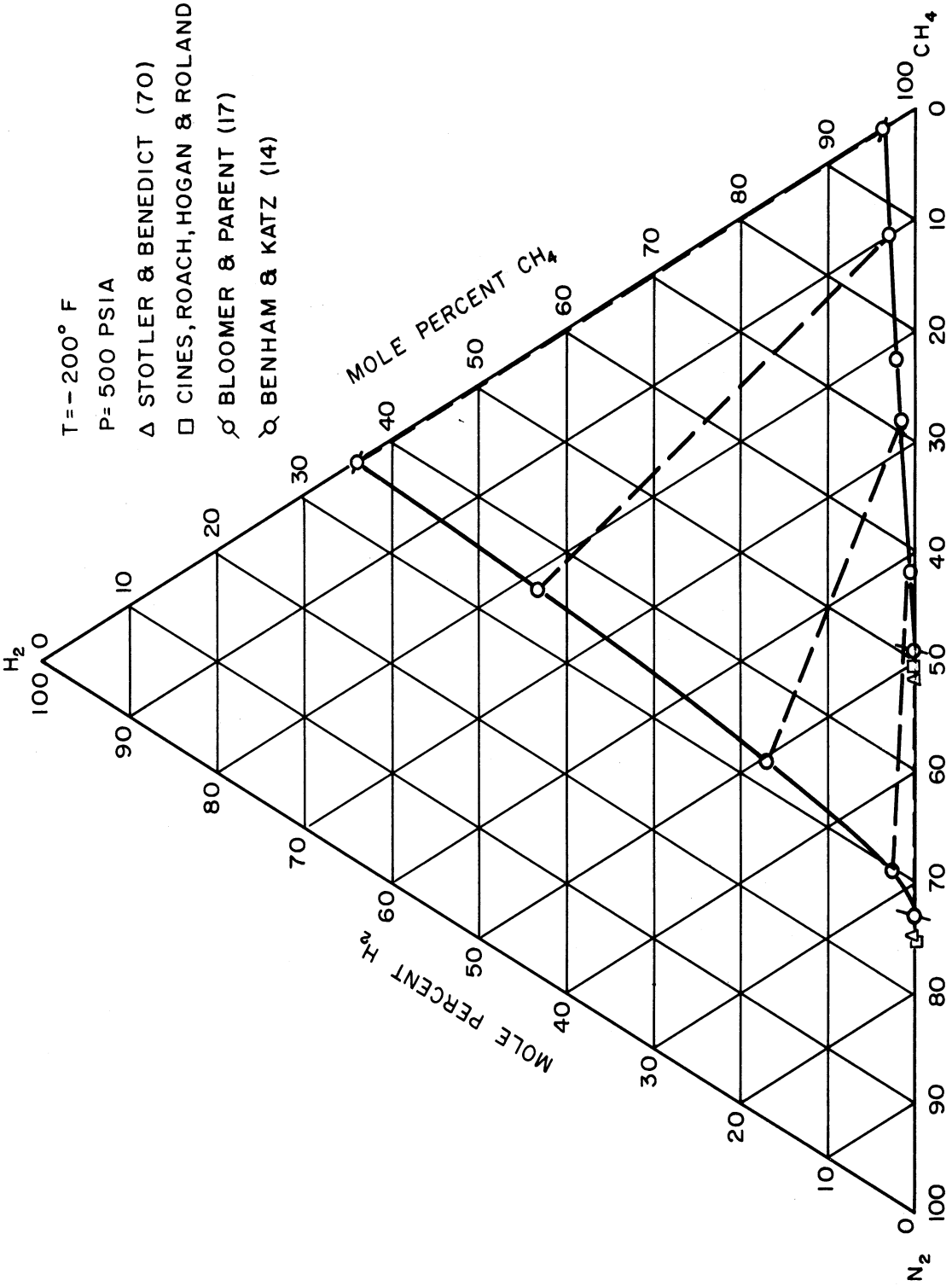

Figure 15. Triangular Composition Diagram for the Hydrogen-Nitrogen-Methane System at -200°F and 500 psia

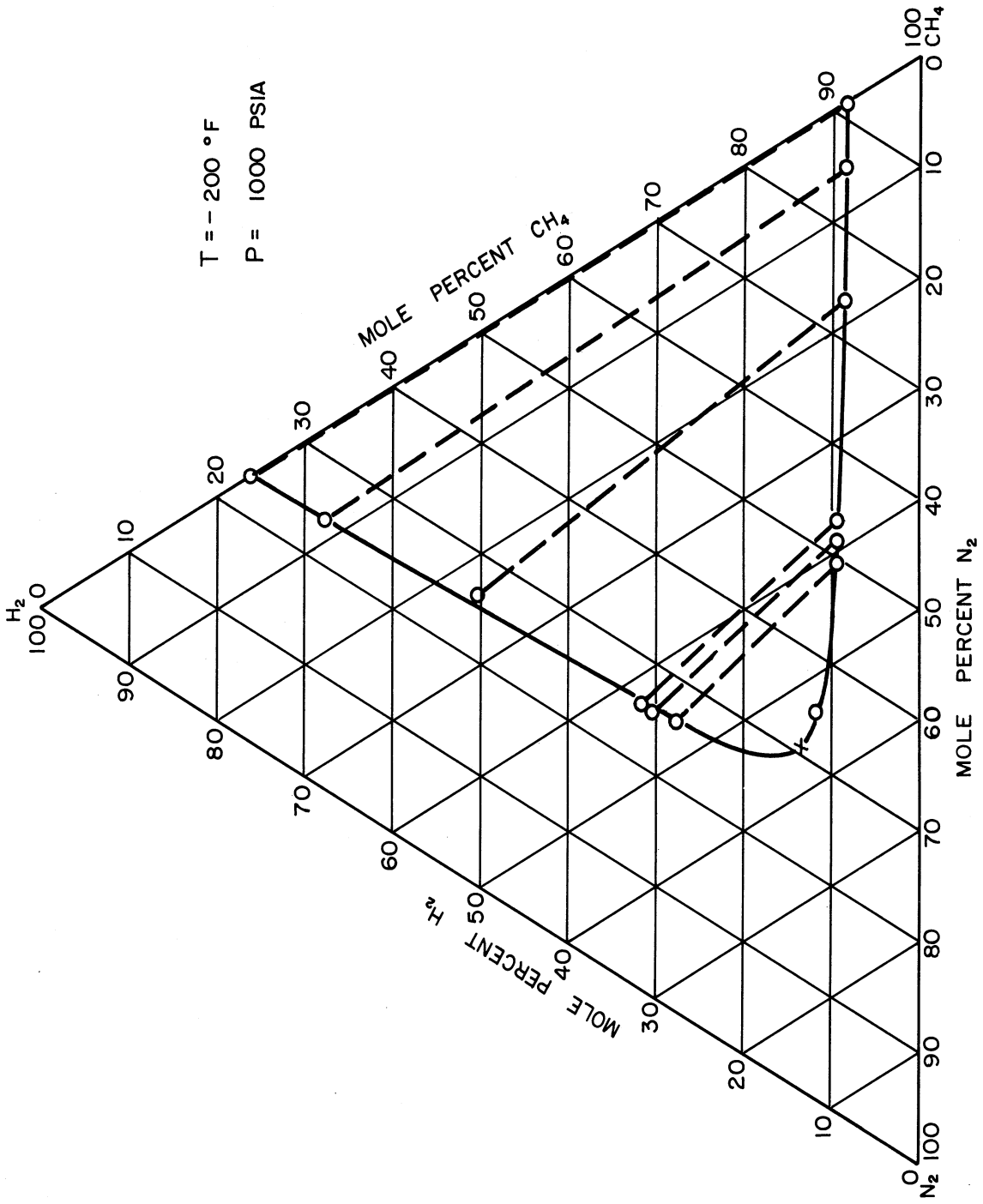

Figure 16. Triangular Composition Diagram for the Hydrogen-Nitrogen-Methane System at -200°F and 1000 psia

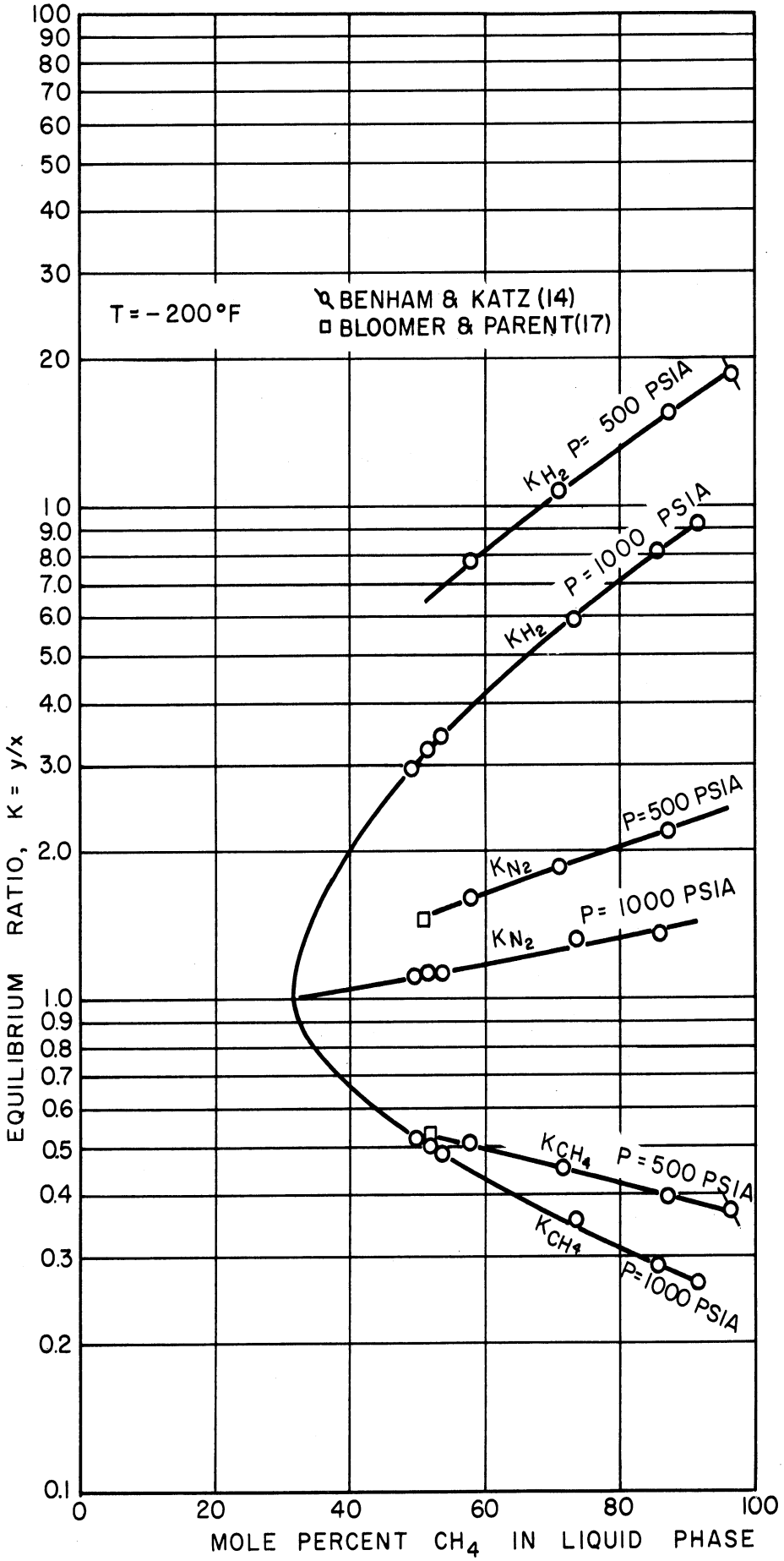

Figure 17. Equilibrium Ratios for Constituents in the Hydrogen-Nitrogen-Methane System at -200°F as a Function of the Mole Percent Methane in the Liquid Phase

phase contains between 24 and 31.0 percent methane, which is less than the amount in the vapor phase at -200°F and 500 psia. The amount of methane in the vapor phase decreases as the amount of nitrogen in the system is increased at 500 psia, but increases as the amount of nitrogen in the system is increased at 1000 psia.

Figure 17 is a plot of the equilibrium ratios for this system at -200°F as a function of the mole percent methane in the liquid phase.

Table X contains the experimental data obtained for the quaternary system hydrogen-nitrogen-methane-ethane. Two runs were made at -100°F and 1000 psia; five runs were made at -200°F and 500 psia. The equilibrium ratios for the constituents of this quaternary system have been calculated and are listed in Table X along with the experimental data. It may be noted that the equilibrium ratios for methane are almost constant for a given temperature and pressure, and are approximately equal to the methane equilibrium ratios in the nitrogen-methane-ethane ternary system at the corresponding temperature and pressure.

From the ternary and quaternary data obtained in the course of this investigation, and from binary data available in the literature, a qualitative understanding of the phase relationships in the quaternary system may be obtained. Figure 18 shows the evolution of the quaternary phase diagram at 500 psia as the temperature is raised from -231°F to 63°F. At approximately -231°F and 500 psia, a critical exists in the nitrogen-methane

TABLE X

EXPERIMENTAL DATA FOR THE HYDROGEN-NITROGEN-METHANE-ETHANE SYSTEM

Run Number		52	53	54	55	56	57	58
Pressure, psia		1000	1000	500	500	500	500	500
Temperature, °F		-100	-100	-200	-200	-200	-200	-200
Liquid	H_2	0.296	1.46	0.462	0.626	0.698	0.743	0.882
Phase	N_2	18.80	14.10	12.15	9.73	7.95	7.05	6.33
Composition	CH_4	8.52	7.91	8.80	8.73	8.41	8.44	8.48
(in mole %)	C_2H_6	72.39	76.53	78.59	80.91	82.95	83.77	84.31
Vapor	H_2	4.10	20.73	24.54	34.48	44.76	50.44	56.76
Phase	N_2	61.96	62.82	70.87	61.01	50.96	45.32	39.32
Composition	CH_4	8.66	8.14	3.98	3.91	3.74	3.71	3.46
in mole %)	C_2H_6	25.28	8.31	0.606	0.608	0.549	0.525	0.456
Equilibrium	H_2	13.9	14.2	53.1	55.1	64.1	67.9	64.4
Ratios	N_2	3.30	4.46	5.83	6.27	6.41	6.43	6.21
	CH_4	1.02	1.03	0.452	0.448	0.445	0.440	0.408
K = y/x	C_2H_6	0.349	0.109	0.00771	0.00751	0.00662	0.00627	0.00541

binary system. As the temperature is raised to -200°F, the ternary system phase diagrams obtained in this work appear on three of the four faces of the quaternary phase diagram. At approximately -131°F the vapor pressure of pure methane is 500 psia, and the hydrogen-nitrogen-methane ternary system can exist only in the vapor phase at this temperature and higher temperatures. As the temperature is increased to -100°F at 500 psia, the hydrogen-methane-ethane and nitrogen-methane-ethane ternary phase diagrams appear as two faces of the quaternary phase diagram. As the temperature is increased at 500 psia from -100°F to -50°F, to 0°F, and finally to 63°F, the quantity of ethane in the vapor phase increases steadily. At approximately 63°F the vapor pressure of ethane is 500 psia, and the quaternary system can exist only in the vapor phase at temperatures greater than 63°F.

Figure 19 shows a similar evolution of the quaternary phase diagram at 1000 psia as the temperature is increased from -200°F to 84°F. At -200°F the ternary phase diagrams for the systems hydrogen-nitrogen-methane and hydrogen-methane-ethane appear on two faces of the quaternary phase diagram. From Figure 12 it can be estimated that a critical point exists in the nitrogen-ethane binary system at 1000 psia and approximately -198°F. Below this temperature the nitrogen-methane-ethane ternary system exists in only one fluid phase. At approximately -120°F and 1000 psia a critical point exists in the hydrogen-methane binary system, and the hydrogen-nitrogen-methane ternary system can exist only in the single phase region at temperatures above -120°F. At -100°F

the ternary phase diagrams for the systems hydrogen-methane-ethane and nitrogen-methane-ethane appear as two of the faces of the quaternary phase diagram. Both of these phase diagrams show ternary critical points. As the temperature is increased from -100°F to -50°F, to 0°F, and finally to 80°F, the amount of ethane in the vapor phase increases. At approximately 80°F and 1000 psia Figure 12 shows that a critical point exists in the nitrogen-ethane binary system. At this temperature and at all higher temperatures the nitrogen-methane-ethane system exists in only one fluid phase. Finally, at approximately 84°F, a critical point exists in the hydrogen-ethane binary system, and the quaternary system ceases to exist in two phases.

It may be noted in Figure 19 that a critical locus exists in the quaternary system at 1000 psia for all temperatures. This system pressure of 1000 psia is well above the critical pressure of all the constituents of the quaternary system.

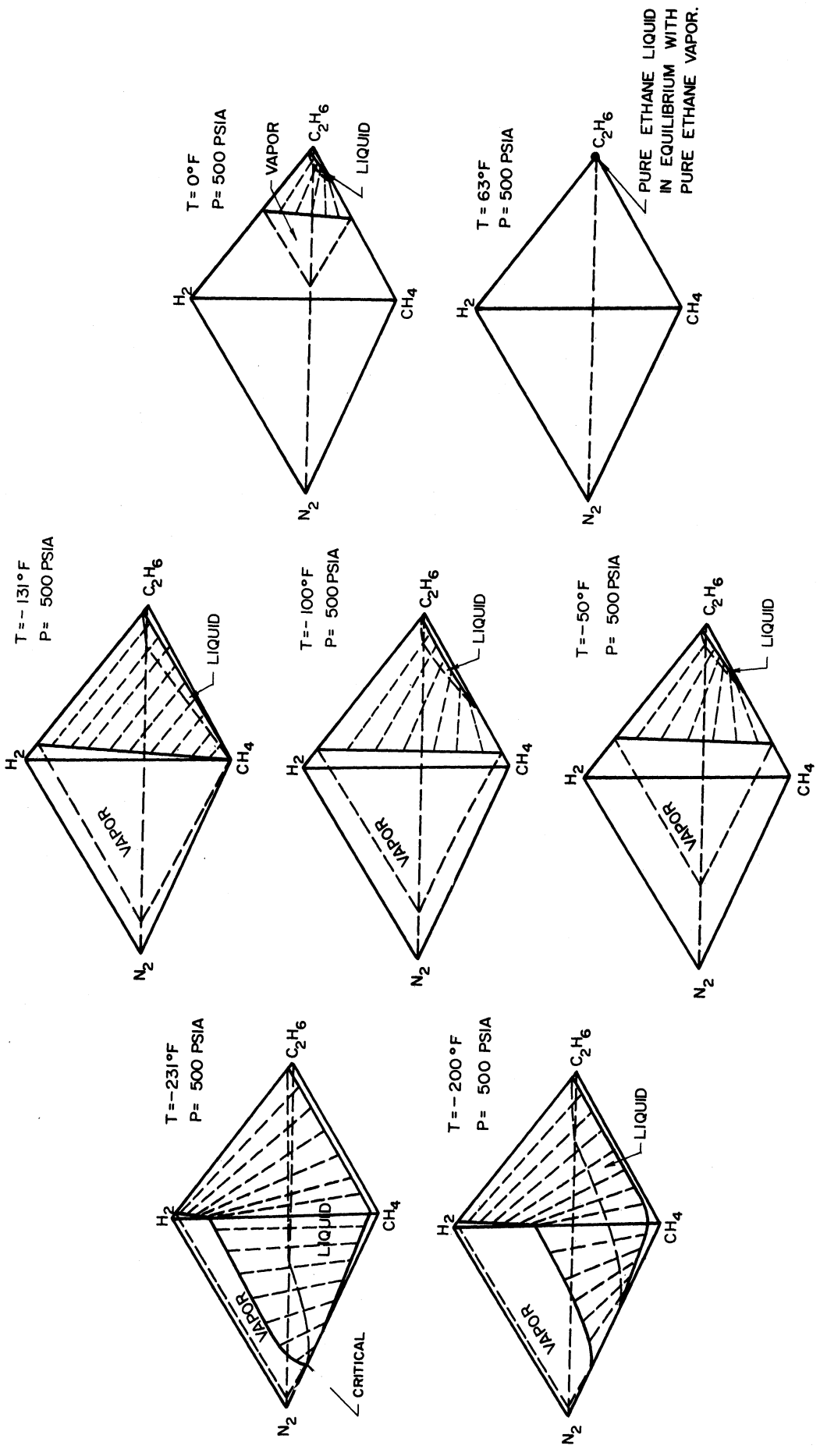

Figure 18. Qualitative Phase Diagrams for the Quaternary System Hydrogen-Nitrogen-Methane-Ethane at 500 psia and Various Temperatures

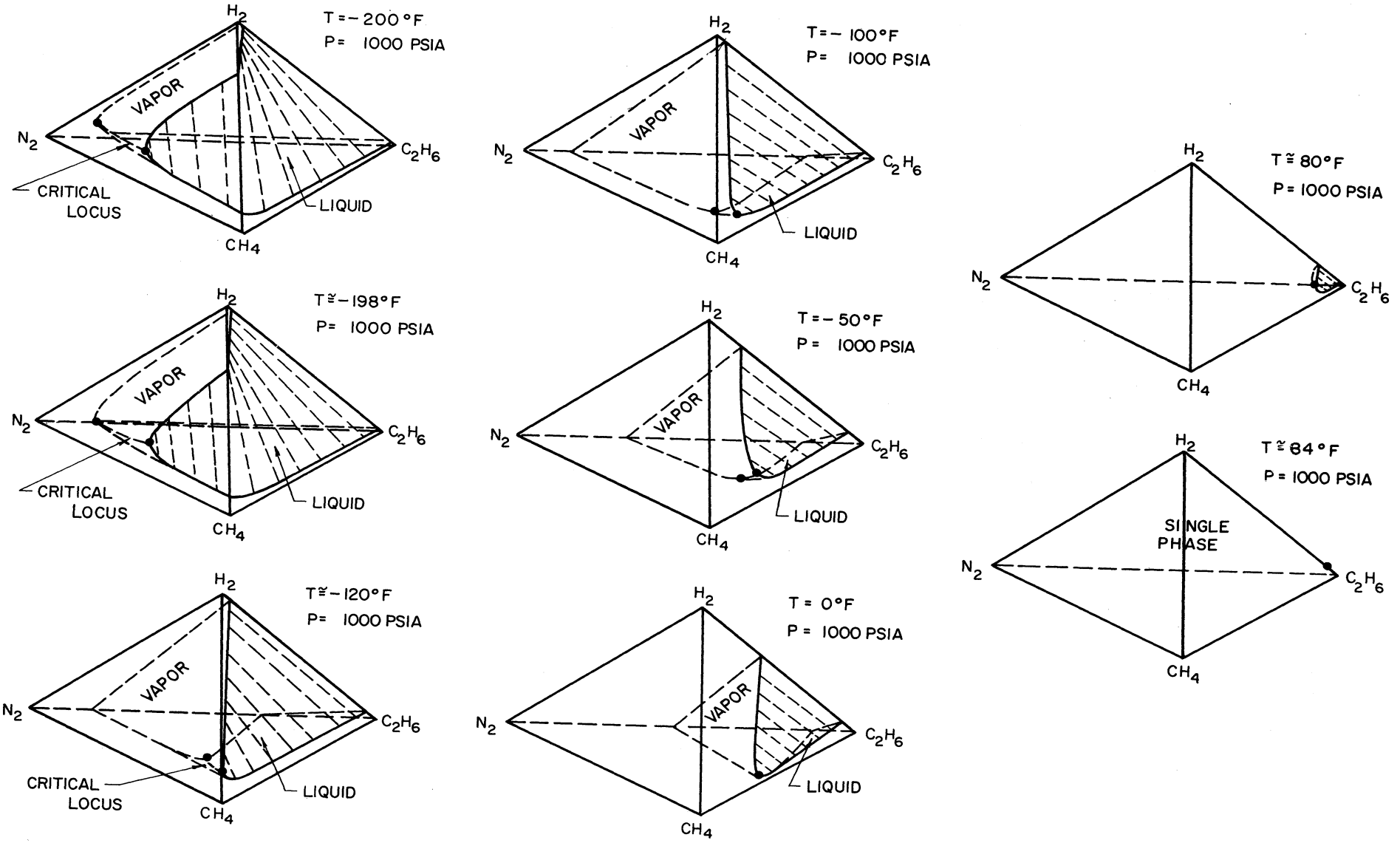

Figure 19. Qualitative Phase Diagrams for the Quaternary System Hydrogen-Nitrogen-Methane-Ethane at 1000 psia and Various Temperatures

ANALYSIS AND CORRELATION

The methods which have been employed by investigators for the correlation of vapor-liquid equilibrium data were reviewed in Appendix A to determine the most feasible approach to the problem of correlating data on systems containing hydrogen, nitrogen, and the light hydrocarbons.

Solubility theory has been used successfully in correlating the binary systems of hydrogen with the light hydrocarbons[13][78], however, little success has been achieved in correlating ternary systems. After reviewing the present state of knowledge in the field of solubility theory, it was decided that an approach to the correlation of ternary and quaternary systems by means of solubility theory was not warranted at this time.

Since the equilibrium ratios in all of the systems studied were found to be functions of composition, ideal solutions could not be assumed. Some means had to be found that would account for the non-ideality of the systems.

The activity coefficient approach to the problem of accounting for the deviations from ideal solutions has proven successful in the region below the critical temperatures of all or most of the components of the system. However, the methods proposed for relating the activity coefficients to the phase compositions for a ternary or quaternary system are very complex mathematically, so that the idea of using this type of

activity coefficient to express deviations from ideality was abandoned.

The use of convergence pressure as a correlating variable was also investigated. The major difficulty encountered in the use of convergence pressure as a variable lies in the estimation of the convergence pressure of the system at given conditions of temperature and pressure and for given phase compositions. At a constant temperature and pressure the convergence pressure of a non-ideal ternary or multicomponent system is a function of the phase compositions. The problem is therefore reduced to one of finding the relationship between phase compositions and convergence pressure. The problem has been changed from that of describing equilibrium ratios as functions of phase composition at constant temperature and pressure to one of describing convergence pressures as functions of phase composition at constant temperature and pressure. While the concept of convergence pressure appeared to offer a possible method for correlating the data, it was decided to investigate other methods for representing the equilibrium ratios as functions of phase compositions or derived concentration variables.

The use of the Benedict-Webb-Rubin equation of state for the correlation of phase behavior data was also investigated. Because of the complexity of the trial-and-error calculations involved in the use of such an equation of state, and because of the uncertainty involved in the specification of the mixture parameters in the equation of state, correlation of the vapor-liquid equilibrium data for systems containing hydrogen, nitrogen, and the light hydrocarbons by means of the Benedict-Webb-Rubin equation was thought to be impracticable. It was also thought

that, over a considerable range of compositions, the liquid phase densities would be outside of the region for which the Benedict-Webb-Rubin equation of state gives satisfactory results when applied to the liquid phase.

The kinetic theory of liquids was also investigated as a possible source of a generalized correlation for vapor-liquid equilibrium data. However, much more work will have to be done in this field before a suitable correlation can be obtained from kinetic theory alone.

It was decided that the use of derived concentration variables such as molal average boiling points of the phases and pseudocritical pressures and temperatures of the phases should be investigated. The equilibrium ratios obtained from the data collected in this work and from data available in the literature were used to determine whether a generalized correlation could be obtained using these derived concentration variables or pseudoreduced temperatures and pressures as the correlating variables. In the course of these investigations several methods other than the usual molal average method of combining the phase composition variables and the critical pressures and temperatures of the pure components were utilized as suggested by Joffe[37]. While the pseudocritical pressures and temperatures, which were calculated using methods of combining the variables other than the usual molal average method, varied slightly from the values of the molal average properties, the difference in their ability to correlate the equilibrium ratios appeared to be insignificant. Since the molal average properties are generally easier to calculate than the more complex average properties

suggested by Joffe, it appears that little advantage is to be gained by use of properties other than the molal average properties. While it was determined that the molal average properties of the system could be used to correlate vapor-liquid equilibrium data for a specific ternary or quaternary system, a generalized correlation for multicomponent systems containing hydrogen, nitrogen, and the light hydrocarbons could not be disclosed using these variables.

Attempts were made to determine a generalized relationship between the equilibrium ratios for the light, intermediate, and heavy components. Figure 20 shows the equilibrium ratios for the light component (hydrogen) in the hydrogen-methane-ethane ternary system as a function of the equilibrium ratios for the heavy component (ethane). Figure 21 gives the equilibrium ratios for the intermediate component (methane) in the hydrogen-methane-ethane ternary system as a function of the product of the equilibrium ratios for the light and heavy components (hydrogen and ethane). Several attempts were made to obtain a generalized relationship for the equilibrium ratio for one of the components of a ternary system as a function of pressure, temperature, and the equilibrium ratios of the other two components. However, no reliable, generalized correlation was developed using these correlating variables.

It was decided that an attempt should be made to correlate the ternary and quaternary systems by a graphical trial-and-error method employing the phase compositions as correlating variables rather than the derived concentration variables. There appeared to be no particular advantage to be gained from the use of the derived concentration variables, and the use of phase compositions (mole percentages of the constituents in either the liquid or vapor phase) simplified the task of adapting the binary

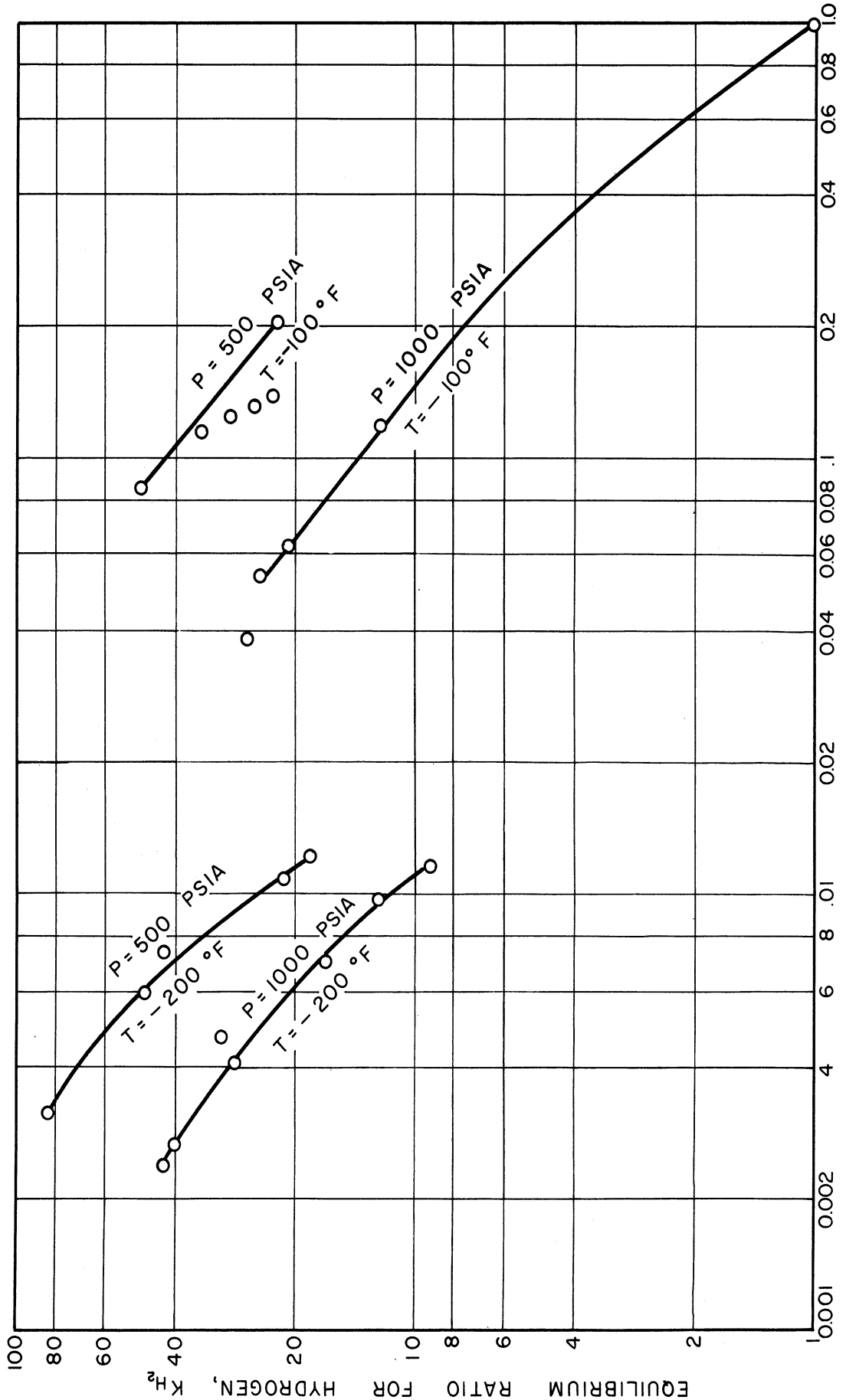

Figure 20. Equilibrium Ratios for Hydrogen in the Hydrogen-Methane-Ethane System as a Function of the Equilibrium Ratios for Ethane

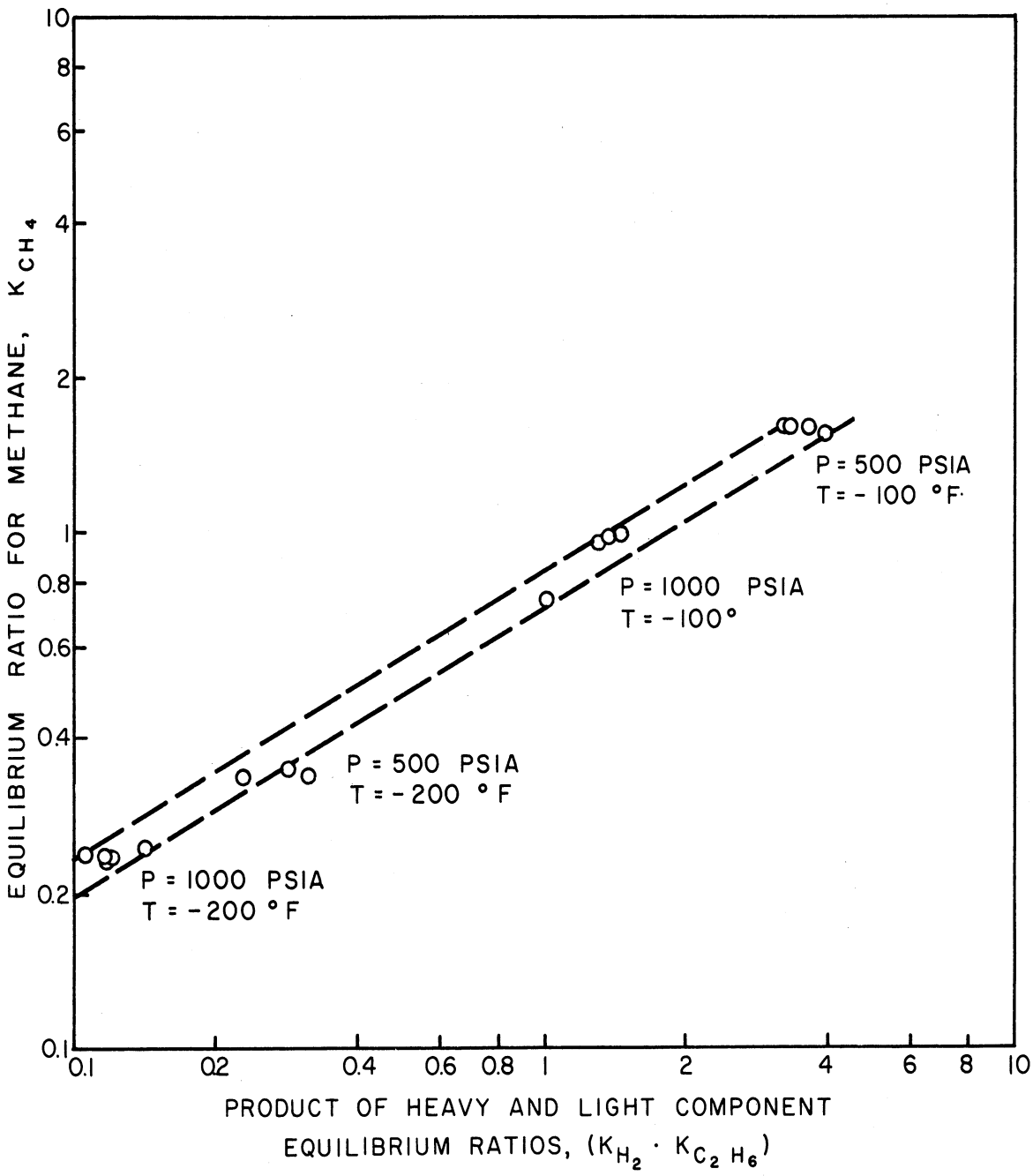

Figure 21. Equilibrium Ratios for Methane in the Hydrogen-Methane-Ethane System as a Function of the Product of the Equilibrium Ratios for Hydrogen and Ethane

and ternary system data available in the literature for use in the correlations. Most of the data available in the literature are represented in terms of the equilibrium liquid and vapor phase compositions rather than in terms of molal average boiling points or pseudocritical properties of the equilibrium phases. These phase compositions could then be used directly as listed in the literature without conversion to the corresponding derived concentration variables for the equilibrium phases.

The methods used in correlating the ternary and quaternary systems studied in the course of this investigation will now be discussed and the binary and ternary system data obtained from the literature for use in these correlations will be noted.

Hydrogen-Methane-Ethane System

Data for the hydrogen-methane-ethane ternary system are available in the literature from the work of Levitskaya[44] at pressures of 441, 588, and 1176 psia (30, 40, and 80 atm) and temperatures of -121, -139, -157, and -175°F. However, these data have been found to be internally inconsistent, and, as a result, proved to be of value in the correlation of the hydrogen-methane-ethane ternary system mainly as an order-of-magnitude approximation at temperatures between -100 and -200°F.

While data on the binary system methane-ethane are available in the literature from the earlier work of Ruhemann[62], the data for this system which were employed in this correlation were obtained from the later work of Bloomer and co-workers[16].

Vapor-liquid equilibrium data for the binary system hydrogen-methane were obtained from the works of Benham and Katz[14] and Freeth and Verschoyle[29], while the data for the hydrogen-ethane binary system were obtained from the work of Williams and Katz[79].

Using the binary and ternary system data mentioned above and the data obtained in this investigation, equilibrium ratios for the constituents in the hydrogen-methane-ethane system were plotted at constant pressures of 500 and 1000 psia as functions of temperature with parameters of mole percent methane in the liquid phase (Figures 29 and 31). The general shapes of the equilibrium ratio curves for the three binary systems, together with the ternary system data from this work and the known mole percentages of methane in the liquid phase of the methane-ethane binary system, permitted the construction of the lines of constant mole percentage methane on these two plots (Figures 29 and 31). The equilibrium ratios were then plotted as a function of temperature in a similar manner for a constant pressure of 250 psia. The equilibrium ratios in the three binary systems again form the boundary curves on this diagram (Figure 28). The variations in the equilibrium ratios with composition at 250 psia are small enough so that, as a first approximation, the lines of constant mole percentage methane in the liquid phase were estimated from the general shapes of the equilibrium ratio curves for the three binary systems and the known mole percentages of methane in the liquid phase of the methane-ethane binary system. Then the equilibrium ratios in the ternary system were plotted at various constant mole percentages of methane in the liquid phase as a function of pressure with parameters

of temperature. The temperature parameters chosen for these plots were -100, -125, -150, -175, and -200°F. Figure 22 shows this type of plot for zero mole percentage methane in the liquid phase. Figure 22 gives the equilibrium ratios for hydrogen and ethane in the hydrogen-ethane binary system with the equilibrium ratios for methane being extrapolated to zero mole percent methane from the values determined in the ternary system at low percentages of methane. Figures 23, 24, 25, and 26 show these plots for 20, 40, 60, and 80 mole percent methane in the liquid phase respectively. Figure 27 gives the equilibrium ratios for hydrogen and methane in the hydrogen-methane binary system together with the equilibrium ratios for ethane which were extrapolated from their values in the ternary system at low percentages of ethane in the liquid phase. Therefore, Figure 27 shows the equilibrium ratios for the constituents in the ternary system at approximately zero mole percent ethane in the liquid phase.

The values of the equilibrium ratios at constant pressures of 250, 500, and 1000 psia for various mole percentages of methane in the liquid phase were sufficient to allow construction of the plots of Figure 22 through Figure 27 from 100 psia to approximately 1500 psia. A trial-and-error procedure was then used to obtain smooth, symmetrical curves consistent with the available data for Figures 22 through 27 and Figures 28, 29, and 31.

After completion of this trial-and-error smoothing process the equilibrium ratios for the constituents in the ternary system at 750 psia and 1500 psia were plotted as a function of temperature with parameters

of mole percent methane in the liquid phase (Figures 30 and 32). The data for the three binary systems were again used to determine the boundary curves and as a guide to the general shape of the lines of constant mole percent methane in the liquid phase. Figures 22 through 27 were then used, as a first approximation, to obtain the lines of constant mole percent methane in the liquid phase for Figures 30 and 32. A trial-and-error procedure was again used until symmetrical curves consistent with all available binary and ternary system data were obtained for Figures 22 through 27 and Figures 28 through 32.

After completion of this second trial-and-error smoothing process the curves of Figure 22 through Figure 27 were extrapolated to their estimated convergence pressures and the curves of Figure 28 through Figure 32 were completed and checked for consistency with the curves of Figure 22 through Figure 27. The general procedure for estimating the convergence pressures in the ternary system was to extrapolate the equilibrium ratio curves for the lightest component (hydrogen) as approximately straight lines to a value of almost unity. A general symmetry was then assumed in bringing the equilibrium ratio curves to their convergence pressures for various temperatures and for varying amounts of methane in the liquid phase. The convergence pressures for the ternary system all occur at pressures between the high convergence pressures found in the hydrogen-ethane binary system and the low convergence pressures found in the hydrogen-methane binary system.

Having established the equilibrium ratios for the ternary system over the desired temperature and pressure range, Figures 22 through 32 may

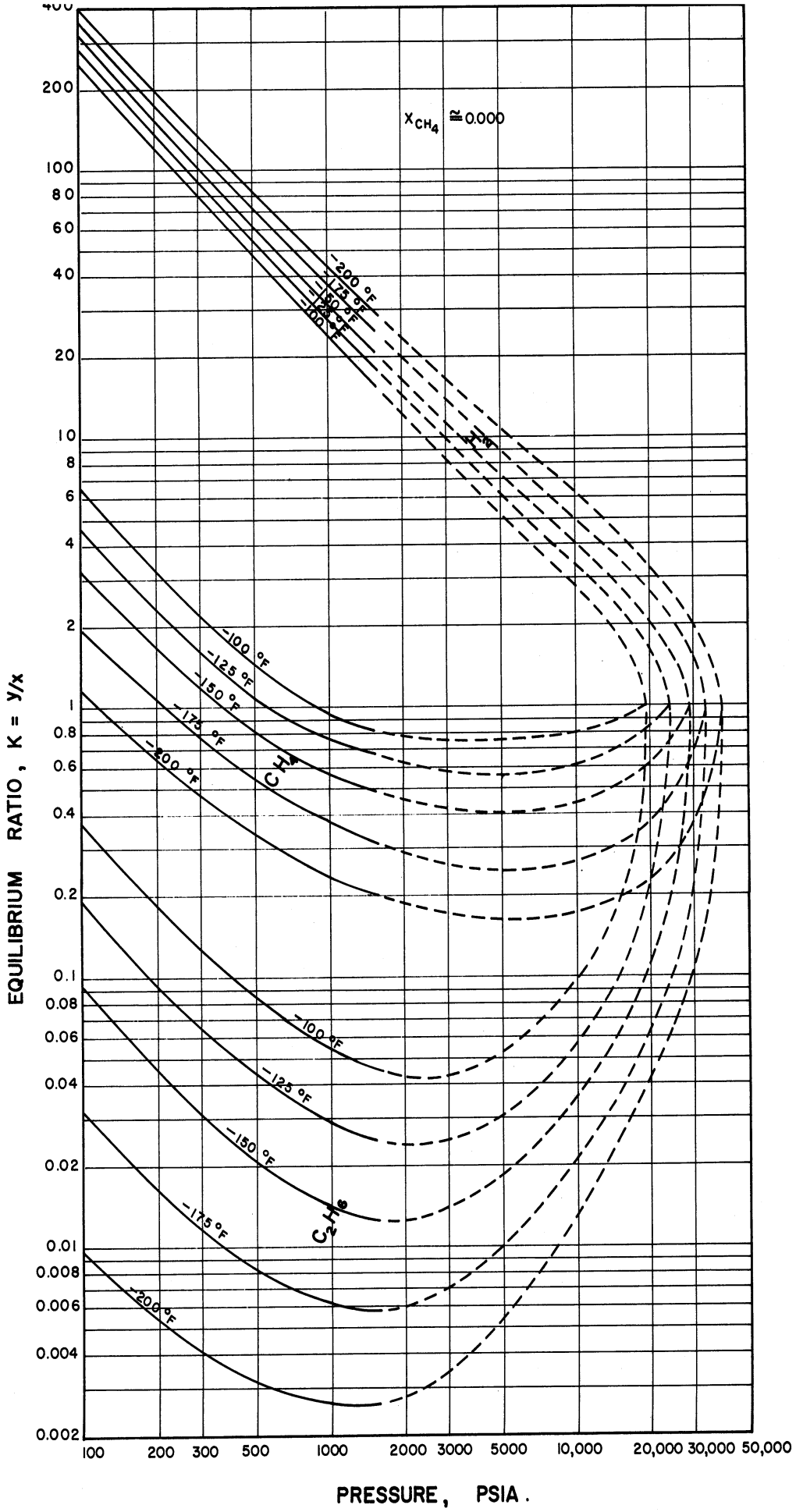

Figure 22. Equilibrium Ratios for Constituents in the Hydrogen-Methane-Ethane System at 0 Mole Percent Methane in the Liquid Phase as a Function of Pressure for Various Temperatures

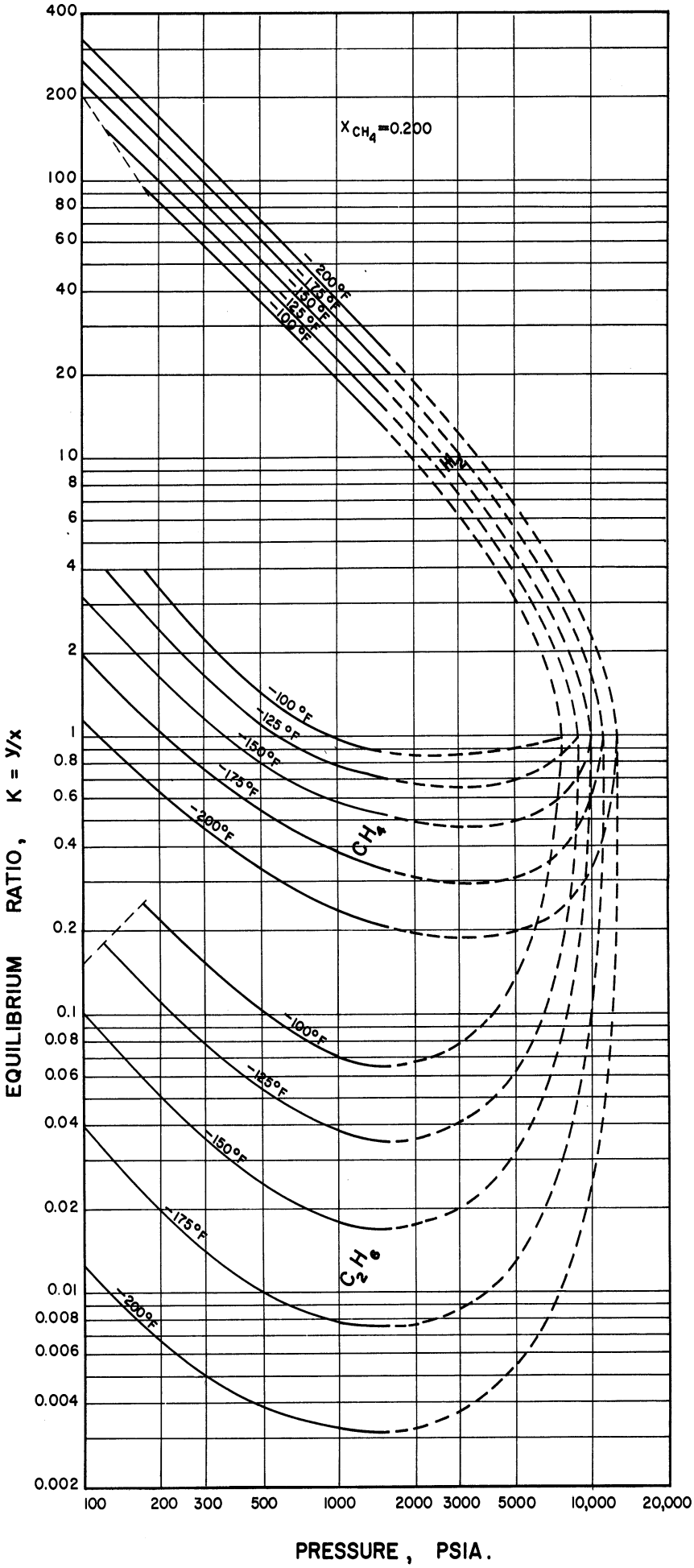

Figure 23. Equilibrium Ratios for Constituents in the Hydrogen-Methane-Ethane System at 20 Mole Percent Methane in the Liquid Phase as a Function of Pressure for Various Temperatures

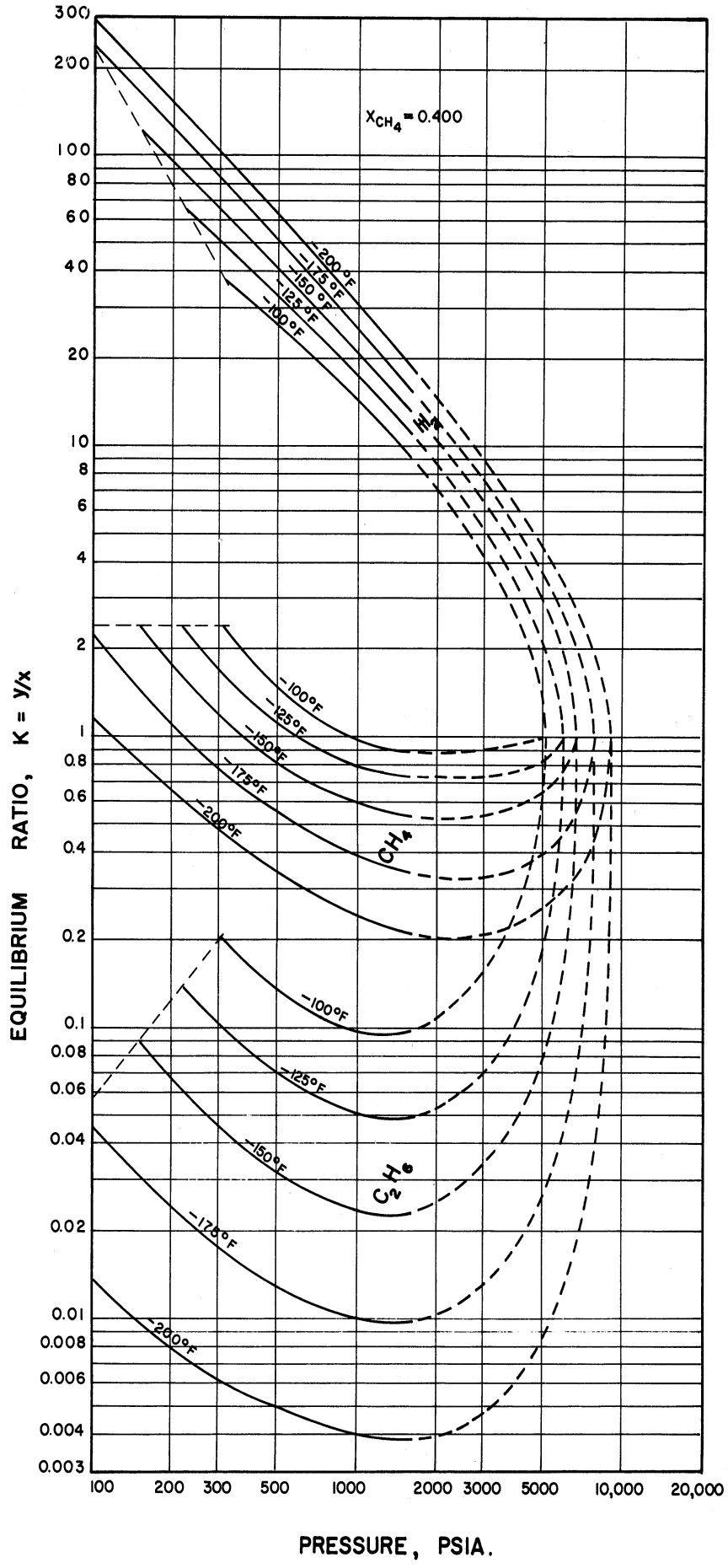

Figure 24. Equilibrium Ratios for Constituents in the Hydrogen-Methane-Ethane System at 40 Mole Percent Methane in the Liquid Phase as a Function of Pressure for Various Temperatures

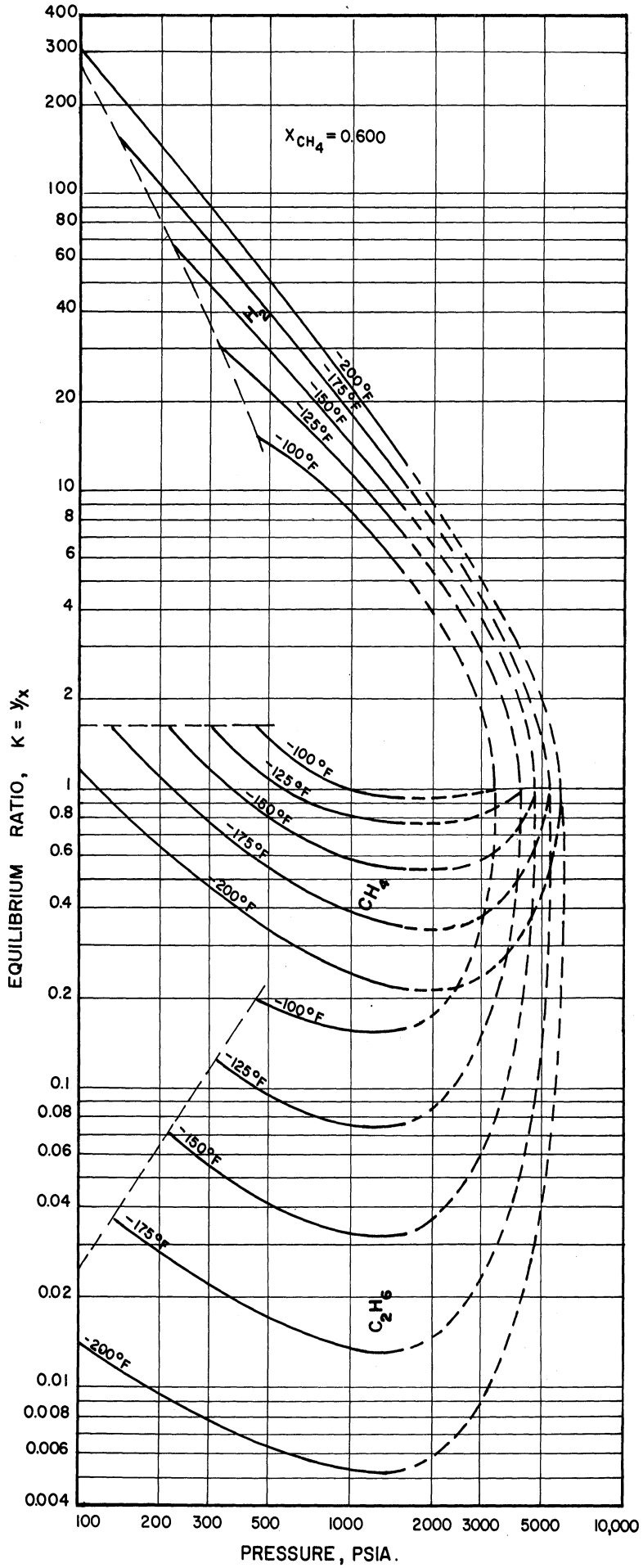

Figure 25. Equilibrium Ratios for Constituents in the Hydrogen-Methane-Ethane System at 60 Mole Percent Methane in the Liquid Phase as a Functionof Pressure for Various Temperatures

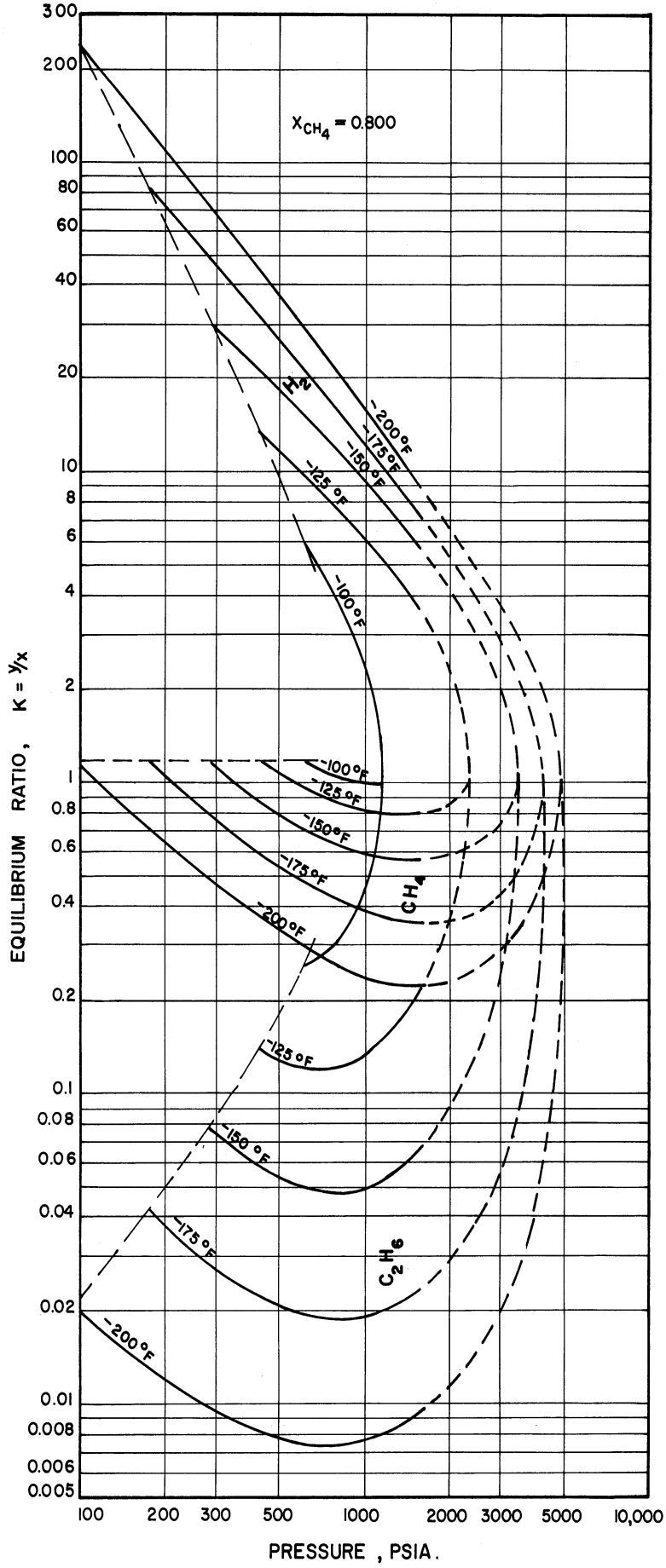

Figure 26. Equilibrium Ratios for Constituents in the Hydrogen-Methane-Ethane System at 80 Mole Percent Methane in the Liquid Phase as a Function of Pressure for Various Temperatures

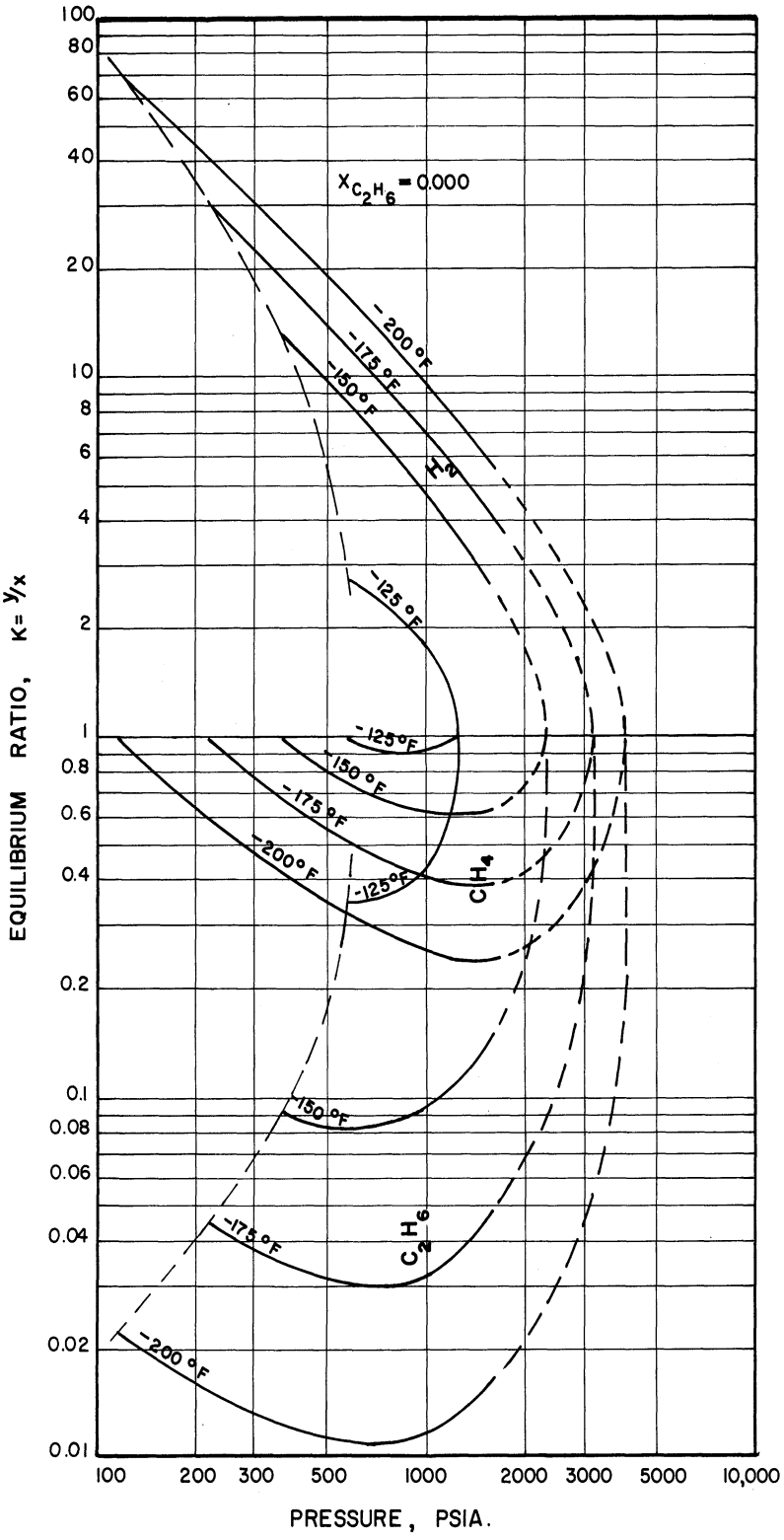

Figure 27. Equiibrium Ratios for Constituents in the Hydrogen-Methane-Ethane System at 0 Mole Percent Ethane in the Liquid Phase as a Function of Pressure for Various Temperatures

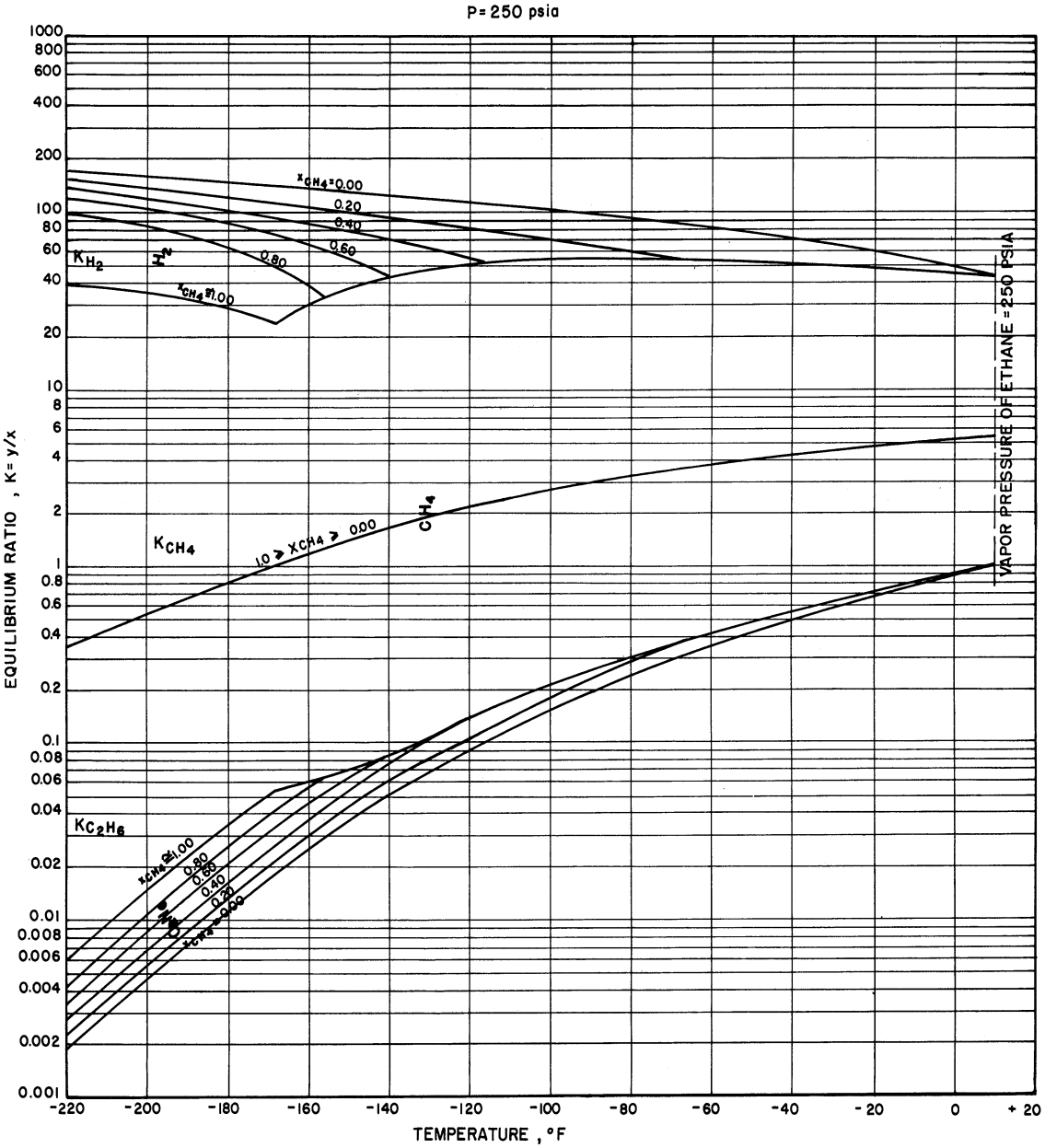

Figure 28. Equilibrium Ratios for Constituents in the Hydrogen-Methane-Ethane System at 250 psia as a Function of Temperature with Varying Amounts of Methane in the Liquid Phase

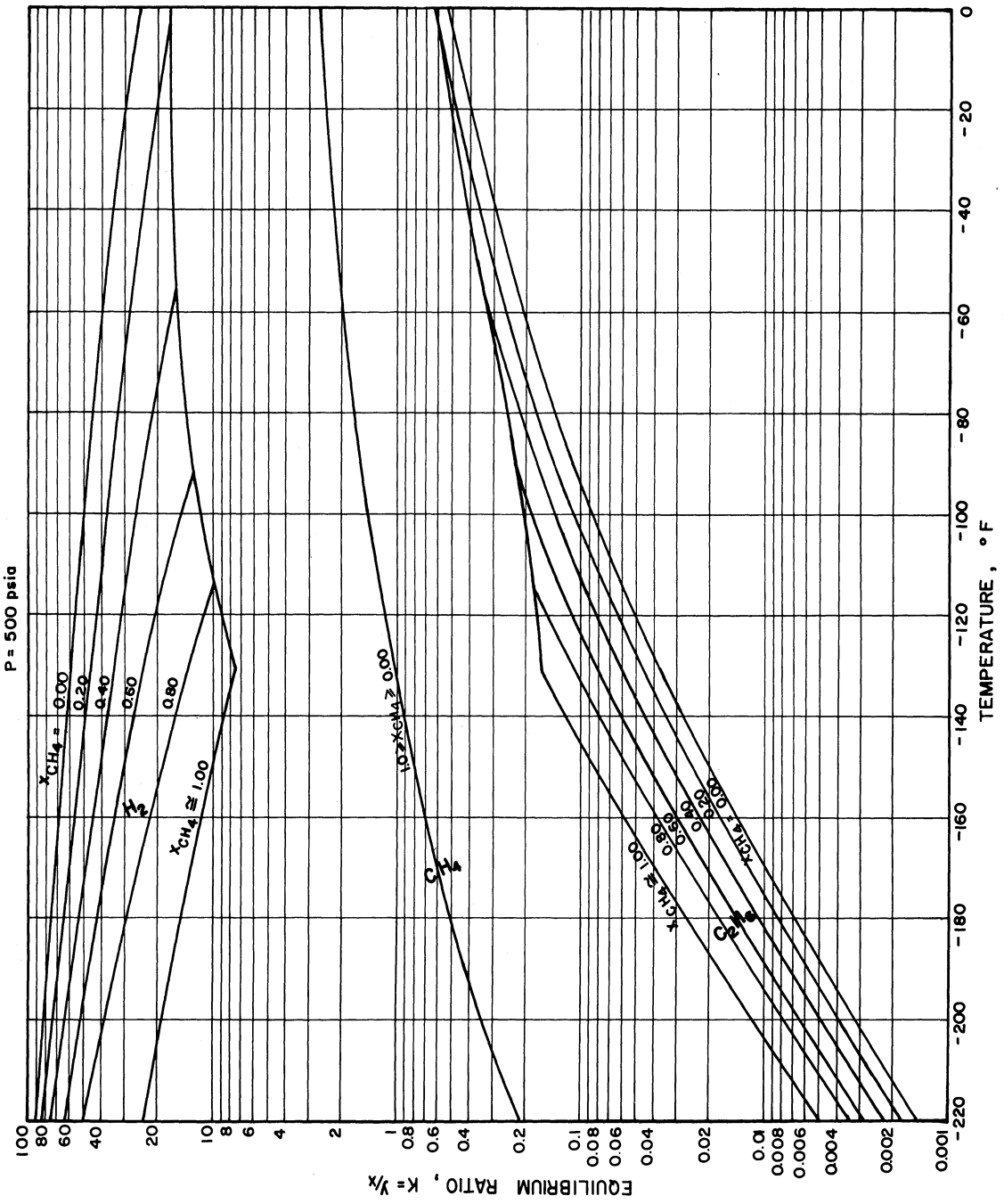

Figure 29. Equilibrium Ratios forConstituents in the Hydrogen-Methane-Ethane System at 500 psia as a Function of Temperature with Varying Amounts of Methane in the Liquid Phase

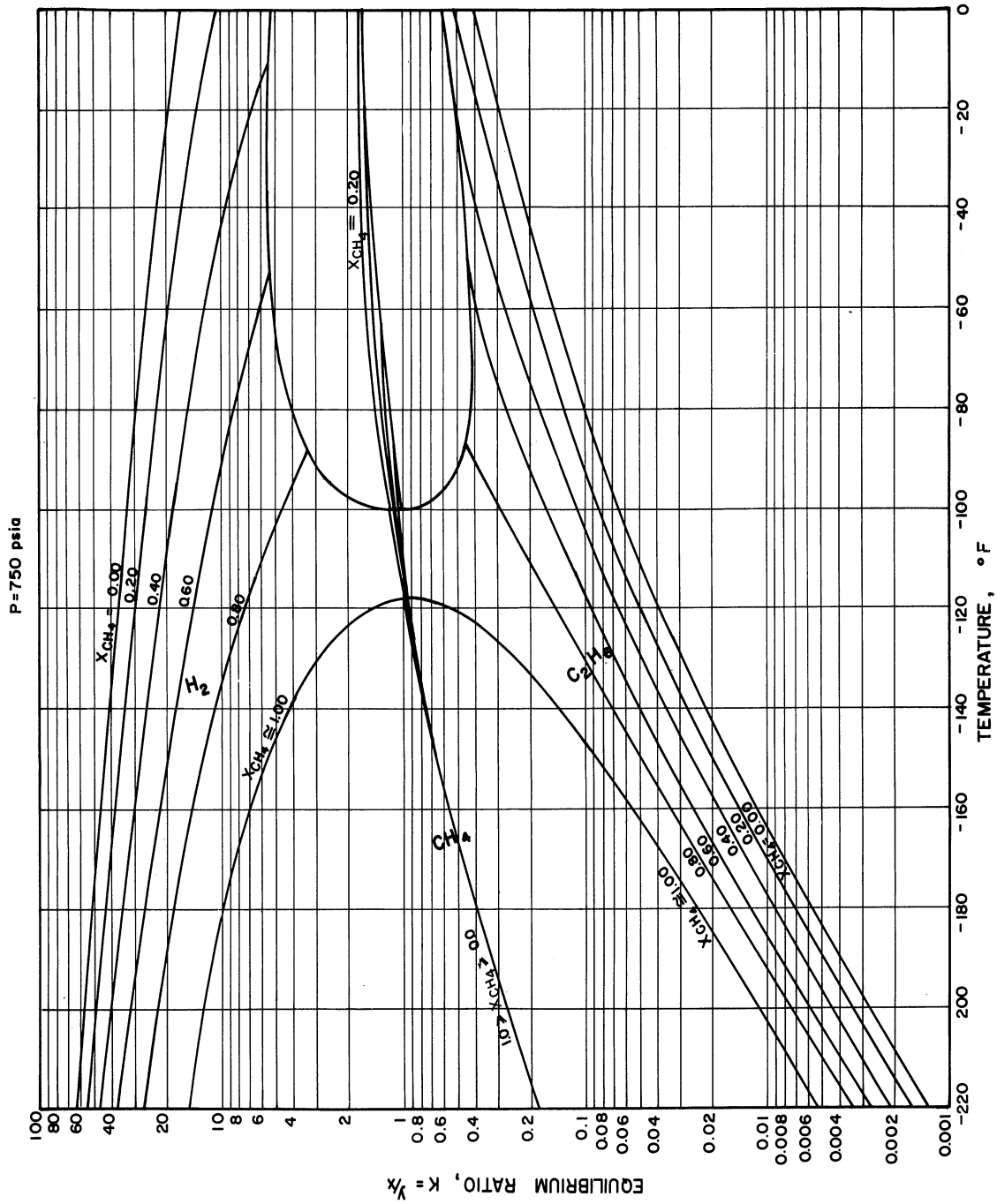

Figure 30. Equilibrium Ratios for Constituents in the Hydrogen-Methane-Ethane System at 750 psia as a Function of Temperature with Varying Amounts of Methane in the Liquid Phase

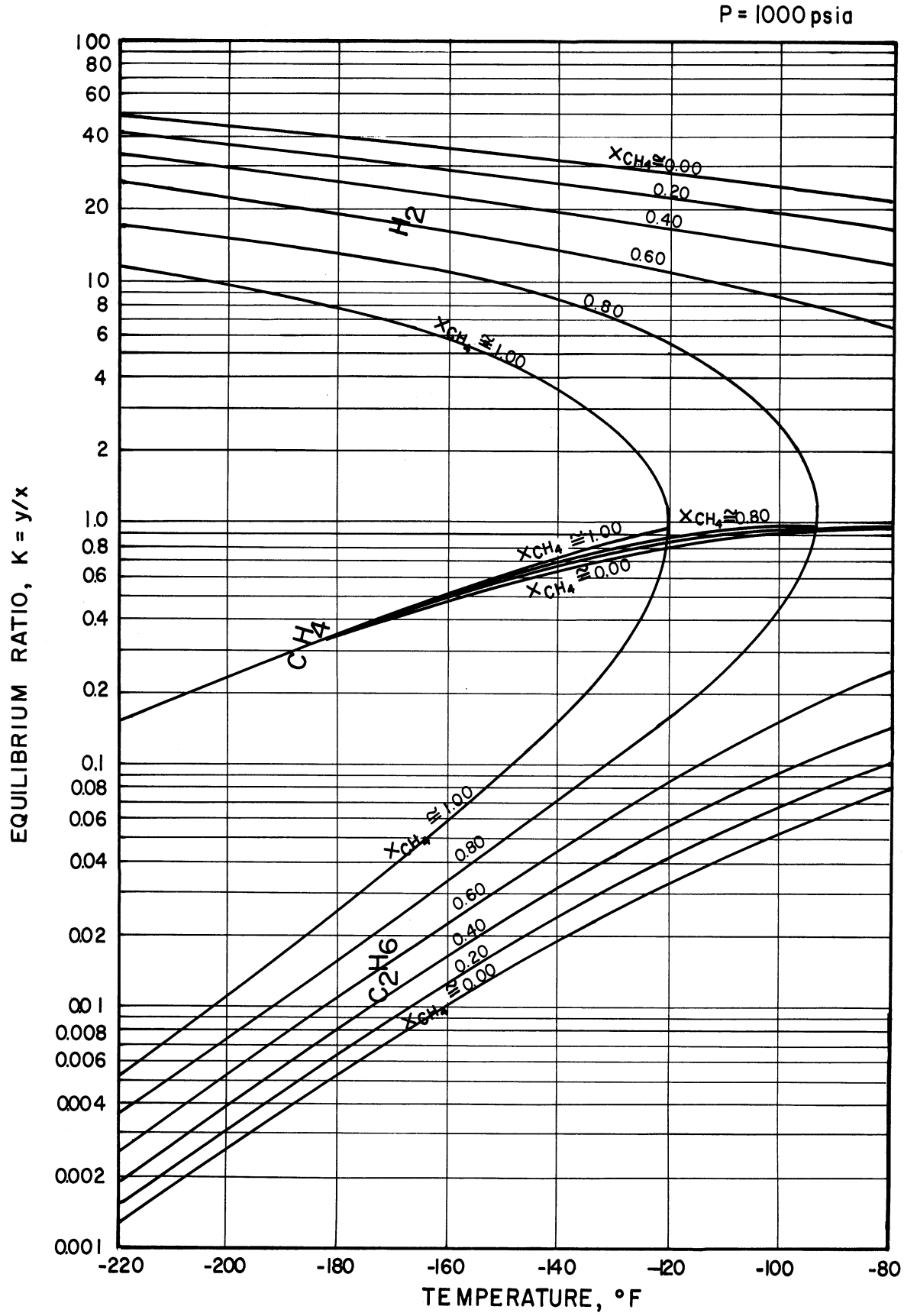

Figure 31. Equilibrium Ratios for Constituents in the Hydrogen-Methane-Ethane System at 1000 psia as a Function of Temperature with Varying Amounts of Methane in the Liquid Phase

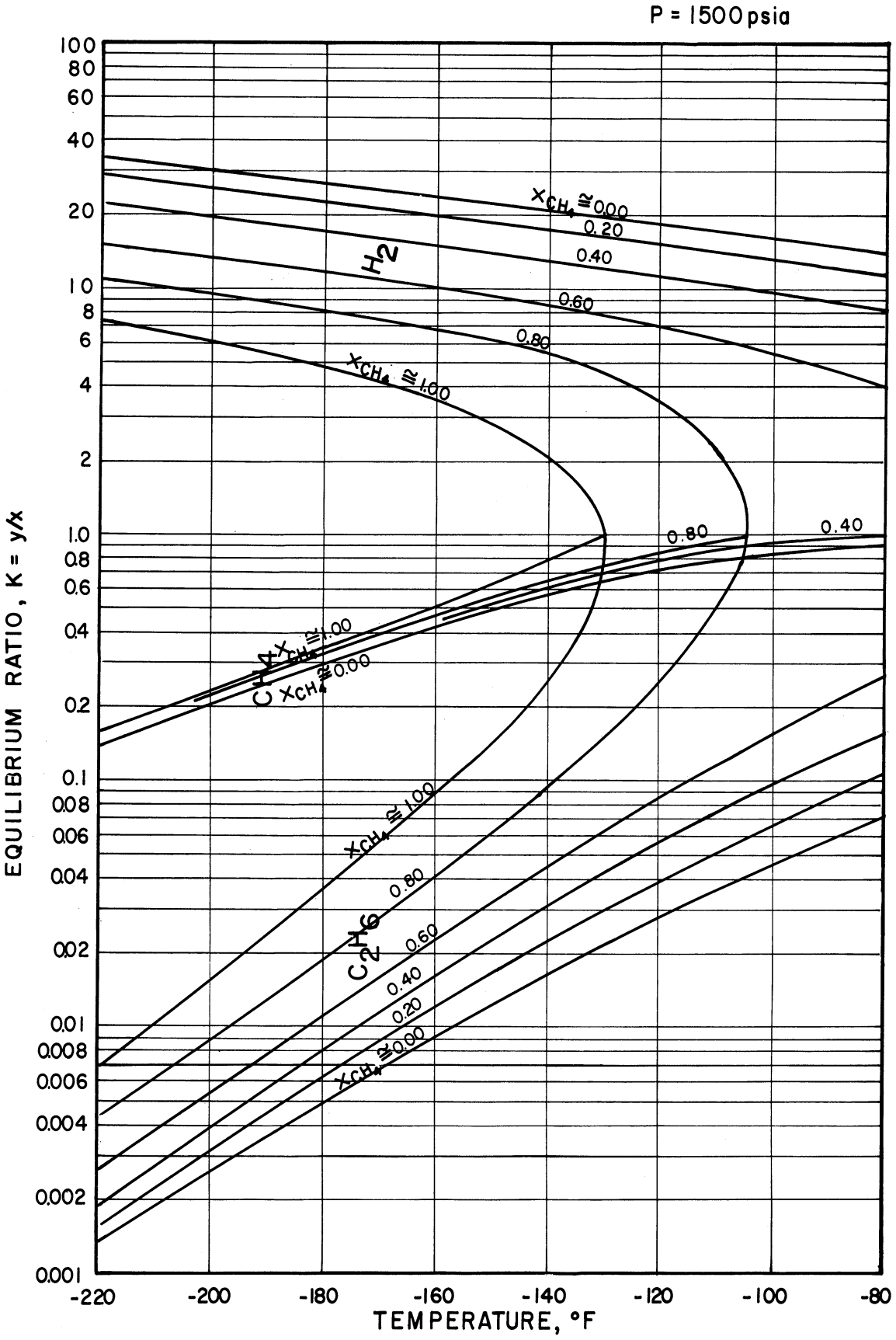

Figure 32. Equilibrium Ratios for Constituents in the Hydrogen-Methane-Ethane System at 1500 psia as a Function of Temperature with Varying Amounts of Methane in the Liquid Phase

be used to determine the equilibrium ratios at intermediate temperatures, pressures, and mole percentages of methane in the liquid phase. However, it is recommended that the values obtained from these plots be used with caution at pressures above 1500 - 2000 psia since the estimated convergence pressures may be in error by several hundred psi and the equilibrium ratios (particularly those of ethane) vary extremely rapidly with variations in pressure near the convergence pressures.

Hydrogen-Nitrogen-Methane System

Data for the hydrogen-nitrogen-methane ternary system are available in the literature from the work of Steckel and Zinn[68] at temperatures of -266°F and -298°F and pressures ranging from 150 to 1500 psia. However, the equilibrium ratios calculated from these ternary system phase composition data show considerable scatter, and the data were of use mainly as a first approximation in the construction of the plots of equilibrium ratios at constant liquid phase methane composition as a function of pressure with temperature parameters.

The nitrogen-methane binary system data used in this correlation were obtained from the work of Bloomer and Parent[17]. These were thought to be the best data available for the nitrogen-methane binary system.

As before, the vapor-liquid equilibrium data for the hydrogen-methane binary system were obtained from the investigations of Benham and Katz[14] and Freeth and Verschoyle[29].

Equilibrium phase composition data are available for the hydrogen-nitrogen binary system from the works of many investigators. The equilibrium ratios of hydrogen and nitrogen in the hydrogen-nitrogen binary

system are shown in Figure 33 as a function of pressure for several temperatures. The data of Verschoyle[77] cover a pressure range from 200 psia to approximately 3000 psia for temperatures of -346, -337, -319, and -301°F. The data of Gonikberg, Fastowsky, and Gurwitsch[32] cover a pressure range from 150 psia to approximately 1500 psia at temperatures of -301, -298, -266, and -256°F. Vapor-liquid equilibrium data for this binary system from the work of Steckel and Zinn[68] include a pressure range from 200 psia to approximately 2500 psia at temperatures of -317, -305, -288, and -264°F. The data of Ruhemann and Zinn[63] include a pressure range from 175 psia to approximately 750 psia at temperatures of -319, -310, and -298°F. These four sets of binary system data were used as a basis for the construction of the equilibrium ratio curves of Figure 33. Interpolation was then employed to yield values at the temperatures desired for use in the correlation of the ternary system hydrogen-nitrogen-methane.

Using the binary and ternary system data mentioned above and the data obtained in this investigation, the equilibrium ratios for the constituents in the hydrogen-nitrogen-methane ternary system were correlated as functions of temperature, pressure, and mole percent methane in the liquid phase. The general method of correlation is the same as the method outlined previously for the correlation of the hydrogen-methane-ethane ternary system. The equilibrium ratios for the constituents in the hydrogen-nitrogen-methane ternary system were plotted at constant pressures of 250, 500, and 1000 psia as functions of temperature with parameters of mole percent methane in the liquid phase (Figures 41, 42, and 44). The general

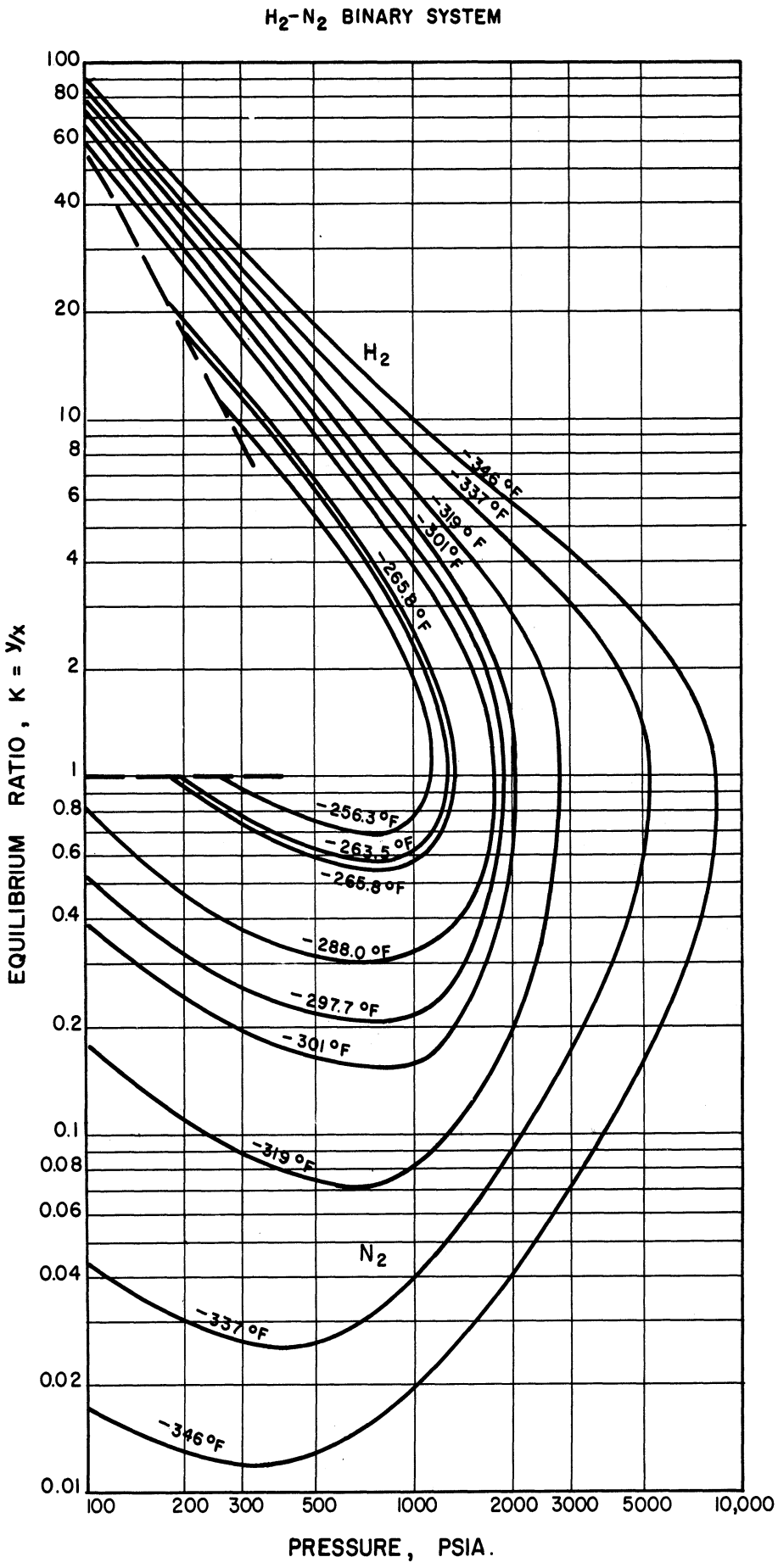

Figure 33. Equilibrium Ratios for Hydrogen and Nitrogen in the Hydrogen-Nitrogen Binary System as a Function of Pressure for Various Temperatures

shapes of the equilibrium ratio curves for the three binary systems were again used, together with the ternary system data from this work and the known mole percentages of methane in the liquid phase of the nitrogen-methane binary system, to construct the lines of constant mole percentage methane in the liquid phase on these plots.

The equilibrium ratios for the ternary system were then plotted at various constant mole percentages of methane in the liquid phase as a function of pressure with parameters of temperature. Figure 34 shows this type of plot for the hydrogen-nitrogen-methane system with zero mole percent methane in the liquid phase. Figure 34 gives the equilibrium ratios for hydrogen and nitrogen in the hydrogen-nitrogen binary system and the equilibrium ratios for methane extrapolated to zero mole percent methane from values determined in the ternary system at low percentages of methane. Therefore, Figure 34 shows the equilibrium ratios for methane when a very small amount of methane is added to a binary system containing hydrogen and nitrogen.

Figures 35, 36, 37, and 38 show the equilibrium ratios for the constituents of the hydrogen-nitrogen-methane ternary system at 20, 40, 60, and 80 mole percent methane in the liquid phase as functions of pressure with temperature parameters. Figure 39 gives the equilibrium ratios for hydrogen and methane in the hydrogen-methane binary system and the equilibrium ratios for nitrogen extrapolated to zero mole percent nitrogen from values in the ternary system at low percentages of nitrogen. Figure 39 shows the equilibrium ratios for nitrogen which may be expected when a small amount of nitrogen is added to a binary system containing hydrogen and methane.

The values of the equilibrium ratios at constant pressures of 250, 500, and 1000 psia for various mole percentages of methane in the liquid phase were sufficient to allow construction of the plots of Figure 34 through Figure 39 from 100 psia to approximately 1500 psia. A trial-and-error procedure was again employed to obtain symmetrical curves consistent with the available data for Figures 34 through 39 and Figures 41, 42, and 44. The ternary system data of Steckel and Zinn [68] were used to obtain a good first approximation in drawing the curves of Figures 34 through 39.

At the completion of this first trial-and-error smoothing process the equilibrium ratios for the constituents in the ternary system at 100, 700, and 1500 psia were plotted as a function of temperature with parameters of mole percent methane in the liquid phase (Figures 40, 43, and 45). Figures 34 through 39 were used, as a first approximation, to obtain the lines of constant mole percent methane in the liquid phase, and the data for the three binary systems were used to determine the boundary curves. A second trial-and-error procedure was then employed until symmetrical curves consistent with all available binary and ternary system data were obtained for Figures 34 through 39 and Figures 40 through 45.

After completion of the second trial-and-error procedure, the curves of Figure 34 through Figure 39 were extrapolated to their estimated convergence pressures. Figures 40 through 45 were then checked for consistency with Figures 34 through 39.

Once the equilibrium ratios for the hydrogen-nitrogen-methane ternary system have been thus established, Figures 34

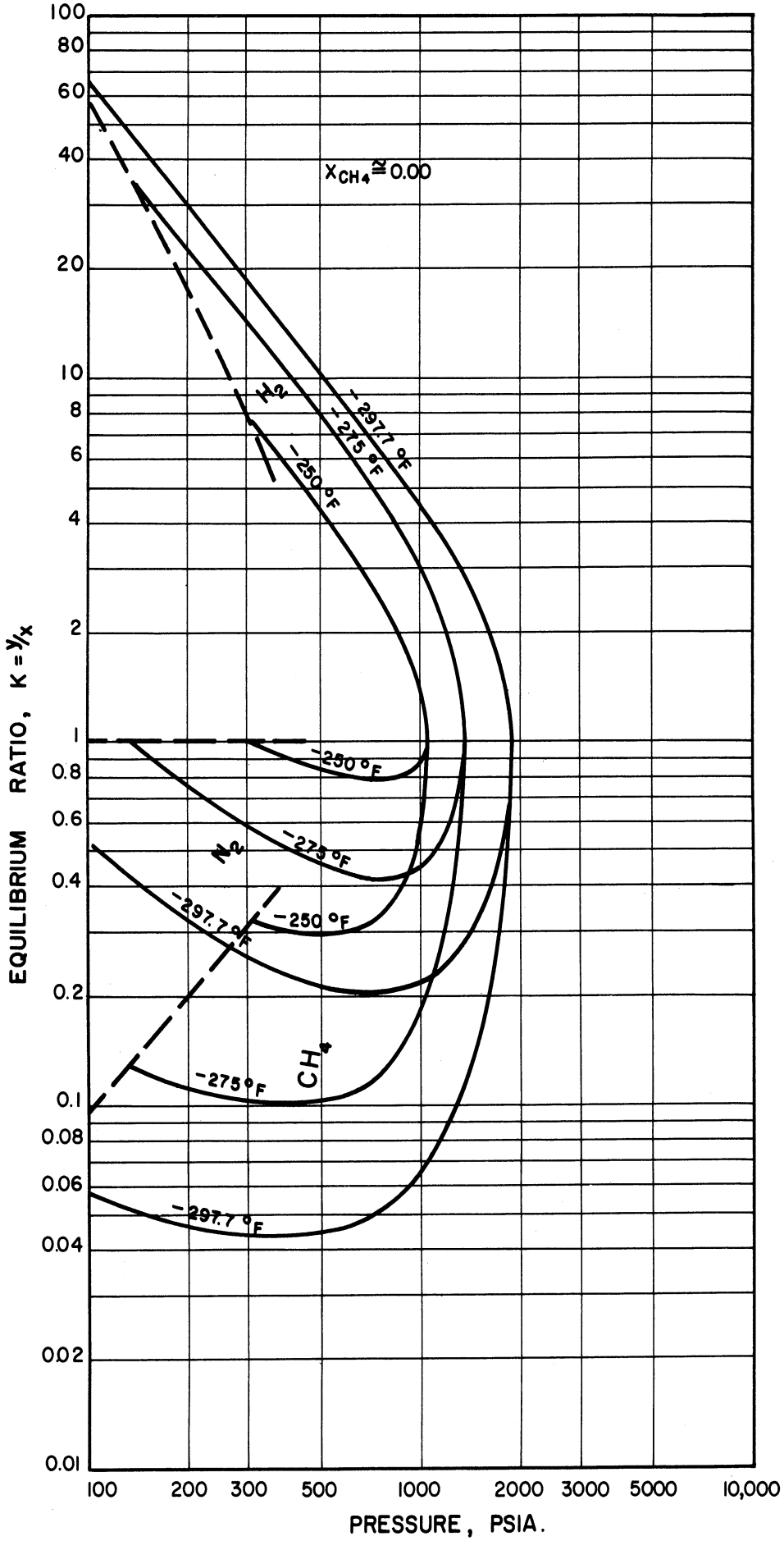

Figure 34. Equilibrium Ratios for Constituents in the Hydrogen-Nitrogen-Methane System at 0 Mole Percent Methane in the Liquid Phase as a Function of Pressure for Various Temperatures

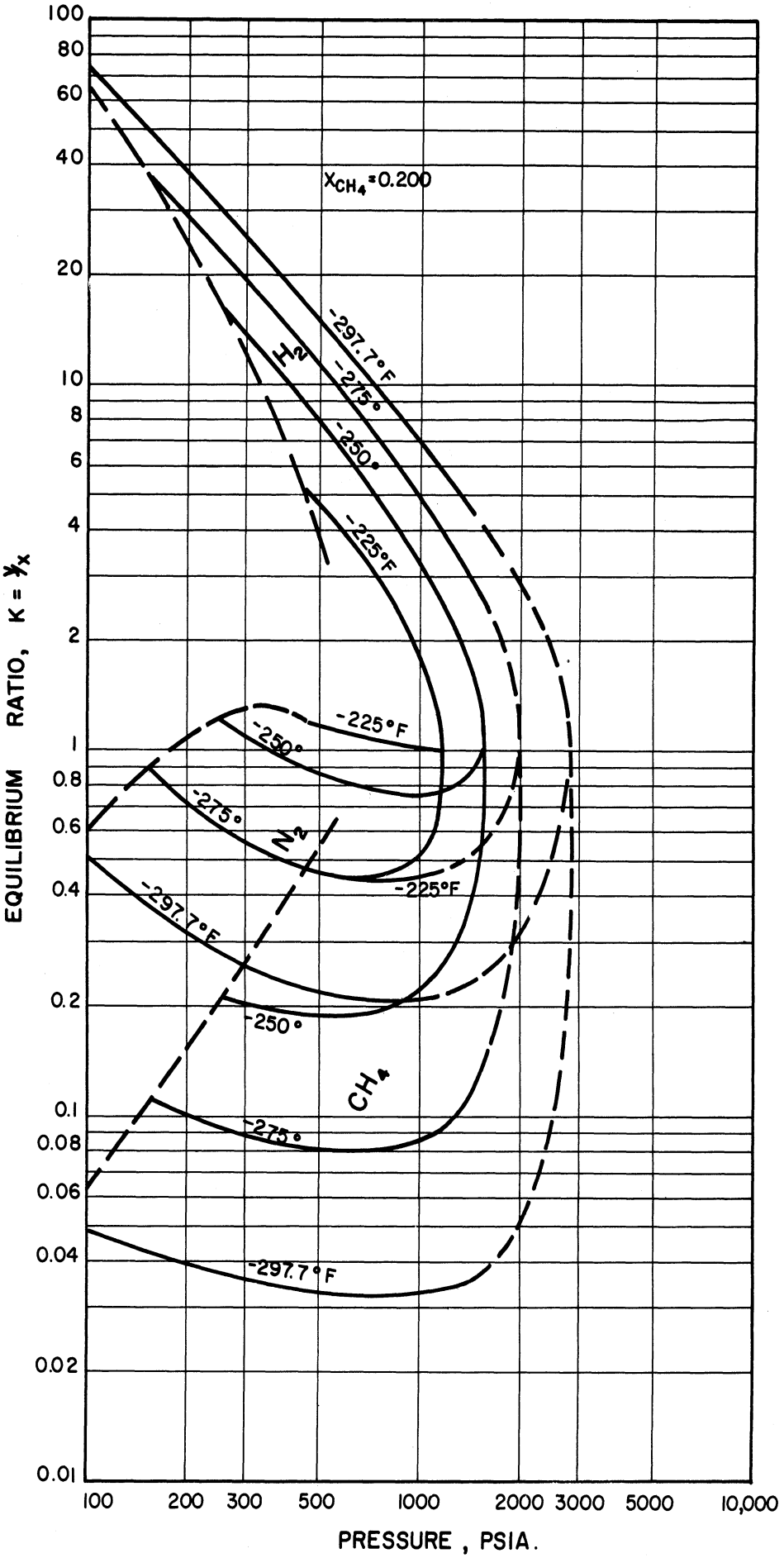

Figure 35. Equilibrium Ratios for Constituents in the Hydrogen-Nitrogen-Methane System at 20 Mole Percent Methane in the Liquid Phase as a Function of Pressure for Various Temperatures

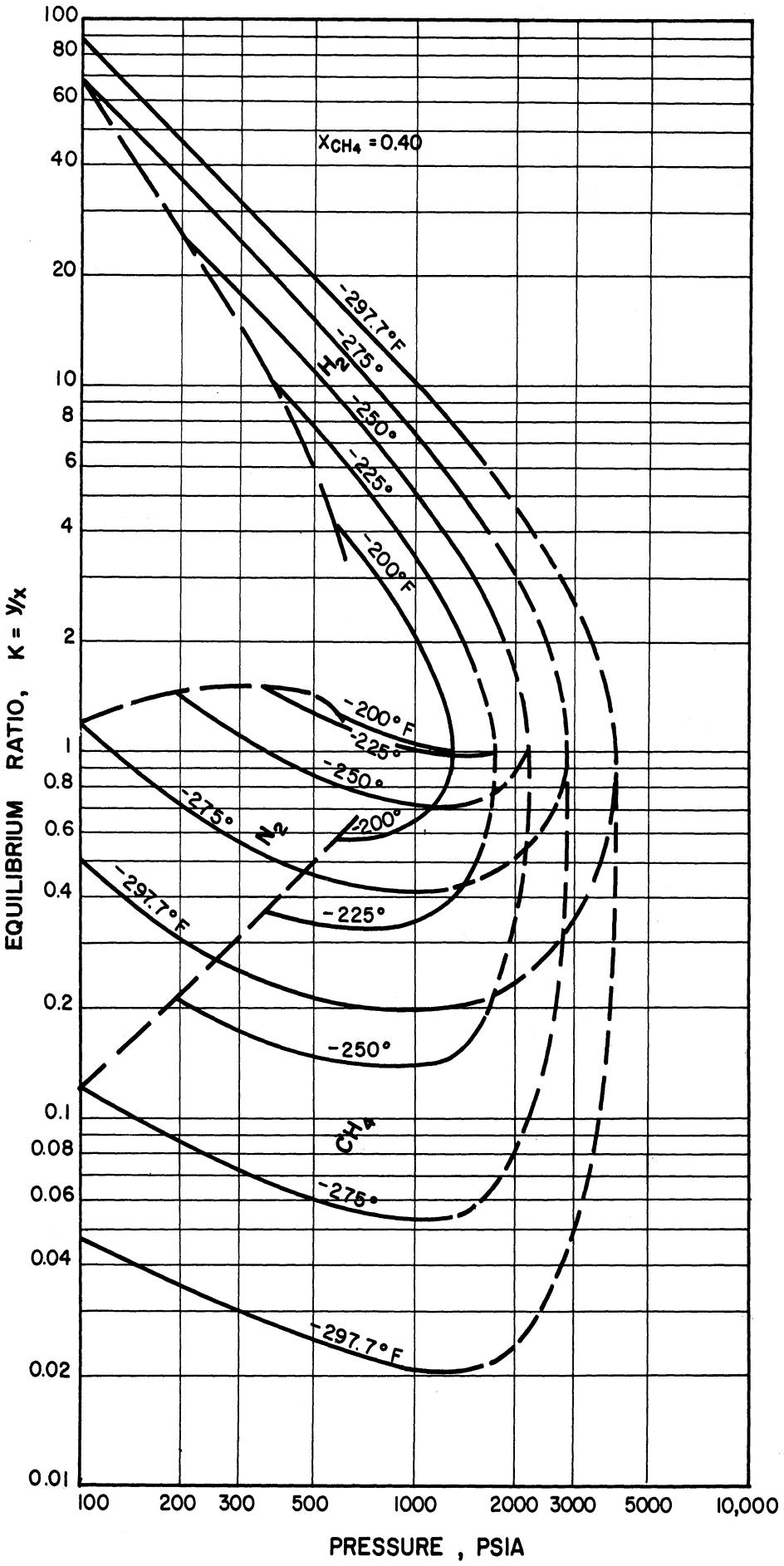

Figure 36. Equilibrium Ratios for Constituents in the Hydrogen-Nitrogen-Methane System at 40 Mole Percent Methane in the Liquid Phase as a Function of Pressure for Various Temperatures

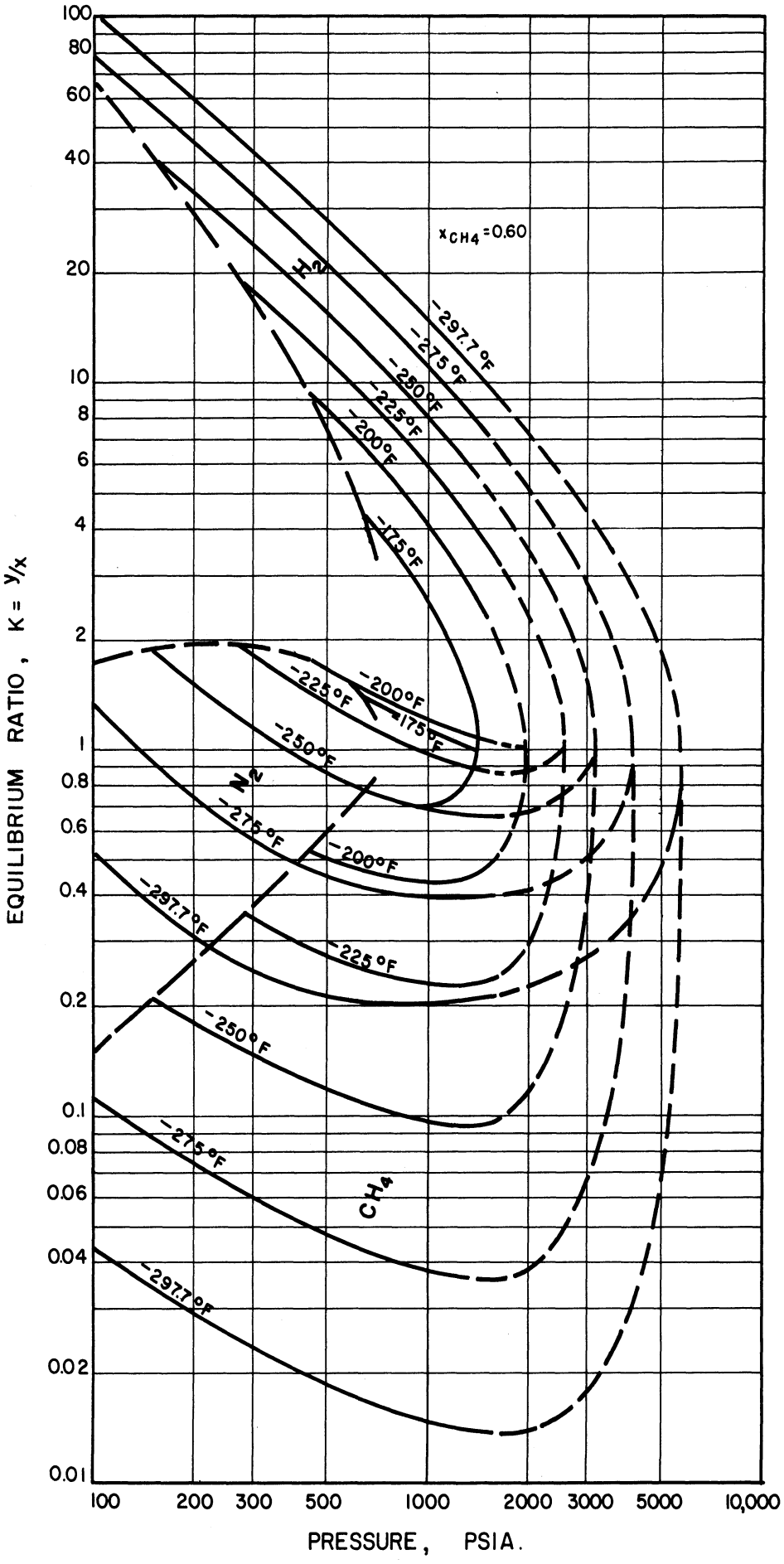

Figure 37. Equilibrium Ratios for Constituents in the Hydrogen-Nitrogen-Methane System at 60 Mole Percent Methane in the Liquid Phase as a Function of Pressure for Various Temperatures

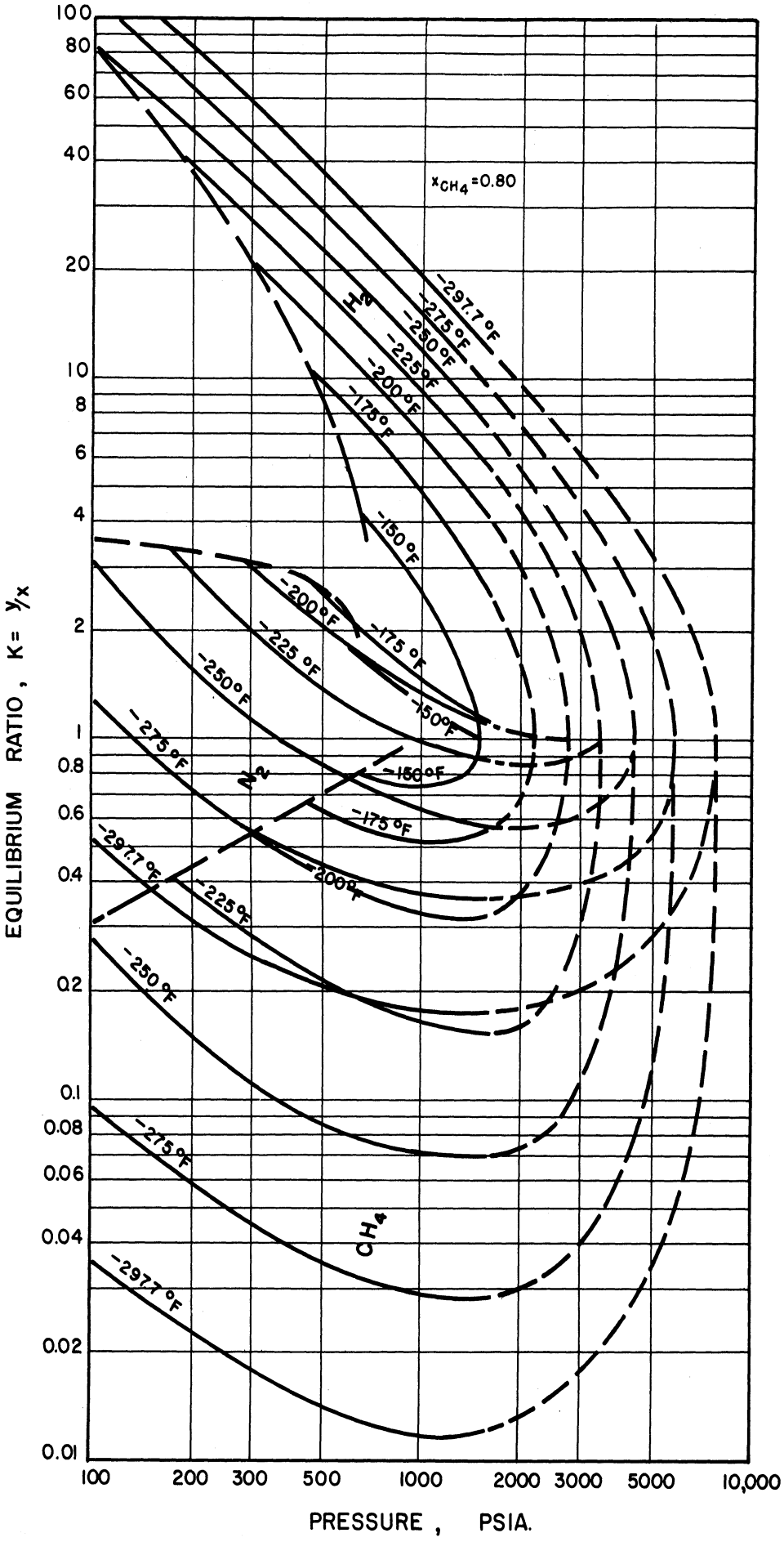

Figure 38. Equilibrium Ratios for Constituents in the Hydrogen-Nitrogen-Methane System at 80 Mole Percent Methane in the Liquid Phase as a Function of Pressure for Various Temperatures

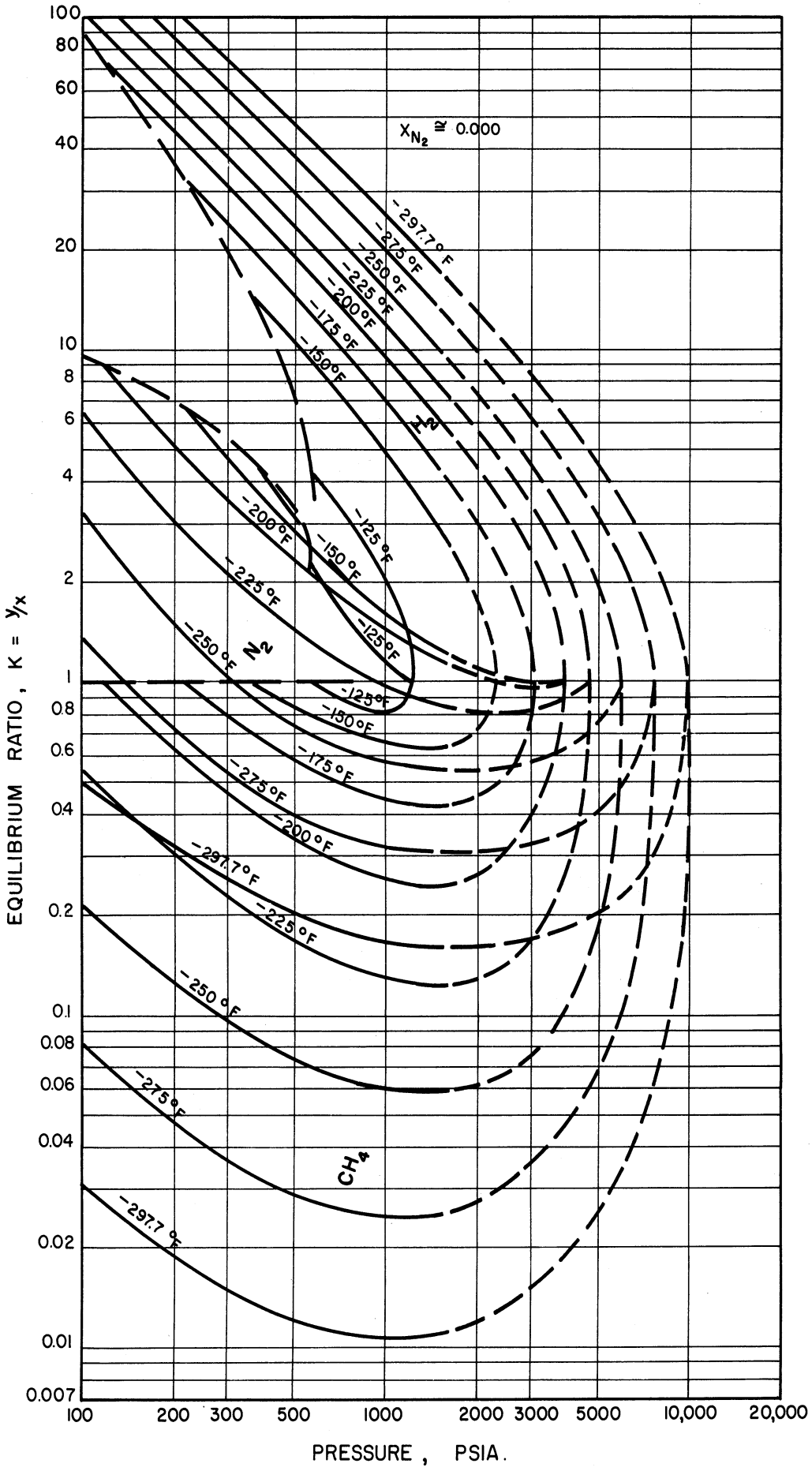

Figure 39. Equilibrium Ratios for Constituents in the Hydrogen-Nitrogen-Methane System at 0 Mole Percent Nitrogen in the Liquid Phase as a Function of Pressure for Various Temperatures

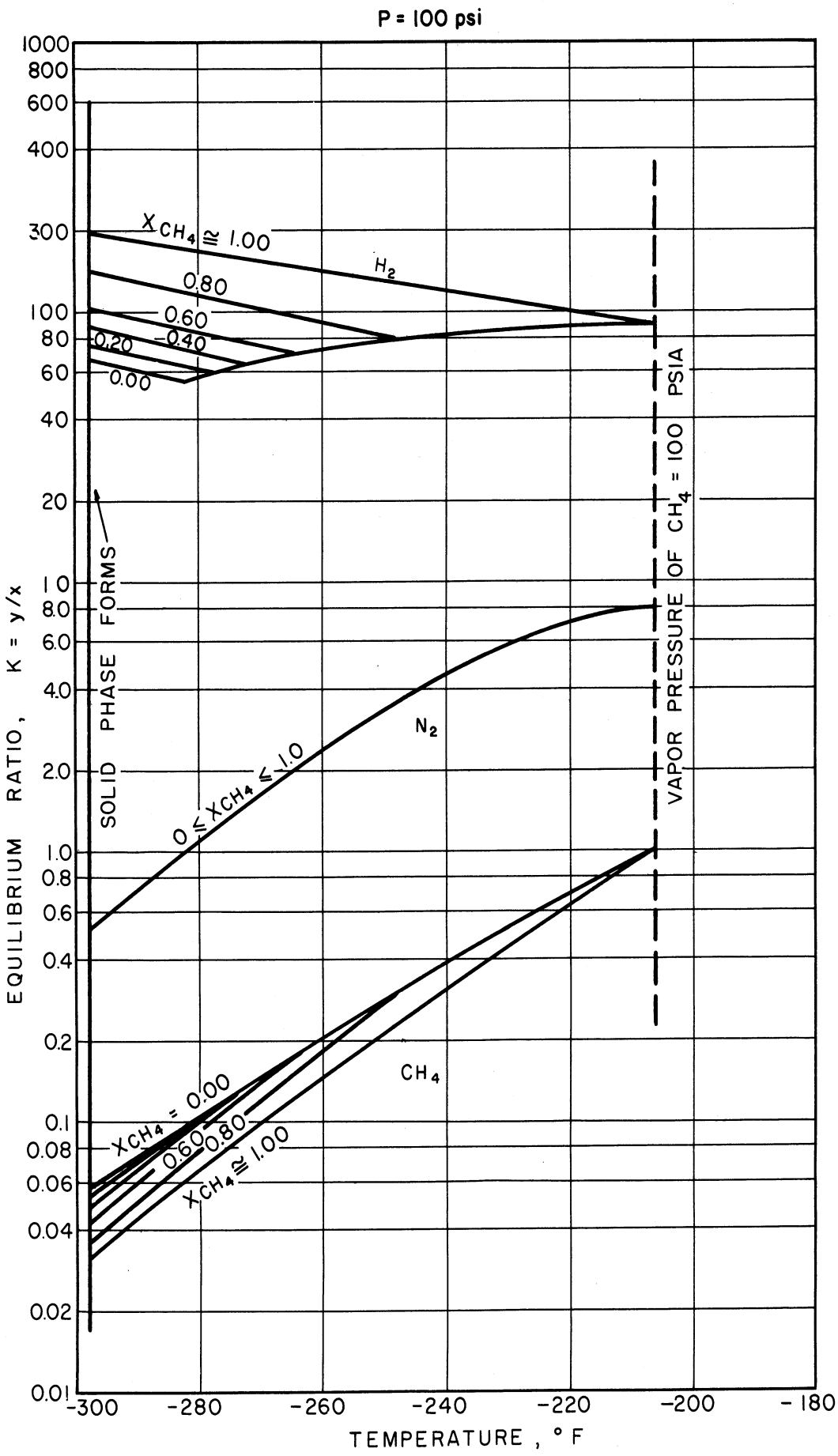

Figure 40. Equilibrium Ratios for Constituents in the Hydrogen-Nitrogen-Methane System at 100 psia as a Function of Temperature with Varying Amounts of Methane in the Liquid Phase

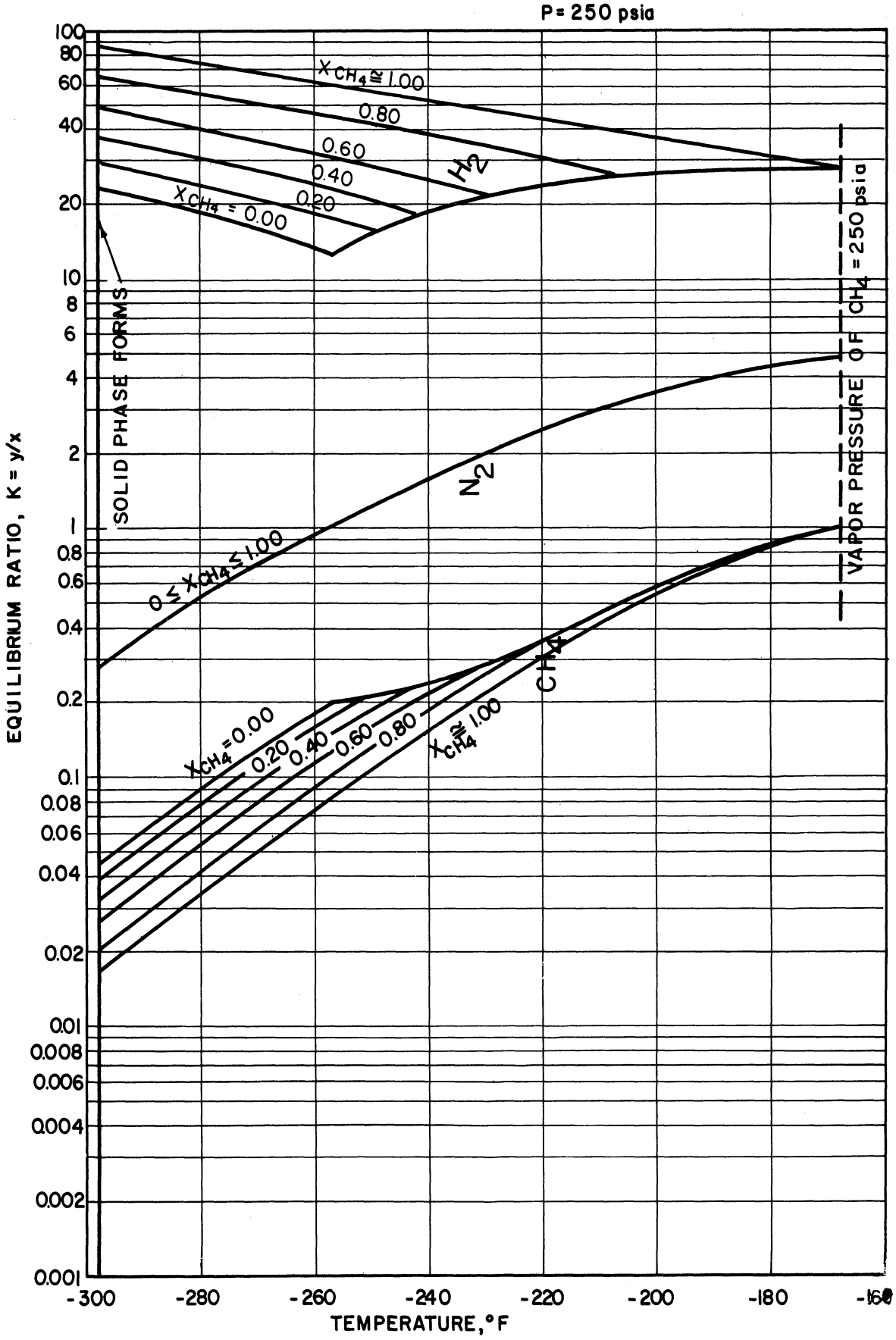

Figure 41. Equilibrium Ratios for Constituents in the Hydrogen-Nitrogen-Methane System at 250 psia as a Function of Temperature with Varying Amounts of Methane in the Liquid Phase

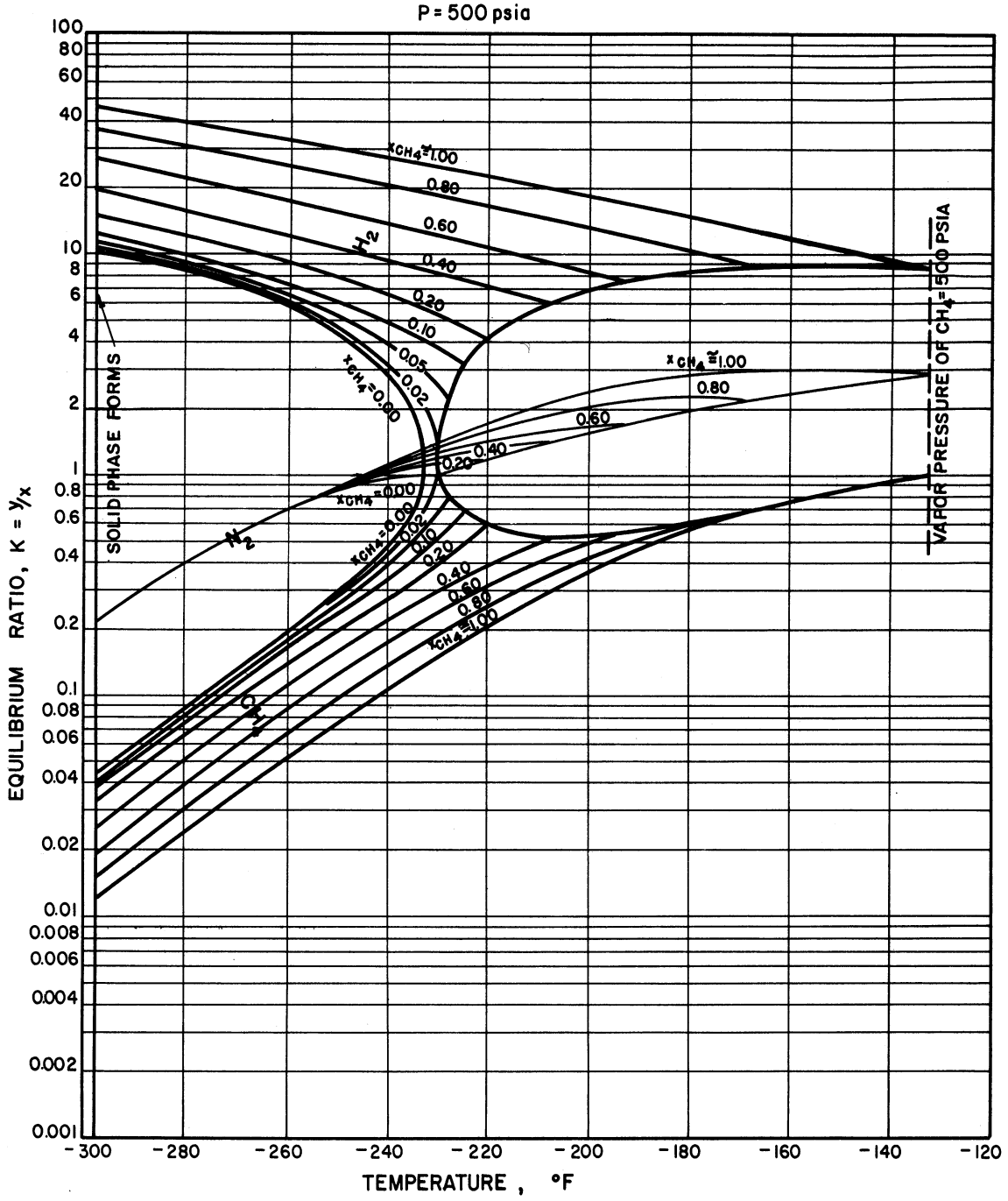

Figure 42. Equilibrium Ratios for Constituents in the Hydrogen-Nitrogen-Methane System at 500 psia as a Function of Temperature with Varying Amounts of Methane in the Liquid Phase

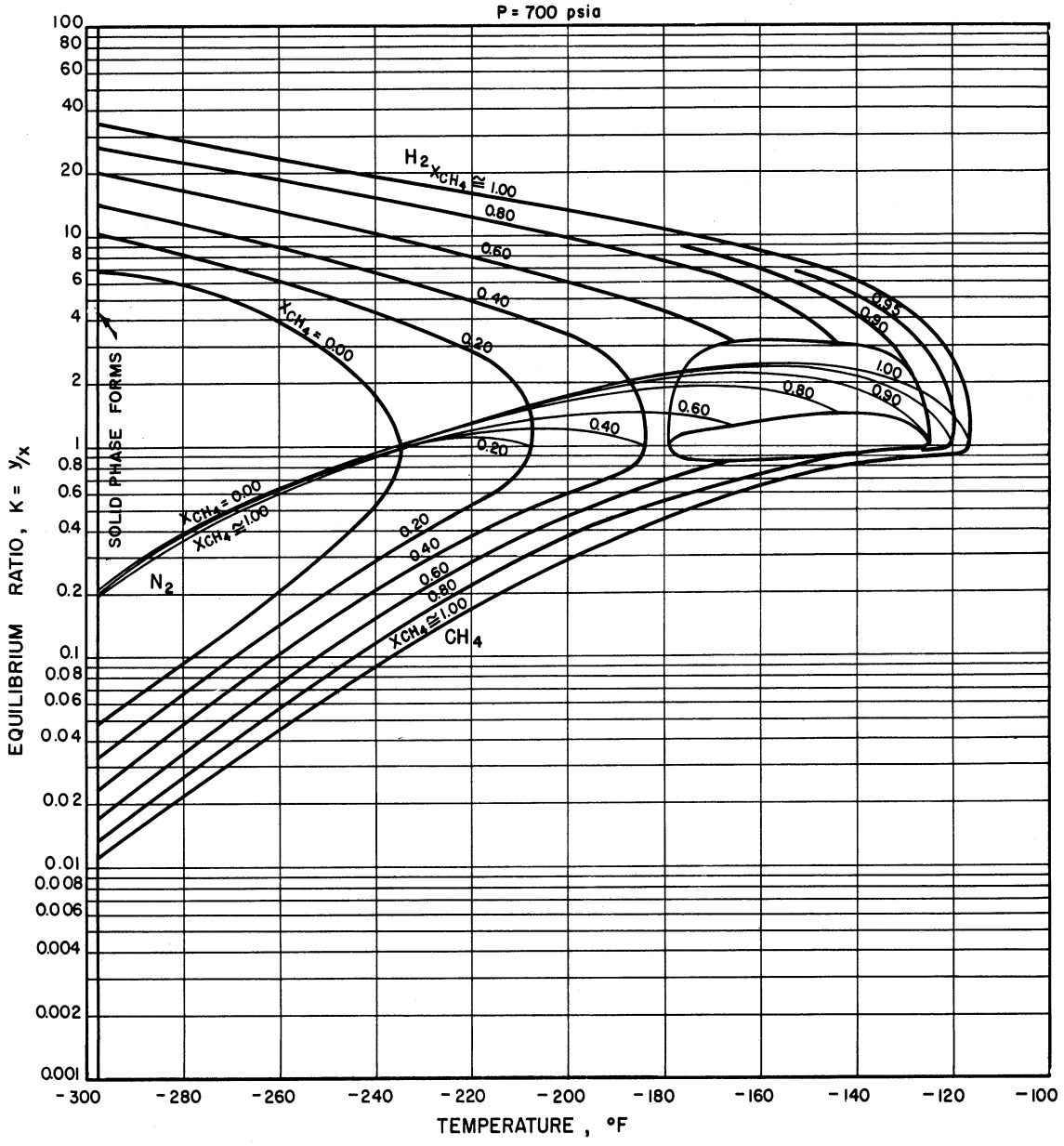

Figure 43. Equilibrium Ratios for Constituents in the Hydrogen-Nitrogen-Methane System at 700 psia as a Function of Temperature with Varying Amounts of Methane in the Liquid Phase

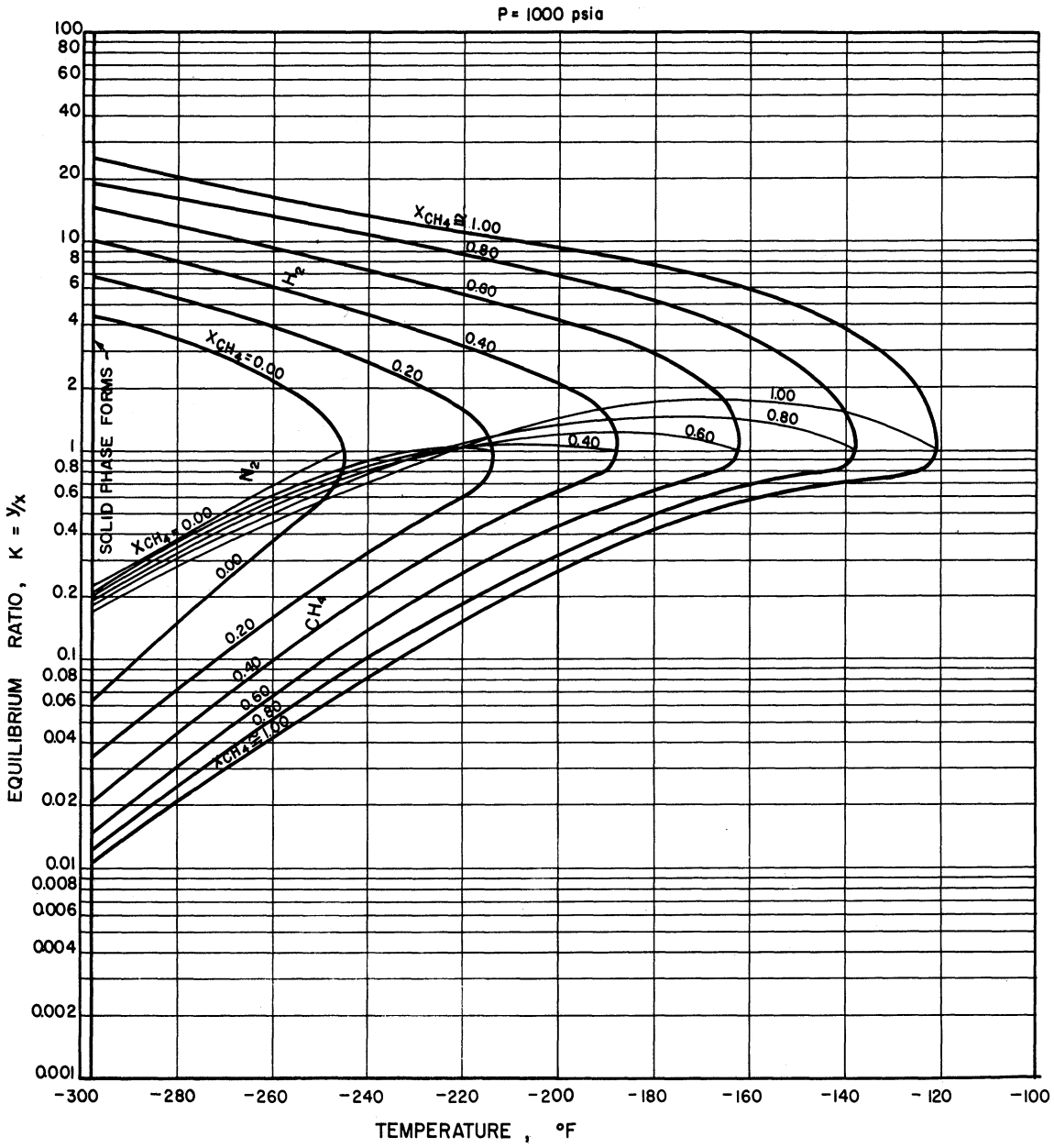

Figure 44. Equilibrium Ratios for Constituents in the Hydrogen-Nitrogen-Methane System at 1000 psia as a Function of Temperature with Varying Amounts of Methane in the Liquid Phase

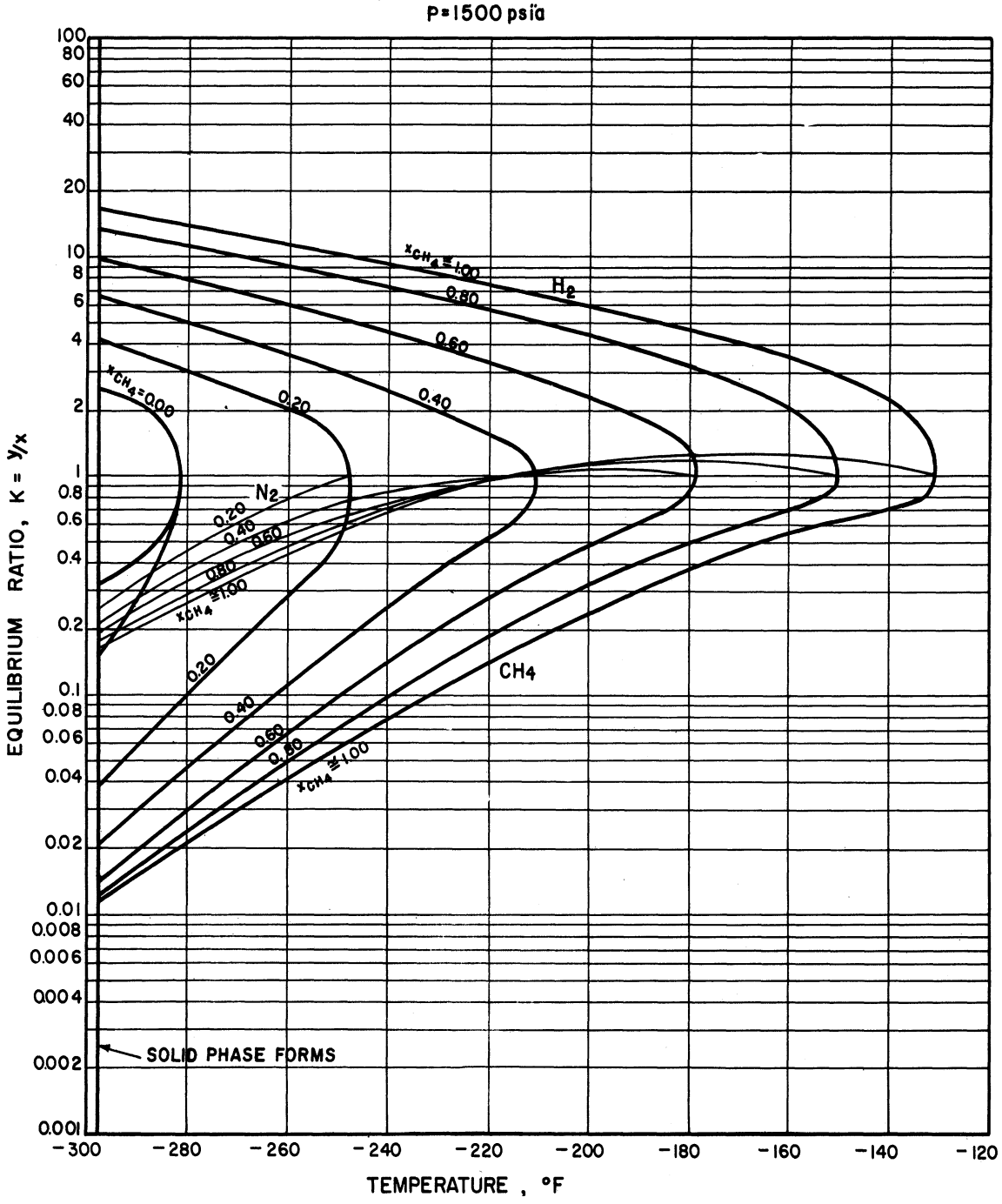

Figure 45. Equilibrium Ratios for Constituents in the Hydrogen-Nitrogen-Methane System at 1500 psia as a Function of Temperature with Varying Amounts of Methane in the Liquid Phase

through 45 may be utilized to obtain equilibrium ratios at intermediate temperatures, pressures, and mole percentages of methane in the liquid phase. Again it is recommended that the values obtained from these plots be used with caution at pressures above 1500-2000 psia.

Nitrogen-Methane-Ethane System

Since no data could be found in the literature for the binary system nitrogen-ethane, the correlation of the nitrogen-methane-ethane ternary system using the methods employed in the correlation of the preceding two ternary systems was found to be impossible. At such time as these data become available, this ternary system could be correlated in a manner similar to the methods outlined above for the correlation of the hydrogen-methane-ethane and hydrogen-nitrogen-methane ternary systems. The binary system phase behavior data could be used, together with the ternary system data obtained in this work, to obtain a correlation which would allow the determination of the equilibrium ratios for all the constituents of the nitrogen-methane-ethane ternary system at any desired temperature, pressure, and mole percentage of methane in the liquid phase. Until the vapor-liquid equilibrium data for the nitrogen-ethanebinary system become available, it is recommended that the ternary system data given in this investigation be interpolated or extrapolated to yield ternary system equilibrium ratios at other temperatures, pressures, and mole percentages of methane in the liquid phase. One other possibility would be the estimation of the required data for the nitrogen-ethane binary system

and the correlation of the ternary system based on the estimated nitrogen-ethane binary data by the methods outlined in the discussion of the correlation for the other two ternary systems.

Hydrogen-Nitrogen-Methane-Ethane System

As may be noted in Table X, the vapor-liquid equilibrium data for the hydrogen-nitrogen-methane-ethane quaternary system at -200°F and 500 psia were obtained at a relatively constant percentage of methane in the liquid phase. For five observations at these conditions of temperature and pressure the amount of methane in the liquid phase varies from 8.41 mole percent to 8.80 mole percent, while three of the observations vary from 8.41 mole percent to 8.48 mole percent. Therefore, these five data points (runs 54 through 58) were obtained at constant temperature, constant pressure, and approximately constant mole percentage of methane in the liquid phase. If the equilibrium ratios for the constituents in the hydrogen-nitrogen-methane-ethane quaternary system were functions of only the three variables of temperature, pressure, and mole percent methane in the liquid phase, then the equilibrium ratios for all four of the components in the system should be constant for runs 54 through 58 since all three of these variables were held constant during these runs.

The fact that the phase behavior in this quaternary system is not adequately described by the variables of temperature, pressure, and mole percent methane in the liquid phase can, perhaps, be best illustrated with reference to Tables V and VII or to Figure 49. Since the ternary systems hydrogen-methane-ethane and

nitrogen-methane-ethane are only special cases of the quaternary system in which the amount of either nitrogen or hydrogen in the system is zero, the equilibrium ratios for methane and ethane at any constant temperature, pressure, and mole percent methane in the liquid phase would have the same values in both of these ternary systems if the equilibrium ratios in the quaternary system were functions of only pressure, temperature, and mole percent methane in the liquid phase. This is not the case as may be seen in Tables V and VII or on Figure 49. As an illustration, the equilibrium ratios for methane and ethane at -200°F, 500 psia, and 10.0 mole percent methane in the liquid phase are found to be 0.340 and 0.00348 respectively in the hydrogen-methane-ethane ternary system. For the same conditions of temperature, pressure, and liquid phase methane composition in the nitrogen-methane-ethane ternary system, the equilibrium ratios for methane and ethane are found to be 0.440 and 0.00999 respectively. Therefore, the hydrogen-nitrogen-methane-ethane quaternary system cannot be adequately described by the three variables of temperature, pressure, and mole percent methane in the liquid phase. Using this same type of argument and referring to the ternary system data listed in Tables V, VII, and IX or the ternary and quaternary system data shown on Figures 48, 49, and 50, it can be seen that any single composition variable (mole percentage of any one of the four components in either the vapor or liquid phase) is insufficient to describe the phase behavior in the hydrogen-nitrogen-methane-ethane quaternary system at constant

temperature and pressure. For this particular quaternary system, all four of the variables required by the Phase Rule are necessary to adequately represent the phase behavior of the system.

Since the variables of temperature, pressure, and mole percent methane in the liquid phase were found to be insufficient for the proper correlation of the quaternary system, it was necessary to choose a second composition variable for the quaternary system correlation. Figure 46 shows the equilibrium ratios for the constituents in the quaternary system at -200°F, 500 psia, and approximately 8.5 mole percent methane in the liquid phase as a function of the mole percent hydrogen in the vapor phase. Figure 47 is a similar plot of these equilibrium ratios at the same conditions of pressure, temperature, and liquid phase methane composition as a function of the mole percent nitrogen in the vapor phase. The experimental data from runs 54 through 58 have been included on both of these plots. It can be seen from Figures 46 and 47 that the equilibrium ratios may be represented reasonably well using as the second composition variable either the mole percent hydrogen or the mole percent nitrogen in the vapor phase. Since the first composition variable had already been chosen as the mole percent of one of the intermediate components (methane) in the liquid phase, it was decided that the mole percent of the other intermediate component (nitrogen) in the vapor phase would be employed as the second correlating variable. It should be pointed out, however, that, while all four of the variables required by the Phase Rule are necessary to adequately represent

the quaternary system, the choice of either mole percent methane in the liquid phase or mole percent nitrogen in the vapor phase as the correlating variables is not required for the proper representation of the quaternary system. Two other composition variables could possibly have correlated the quaternary system as well as those variables chosen.

Having chosen the mole percent nitrogen in the vapor phase as the second correlating variable, the equilibrium ratios for the constituents in the quaternary system at -200°F and 500 psia were plotted as functions of the mole percent nitrogen in the vapor phase with parameters of mole percent methane in the liquid phase (Figures 48, 49, and 50). Figure 48 shows the equilibrium ratios for hydrogen and nitrogen in the quaternary system at -200°F and 500 psia. Figure 49 gives the equilibrium ratios for ethane in the quaternary system at -200°F and 500 psia, and Figure 50 gives the equilibrium ratios for methane in the quaternary system at these same conditions of temperature and pressure. The experimentally-determined equilibrium ratios from runs 54 through 58 are included on these plots. The equilibrium ratios for the constituents in the four ternary systems (hydrogen-methane-ethane, hydrogen-nitrogen-methane, nitrogen-methane-ethane, and hydrogen-nitrogen-ethane) form the boundary curves in Figures 48, 49, and 50. The lines of constant mole percent methane in the liquid phase were constructed on Figures 48 and 49 from a knowledge of the mole percentages of methane in the liquid phase of the three ternary systems studied in this investigation, and

from the shape of the lines of constant 8.5 mole percent methane in the quaternary system as given in Figure 47. As shown in Figure 50, the variation in the equilibrium ratios for methane is small, and as a result, no attempt has been made to estimate the lines of constant percentage methane in the liquid phase on this plot.

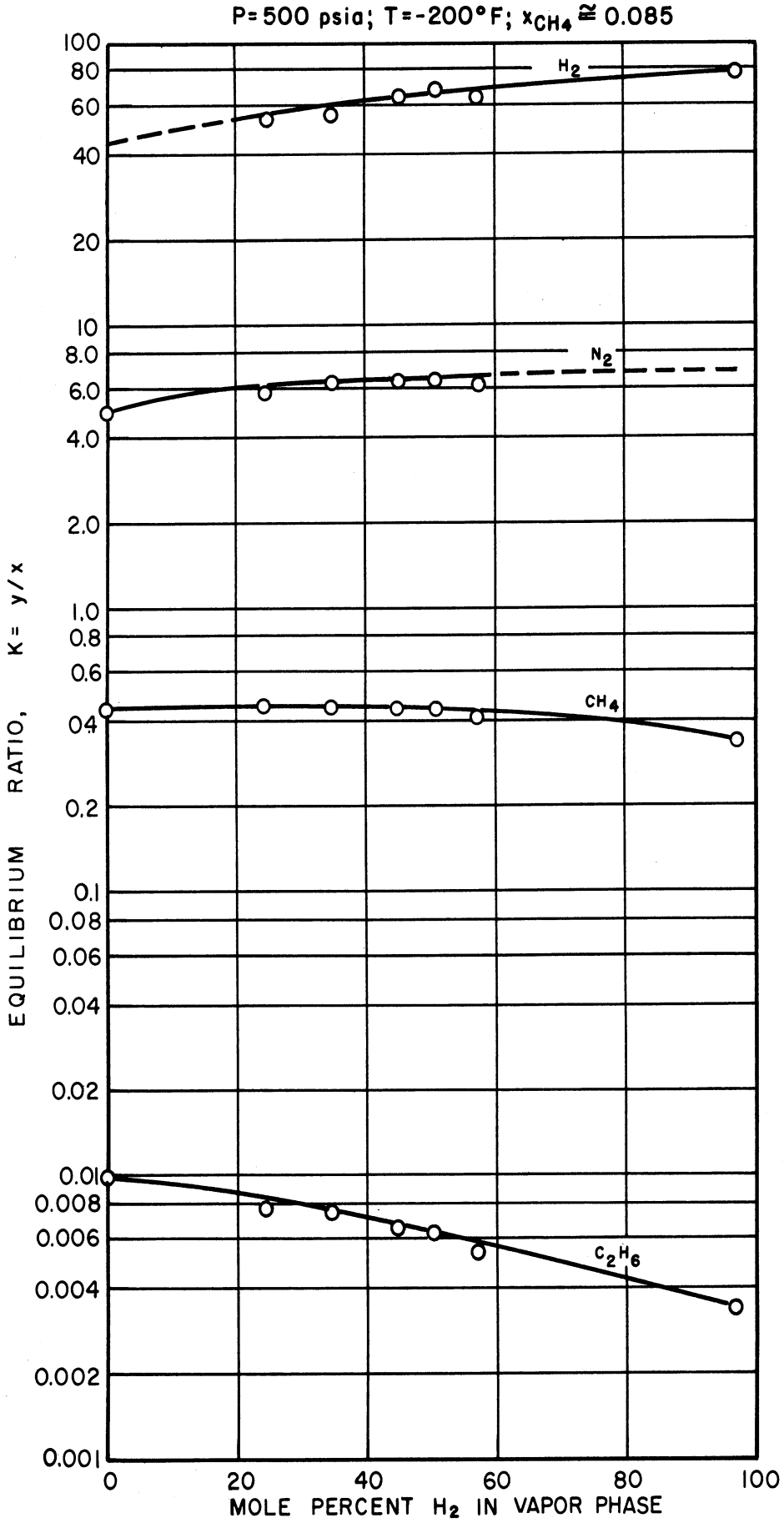

Figure 46. Equilibrium Ratios for Constituents in the Hydrogen-Nitrogen-Methane-Ethane Quaternary System at 500 psia and -200°F as a Function of the Mole Percent Hydrogen in the Vapor Phase at a Constant 8.5 Mole Percent Methane in the Liquid Phase

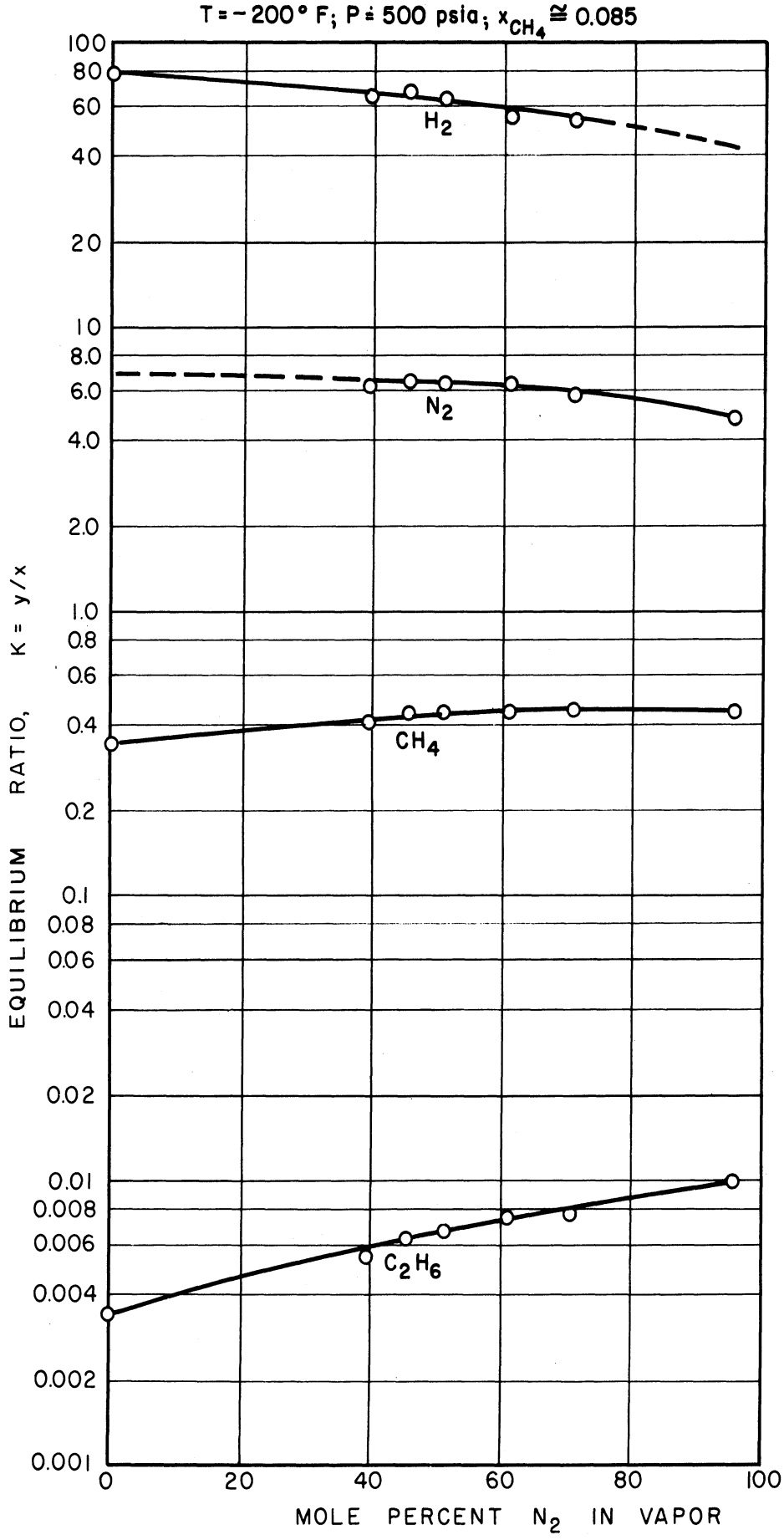

Figure 47. Equilibrium Ratios for Constituents in the Hydrogen-Nitrogen-Methane-Ethane Quaternary System at 500 psia and -200°F as a Function of the Mole Percent Nitrogen in the Vapor Phase at a Constant 8.5 Mole Percent Methane in the Liquid Phase

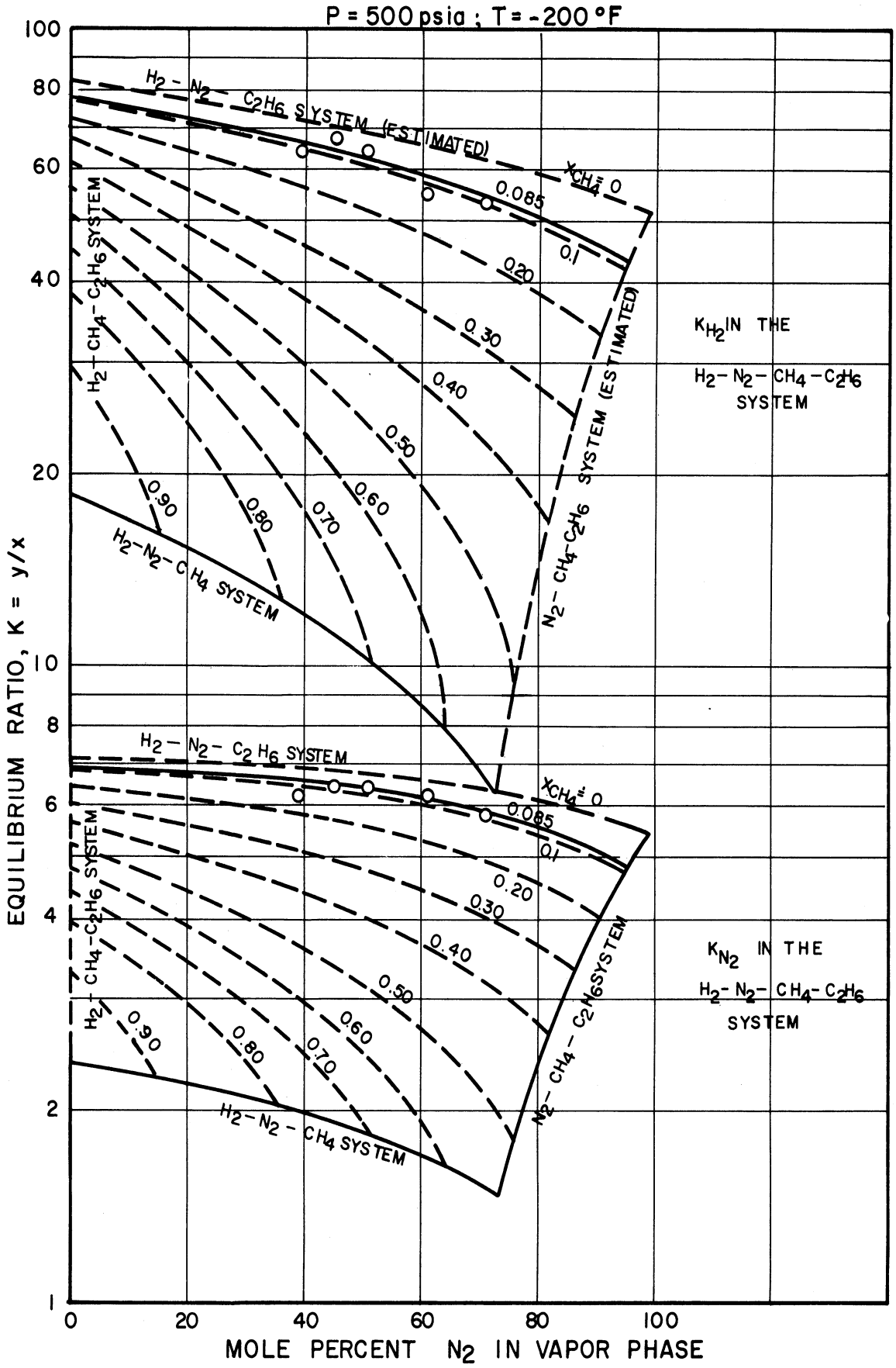

Figure 48. Equilibrium Ratios for Hydrogen and Nitrogen in the Hydrogen-Nitrogen-Methane-Ethane Quaternary System at 500 psia and -200°F as a Function of the Mole Percent Nitrogen in the Vapor Phase with Varying Amounts of Methane in the Liquid Phase

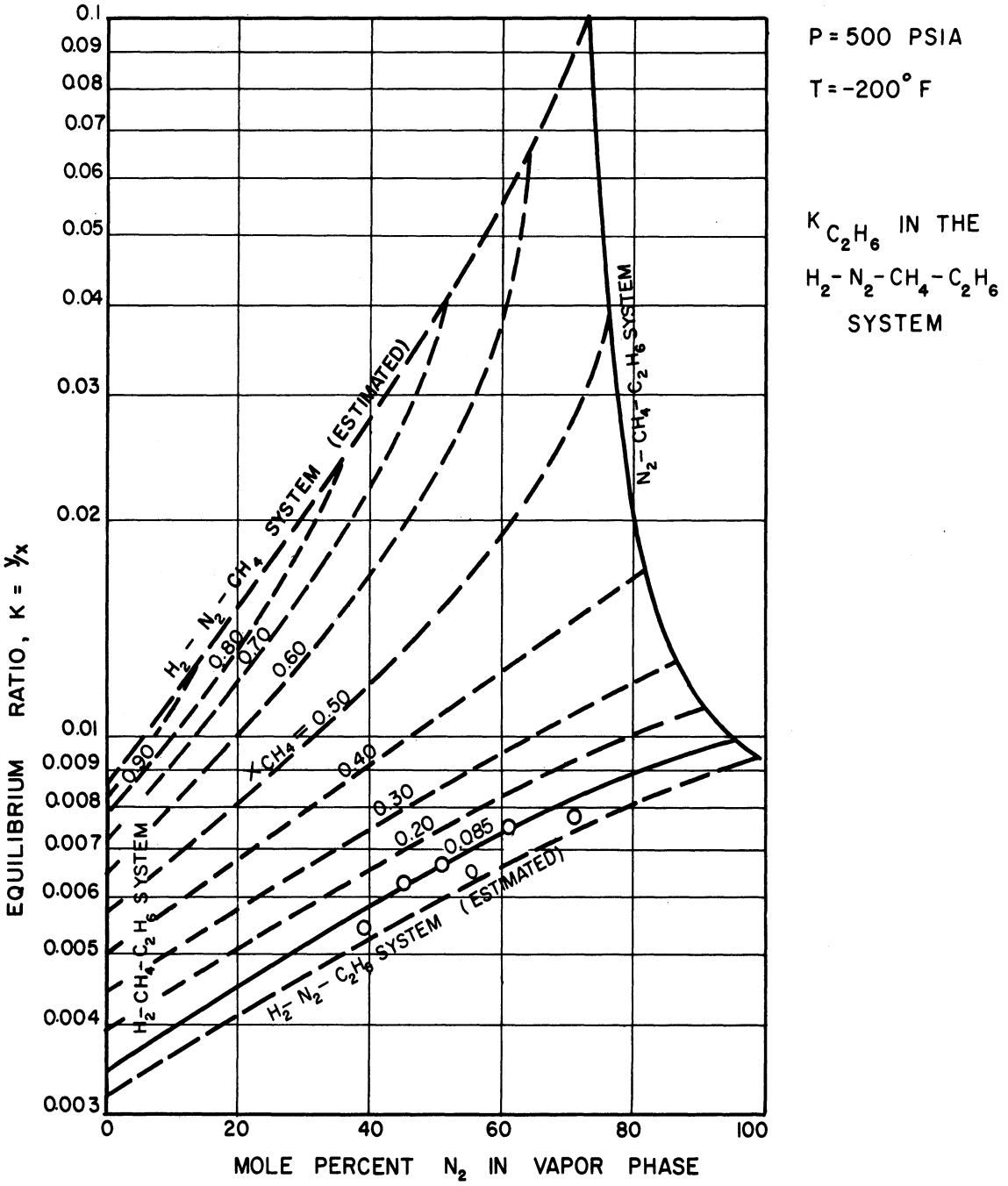

Figure 49. Equilibrium Ratios for Ethane in the Hydrogen-Nitrogen-Methane-Ethane Quaternary System at 500 psia and -200°F as a Function of the Mole Percent Nitrogen in the Vapor Phase with Varying Amounts of Methane in the Liquid Phase

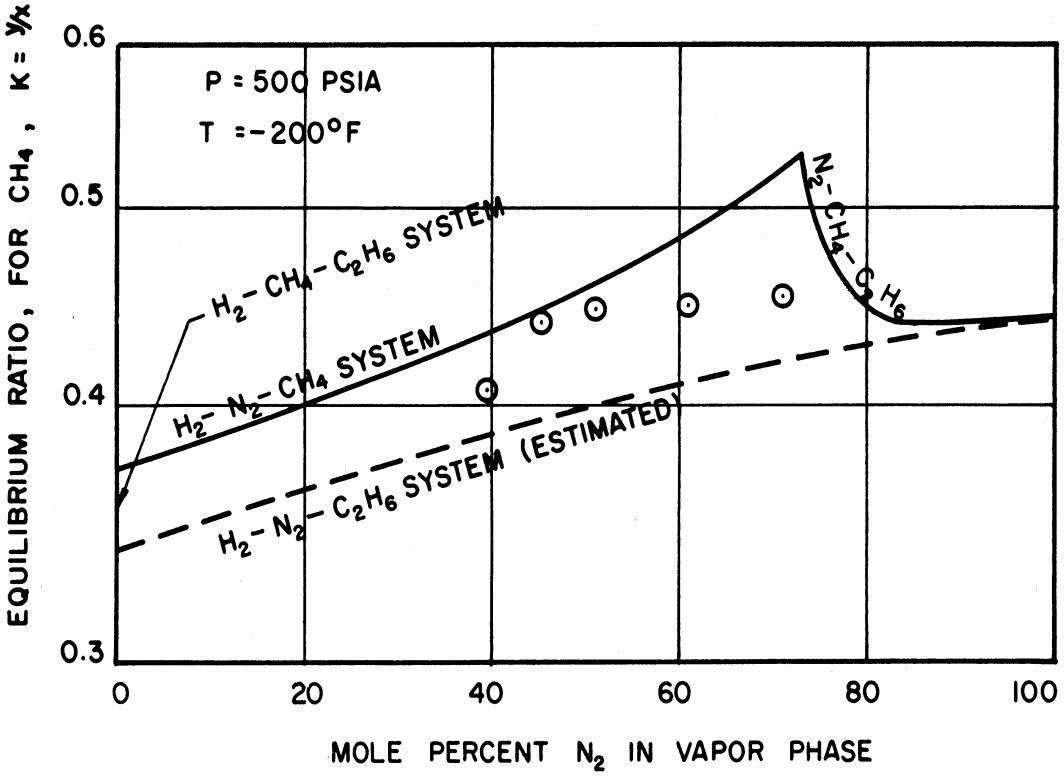

Figure 50. Equilibrium Ratios for Methane in the Hydrogen-Nitrogen-Methane-Ethane Quaternary System at 500 psia and -200°F as a Function of the Mole Percent Nitrogen in the Vapor Phase

SUMMARY AND CONCLUSIONS

The compositions of the equilibrium liquid and vapor phases were obtained for the hydrogen-methane-ethane ternary system at temperatures of -100 and -200°F and at pressures of 500 and 1000 psia. The equilibrium phase compositions were obtained for the nitrogen-methane-ethane ternary system at -100°F and pressures of 500 and 1000 psia, and at -200°F and 500 psia. Equilibrium phase compositions were also obtained for the hydrogen-nitrogen-methane ternary system at -200°F and pressures of 500 and 1000 psia, and for the hydrogen-nitrogen-methane-ethane quaternary system at -100°F and 1000 psia and at -200°F and 500 psia.

The data have been presented graphically in various ways as summarized in Table XI. Both the experimental data and the smoothed values of phase compositions and equilibrium ratios have been presented in tabular form. The equilibrium ratios for all of the systems studied have been found to be functions of phase composition as well as functions of the temperature and pressure.

The application of the Phase Rule to the correlation of vapor-liquid equilibrium data has been discussed and several methods which have been employed in the correlation of vapor-liquid equilibrium data have been reviewed. The use of these methods in the correlation of equilibrium data for systems containing hydrogen, nitrogen, and the light hydrocarbons has been shown to be difficult or impossible.

Attempts to obtain a generalized correlation for multicomponent systems containing hydrogen, nitrogen, and the light hydrocarbons by either

graphical or analytical methods have proven unsuccessful. For these multicomponent systems at least four, and perhaps more than four variables in the case of systems containing more than four components, will have to be used in order to properly represent the phase behavior of the system.

TABLE XI

SUMMARY OF DATA PRESENTED GRAPHICALLY IN THIS THESIS

SYSTEM	ORDINATE	ABSCISSA	PLOT PARAMETER	VARIABLES HELD CONSTANT	NO. OF PLOTS
H_2-N_2	Equilibrium Ratios	Pressure	Temperature	---	1
N_2-C_2H_6	Pressure	Mole Percent N_2	Temperature	---	1
Binary Systems containing H_2, N_2, CH_4, and C_2H_6	Critical Pressure or Vapor Pressure	Temperature	System	---	1
H_2-CH_4-C_2H_6	Phase Composition	Phase Composition	---	Pressure and Temperature	4
	Equilibrium Ratios	Mole Percent CH_4 in Liquid Phase	Temperature	Pressure	1
	Equilibrium Ratios for H_2	Equilibrium Ratios for C_2H_6	Pressure and Temperature	---	1
	Equilibrium Ratios for CH_4	$K_{C_2H_6} \times K_{H_2}$	Pressure and Temperature	---	1
	Equilibrium Ratios	Pressure	Temperature	Mole Percent CH_4 in Liquid Phase	5
	Equilibrium Ratios	Pressure	Temperature	Mole Percent C_2H_6 in Liquid Phase	1
	Equilibrium Ratios	Temperature	Mole Percent CH_4 in Liquid Phase	Pressure	5
N_2-CH_4-C_2H_6	Phase Composition	Phase Composition	---	Pressure and Temperature	3
	Equilibrium Ratios	Mole Percent CH_4 in Liquid Phase	Pressure	Temperature	2
H_2-N_2-CH_4	Phase Composition	Phase Composition	---	Pressure and Temperature	2
	Equilibrium Ratios	Mole Percent CH_4 in Liquid Phase	Pressure	Temperature	1
	Equilibrium Ratios	Pressure	Temperature	Mole Percent CH_4 in Liquid Phase	5
	Equilibrium Ratios	Pressure	Temperature	Mole Percent N_2 in Liquid Phase	1
	Equilibrium Ratios	Temperature	Mole Percent CH_4 in Liquid Phase	Pressure	6
H_2-N_2-CH_4-C_2H_6	Equilibrium Ratios	Mole Percent H_2 in Vapor Phase	---	Pressure, Temp. and Mole Percent CH_4 in Liquid Ph.	1
	Equilibrium Ratios	Mole Percent N_2 in Vapor Phase	---	Pressure, Temp. and Mole Percent CH_4 in Liquid Ph.	1
	Equilibrium Ratios	Mole Percent N_2 in Vapor Phase	Mole Percent CH_4 in Liquid Phase	Pressure and Temperature	3
	Phase Composition	Phase Composition	Temperature	Pressure	2

APPENDIX A

METHODS USED FOR CORRELATING VAPOR-LIQUID EQUILIBRIUM DATA

Many attempts have been made to predict phase behavior theoretically or empirically, however, no single method of correlation has been successful in describing all of the binary and multicomponent vapor-liquid equilibrium data which have been published in the literature. Indeed, most of the presently available correlations have been successful in describing only an exceedingly small fraction of the available data.

Since no consideration of the methods used for correlating vapor-liquid equilibrium data would be complete without reference to the information which can be supplied by the Phase Rule, the application of this rule to the correlation problem will be discussed. Various methods which have been used for correlating the data will then be reviewed.

The Phase Rule

The Phase Rule, first enunciated by J. Willard Gibbs in 1876 [22], may be used to determine the maximum number of variables required to describe vapor-liquid equilibrium.

Mathematically, the Phase Rule may be stated:

$$P + F = C + 2 \qquad (1)$$

where:

F = number of degrees of freedom in the system

C = number of Phase Rule components in the system

P = number of phases present in the system

Since this work is mainly concerned with two phase (vapor and liquid) systems, the Phase Rule may be reduced to the form:

$$F = C$$

Therefore, the number of degrees of freedom allowed for a non-reacting two-phase system is equal to the number of components in the system.

Consideration of a three-component, non-reacting system in two phases reveals that three degrees of freedom exist, and, since the Phase Rule variables are pressure, temperature, and the compositions of each phase, functional relationships of the following forms are predicted by the Phase Rule:

$$\varphi(x_i, x_j, P, T) = 0 \tag{2}$$

$$\varphi(x_i, y_i, P, T) = 0 \tag{3}$$

$$\varphi(x_i, y_j, P, T) = 0 \tag{4}$$

$$\varphi(y_i, y_j, P, T) = 0 \tag{5}$$

where the subscripts "i" and "j" refer to any two of the three components in the system, and φ represents some function of the variables.

Several derived concentration variables have come into popular use. A few of these are the equilibrium ratio, the molal average boiling points of the liquid and vapor phases, the pseudocritical pressures and temperatures of the liquid and vapor phases, and the molal average molecular weights of the phases.

These derived concentration variables are defined as follows:

$$K_i = (y_i/x_i) \tag{6}$$

$$MABP = \sum_{i=1}^{C} z_i(nBP_i) \tag{7}$$

$$MW = \sum_{i=1}^{C} z_i M_i \tag{8}$$

$$P_{pc} = \sum_{i=1}^{C} z_i P_{c_i} \tag{9}$$

$$T_{pc} = \sum_{i=1}^{C} z_i T_{c_i} \tag{10}$$

where:

K_i = equilibrium ratio of component "i",

MABP = molal average boiling point,

z_i = mole fraction of component "i" in liquid or vapor,

nBP_i = normal boiling point of component "i",

MW = molal average molecular weight,

M_i = molecular weight of component "i",

P_{pc} = pseudocritical pressure,

T_{pc} = pseudocritical temperature,

P_{c_i} = critical pressure of component "i",

T_{c_i} = critical temperature of component "i",

C = total number of components,

i = individual component.

With the exception of the equilibrium ratio, all of the derived concentration variables listed above are found to be of the form:

$$\Theta = \sum_{i=1}^{C} (a_i \; z_i) \tag{11}$$

where Θ is the derived concentration variable and a_i is a constant for a given component. The value of a_i may be the normal boiling point, the molecular weight, the critical pressure, or the critical temperature of component "i", depending upon which of the derived concentration variables is to be represented by Θ.

These derived concentration variables, which are equivalent to the Phase Rule variables (phase compositions) and may be used in place of them, have been employed by many investigators to correlate vapor-liquid equilibrium data. In these cases, for a three component system, the Phase Rule predicts:

$$\varphi(K_i, \Theta, P, T) = 0 \tag{12}$$

where Θ represents any one of the derived concentration variables for either the vapor or liquid phase. The equilibrium ratio, K_i is found to be a function of the pressure, temperature, and one derived concentration variable for the case of two-phase equilibrium in a three component system.

In a similar manner it can be shown that, for the case of vapor-liquid equilibrium in an "n" component system, the Phase Rule describes the equilibrium ratio as a function of pressure, temperature, and (n-2) derived concentration variables.

While the Phase Rule can predict the maximum number of variables required to describe vapor-liquid equilibrium, it can not reveal which of the variables to use or how these variables are inter-related. The choice of which variables to use in order to obtain the simplest and most accurate correlation is left to the individual. Also, the Phase Rule can predict only the maximum number of variables required in the general case, and gives no information as to the number of variables actually required in order to obtain a sufficiently good correlation in any particular system. For any system which may be described by Raoult's Law, the pressure and temperature are the only variables required to describe the vapor-liquid equilibria of the system. A notable example of such a system is one containing only the paraffin hydrocarbons below their critical temperatures.

The fact that the vapor-liquid equilibria of a particular system apparently require less than the number of variables dictated by the Phase Rule in order to adequately represent the data does not invalidate the Phase Rule. Rather, it shows that, due to a fortuitous selection of the range of phase compositions being investigated, the liquid phase closely follows the laws of ideal solutions and a sufficiently good correlation can be obtained using fewer variables than are normally required. Thus, in the systems of the light hydrocarbons, one of the derived concentration variables may be used to account for the effect of all the more volatile components, and another may be used to account for the effect of all the remaining heavier components.

Solubility

One approach to the problem of correlating vapor-liquid equilibrium data has been through the concept of solubility. Gases dissolve in liquids to form solutions with the degree of solubility depending on the nature of the gas, the nature of the solvent, the pressure, and the temperature. Frequently chemical similarity between solute and solvent leads to a higher solubility, as is evidenced by the fact that gases like hydrogen and helium dissolve in liquid hydrocarbons only to a slight extent, while other hydrocarbon vapors are readily soluble in these same liquid hydrocarbons. Yet, chemical similarity or dissimilarity is not an infallible criterion of solubility.

One expression which has been used for the prediction of the solubility of a gas in a liquid is Henry's Law. Henry's Law states that the solubility of a gas in a liquid is directly proportional to the partial pressure of the gas above the liquid at equilibrium. Thus, at constant temperature:

$$x_i = H_i P_i \qquad (13)$$

where

H_i = Henry's Law Constant for component "i" (usually obtained from experimental data)

Strictly speaking, Henry's Law is an ideal gas law and is therefore applicable without error only to actual gases at very low pressures. At higher pressures the law becomes increasingly less exact. As with other ideal gas laws, the higher the temperature and the lower the pressure, the more exactly the law is obeyed.

At constant pressure the solubility of a gas in a liquid varies with the temperature in such a manner that, normally, the solubility decreases with increase in temperature. There are, however, numerous exceptions to this. In 1941, Kay [40] discovered that hydrogen dissolved in petroleum naphtha exhibits a minimum in the bubble point curve and reverse order solubility over a considerable range of temperatures and pressures at low concentrations of hydrogen in the liquid phase. At higher concentrations of hydrogen in the liquid phase, Kay found that the hydrogen did not exhibit the minimum in the bubble point curve, but that it did show reverse order solubility. By reverse order solubility is meant that the solubility of a substance increases with an increase in temperature.

The work of Benham [13] proves that a similar region of reverse order solubility also exists in the system hydrogen-methane. Benham shows that the reverse order solubility exists for hydrogen dissolved in methane over the entire range of pressures and temperatures except near the vapor pressure of methane.

This is true also for the systems: hydrogen-ethylene, hydrogen-ethane, hydrogen-propylene, and hydrogen-propane. These systems were studied by Williams [78] [79], who found that over the entire temperature range of the two phase region, and for all pressures investigated (8000 psia or less), all the hydrogen-hydrocarbon systems studied exhibited reverse order solubility. The solubility of the hydrogen in the liquid phase decreased with decrease in temperature except near the vapor pressure of the hydrocarbon.

Aroyan[4,5] worked with the system hydrogen-butane and proved that, for hydrogen dissolved in normal butane, the typical region of reverse order solubility existed. Aroyan[4] also gives an excellent description of minimum solubility and reverse order solubility, and shows that these are not unusual phenomena. Ordinary substances exhibit reverse order solubility in the region of retrograde vaporization as described by Katz and Kurata[39].

This phenomenon of reverse order solubility may best be illustrated with reference to Figure 1. Figure 1 (a) shows a very common type of pressure-temperature diagram. The critical point on this diagram occurs at, or very near, the highest temperature at which two phases may exist in the system. The region of reverse order solubility in this system is synonomous with the region of retrograde vaporization. This region is bounded by the bubble point curve and the loci of the maxima in the curves of constant percentage liquid.

Figure 1 (b) shows the pressure-temperature diagram for the binary system hydrogen-methane. The region of reverse order solubility exists for this system over the entire range of pressures and temperatures except near the vapor pressure of methane. An explanation for this extremely large region of reverse order solubility may be found by postulating a "hypothetical behavior" for the hydrogen-methane binary system below the solidification temperature of methane. Referring to Figure 1 (b), it can be seen that the formation of solid phase occurs before the maxima in the bubble point curves are reached (in the zone of

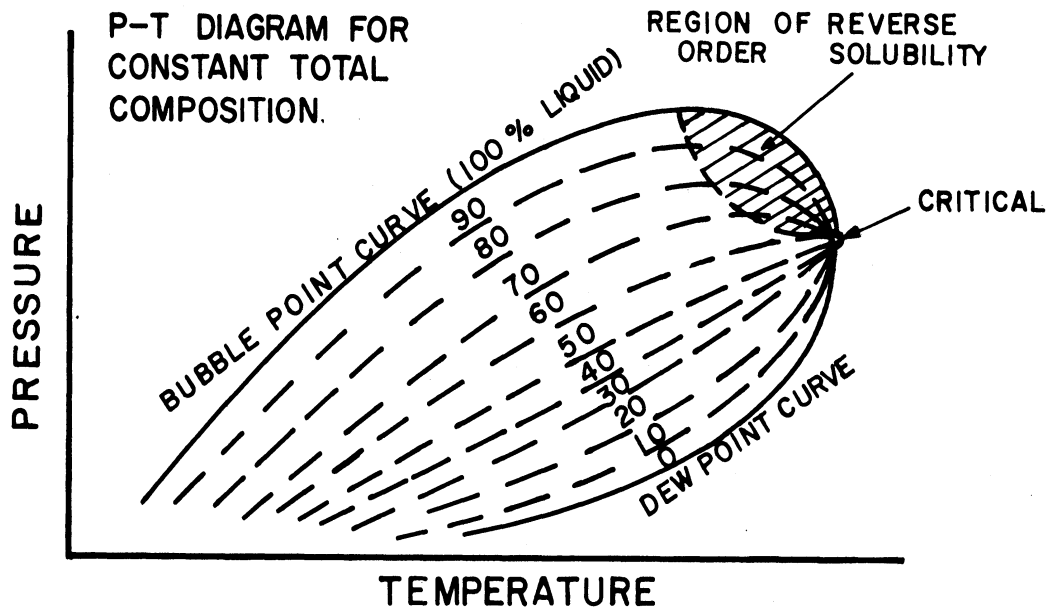

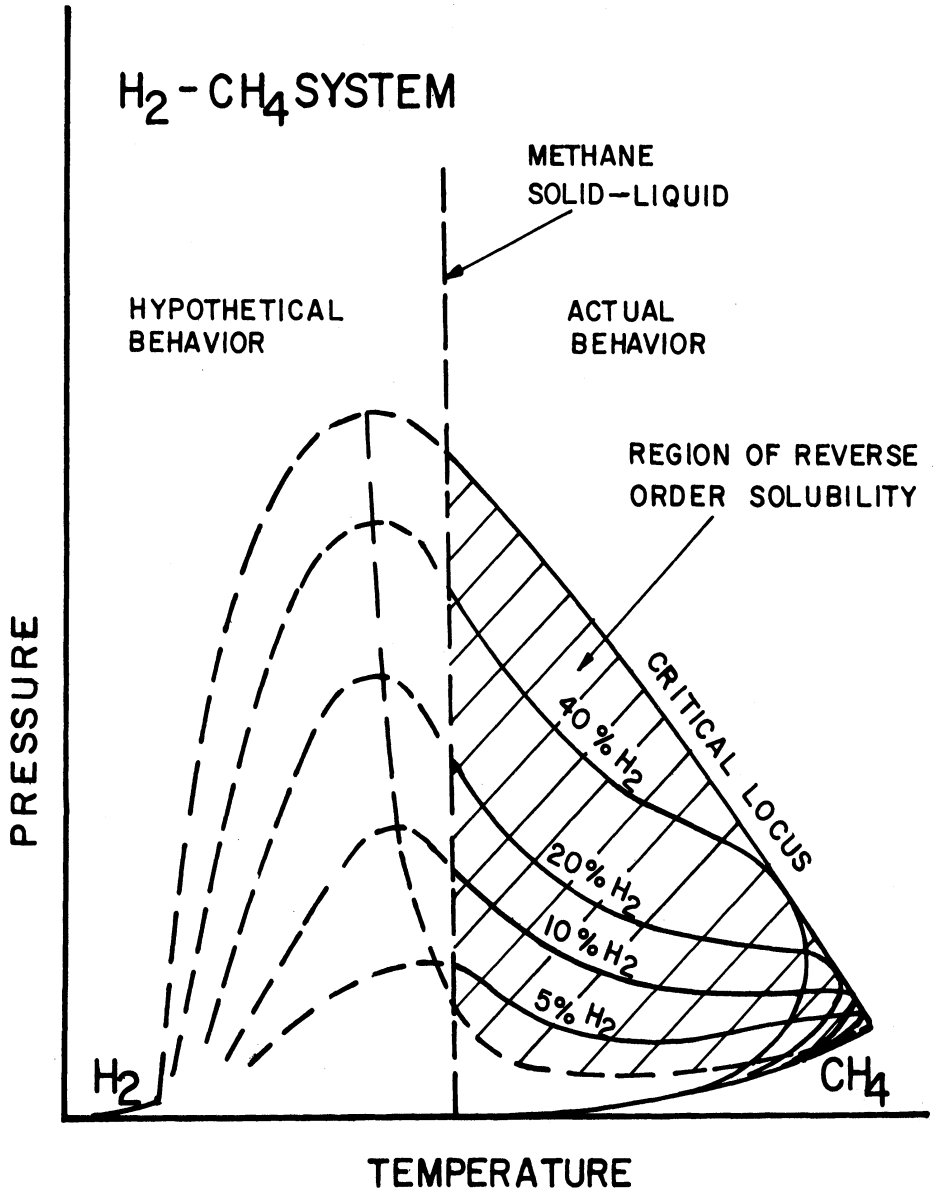

Figure 1. Schematic Pressure-Temperature Diagram for: a) Normal Mixtures, b) Hydrogen-Methane Binary System

hypothetical behavior). Otherwise, the behavior of this binary system is completely similar to the behavior of normal systems in the region of retrograde vaporization. In the hydrogen-methane binary system this region of retrograde vaporization is very large --- extending to the temperatures at which solid phase forms. It may also be noted that, for the hydrogen-methane binary system, a minimum occurs in the bubble point curve at approximately 5 percent hydrogen in the liquid phase.

Ideal Solutions

In cases where ideal solutions may be assumed, Raoult's Law has been used to describe vapor-liquid equilibrium. Raoult's Law states that the partial pressure of any volatile constituent of a solution is equal to the vapor pressure of the pure constituent multiplied by the mole fraction of that constituent in solution. Thus:

$$p_i = p_i^o x_i \tag{14}$$

Then, combining Raoult's Law with Dalton's Law ($p_i = P y_i$), the following relationships are obtained:

$$P y_i = p_i^o x_i \tag{15}$$

or

$$K_i = (y_i/x_i) = (p_i^o/P) \tag{16}$$

where:

p_i = partial pressure of component "i" in the vapor phase,

p_i^o = vapor pressure of component "i" at the temperature, T,

x_i = mole fraction of component "i" in the liquid,

P = total pressure of the system,

y_i = mole fraction of component "i" in the vapor,

K_i = equilibrium ratio of component "i".

For systems that obey Raoult's and Dalton's Laws, the vapor-liquid equilibrium ratio, K, may be correlated using only the variables of system temperature and pressure, as long as the temperature and pressure of the system are below the critical temperature and pressure of the most volatile component. Katz and Hackmuth [38] were able to satisfactorily correlate the vapor-liquid equilibrium data for mixtures of natural gas and Midcontinent crude oil using only the variables of system temperature and pressure. However, a satisfactory correlation for most multicomponent systems requires the use of a method to account for the effect of various concentration variables on the individual vapor-liquid equilibrium ratios.

Gilliland and Scheeline [31] present an empirical correlation for predicting equilibrium data for two component hydrocarbon systems in the critical region based on the general shape of the isotherms when the equilibrium ratio is plotted versus the pressure of the system. This correlation is based on the assumption that the minimum value of the equilibrium ratio for the heavy component occurs at a pressure corresponding approximately to the arithmetic average of the vapor pressure of the heavy component at the temperature in question and its critical pressure.

Non-Ideal Solutions - Activity Coefficients

Smith and Watson [67] approached the problem of correlating vapor-liquid equilibria in paraffin hydrocarbon mixtures by introducing the concept of liquid phase and vapor phase activity coefficients which express deviations from the laws of ideal solutions in two phase mixtures at high pressures. These phase activity coefficients, which were used to correct the equilibrium ratios as the critical pressure of the system was approached, were correlated as functions of the pseudoreduced pressure, pseudoreduced temperature, critical temperatures of the components and of the mixture, liquid mole fractions and normal boiling points. Briefly, the correlation was as follows:

$$K_i = K_{(ideal)} \left(\varphi_{L_i}/\varphi_{V_i}\right) \qquad (17)$$

where:

φL_i = liquid-phase activity coefficient for component "i" expressing deviations from the laws of ideal solutions in the liquid state as a result of differences in the molecular size or volatility,

φV_i = vapor-phase activity coefficient for component "i" expressing deviations resulting from differences in molecular size or volatility in the vapor phase.

These activity coefficients were shown graphically as functions of the following variables:

$$\varphi_{L_i} = \varphi_1 \left[(T_R)_L, (P_R)_L, (r) \right] \tag{18}$$

$$\varphi_{V_i} = \varphi_2 \left[(T_R)_V, (P_R)_V, (T_{c_i}/T_{pc})_V \right] \tag{19}$$

$$r = \varphi_3 \left[(nBP), (x), (P_R)_L \right] \tag{20}$$

where:

T_R = pseudoreduced temperature,

P_R = pseudoreduced pressure,

r = volatility ratio,

T_{c_i} = critical temperature of component "i",

T_{pc} = pseudo critical temperature

nBP = normal boiling points of the liquid phase constituents,

x = mole fractions of the liquid phase constituents,

$\varphi_1, \varphi_2, \varphi_3$ = functions of the indicated variables.

The subscripts "V" and "L" represent the vapor and liquid phases respectively.

Many other investigators have used the approach of evaluating the non-ideality of vapor-liquid equilibrium systems by means of activity coefficients which represent the deviation from ideal solutions. Van Laar[76], Margules[49], Scatchard and Hamer[65], Benedict and co-workers[6], Redlich and Kister[61], and Wohl[81], have used activity coefficients to represent this deviation, and, in turn, all of these investigators have used various semi-empirical expressions to relate the activity coefficients to the concentration.

The activity coefficient, γ_i, may be defined as follows:

$$y_i f^o_{V_i} = \gamma_i \, f^o_{L_i} \, x_i \tag{21}$$

or

$$\gamma_i = \frac{y_i f^o_{V_i}}{x_i f^o_{L_i}} = \left[\frac{K(\text{actual})}{K(\text{ideal})} \right]_i \tag{22}$$

where

$f^o_{L_i}$ = fugacity of pure component "i" as liquid at the same temperature and total pressure,

$f^o_{V_i}$ = fugacity of pure component "i" as vapor at the same temperature and total pressure,

$\frac{f^o_{L_i}}{f^o_{V_i}} = K_{(\text{ideal})}$ as defined by Souders, Selheimer and Brown[67A]

The activity coefficient may then be related to concentration variables using any one of the equations proposed by the above-mentioned authors. To illustrate the form and complexity of these equations, a three-suffix (so-designated because the last term refers to a three-way interaction) Margules equation for a ternary system is shown here:

$$\log \gamma_1 = x_2^2 \left[A_{1-2} + 2x_1 (A_{2-1} - A_{1-2})\right]$$
$$+ x_3^2 \left[A_{1-3} + 2x_1 (A_{3-1} - A_{1-3})\right]$$
$$+ x_2 x_3 \left[1/2 (A_{2-1} + A_{1-2} + A_{3-1} + A_{1-3} - A_{2-3} - A_{3-2})\right.$$
$$+ x_1 (A_{2-1} - A_{1-2} + A_{3-1} - A_{1-3})$$
$$\left. + (x_2 - x_3)(A_{2-3} - A_{3-2}) - (1-2x_1) C^*\right] \qquad (23)$$

or:

$$\log \left(\frac{\gamma_1}{\gamma_2}\right) = x_2^2 A_{1-2} - x_1^2 A_{2-1} + 2x_1 x_2 (A_{2-1} - A_{1-2})$$
$$+ x_3 \left[2x_1 A_{3-1} - 2x_2 A_{3-2} + x_3 (A_{1-3} - A_{2-3})\right. \qquad (24)$$
$$\left. + (x_2 - x_1)[1/2 (A_{1-2} + A_{2-1} + A_{1-3} + A_{3-1} + A_{2-3} + A_{3-2}) - C^*]\right]$$

where:

γ_i = activity coefficient for component "i",

x_i = mole fraction of component "i" in the liquid phase,

C^* = ternary constant for the system,

A_{i-j} = end values of the logarithms of the activity coefficients in the binary systems.

The values of A_{i-j} may be defined as:

$$A_{i-j} = \underset{\substack{x_i \to 0 \\ x_j \to 1}}{\text{limit}} \log \gamma_i \qquad (25)$$

Values of $\log \gamma_2$, $\log \gamma_3$, $\log \frac{\gamma_2}{\gamma_3}$, and $\log \frac{\gamma_3}{\gamma_1}$ may be obtained by application of the "rotation principle" whereby the subscripts in the equations for $\log \gamma_1$, and $\log (\frac{\gamma_1}{\gamma_2})$ are changed by writing 2 instead of 1, 3 instead of 2, and 1 instead of 3.

For a symmetrical ternary system:

$$A_{i-j} = A_{j-i} = A_{ij} = A_{ji} \qquad (26)$$

The equation for $\log \gamma_1$ can then be simplified to give the following expression:

$$\log \gamma_1 = A_{12}x_2^2 + A_{13}x_3^2 + x_2x_3[A_{12} + A_{13} - A_{23} - C^* (1-2x_1)] \qquad (27)$$

The equation for $\log (\frac{\gamma_1}{\gamma_2})$ in a symmetrical ternary system can be obtained in a similar manner and the equations for $\log \gamma_2$, $\log \gamma_3$, $\log (\frac{\gamma_2}{\gamma_3})$, and $\log (\frac{\gamma_3}{\gamma_1})$ can again be obtained by application of the "rotation principle."

Wohl[81] presents a rather extended discussion of the various equations for representing the dependence of the activity coefficients on concentration for binary and ternary systems. He presents a five-suffix equation and shows that the two-suffix Van Laar, three-suffix Margules, and three-suffix Scatchard-Hamer equations an be derived from this five-suffix equation if the proper simplifications are applied.

He also develops three-suffix and four-suffix equations of the Van Laar type and four-suffix equations of the Margules and Scatchard-Hamer types. In addition, the later equation of Redlich and Kister [61] appears to be similar in form to Wohl's four-suffix Margules type equation.

This activity coefficient approach to the correlation of vapor-liquid equilibria has proved useful in the region below the critical temperatures of all the components of the system. It is particularly useful in correlating data for systems in which one or more azeotropes are formed. However, as may be observed from equations 23, 24, or 27, the types of relationships involving the activity coefficients and the phase composition variables are very complex and the use of a digital computer is almost a necessity if a number of calculations are to be made using these equations.

Convergence Pressure

Many investigators have used the concept of "convergence pressure" in correlating vapor-liquid equilibrium data [33] [34] [43] [56] [57] [64] [80]

Most of these correlations predict the equilibrium ratios of the light hydrocarbons in binary, ternary, or multicomponent mixtures of the normal paraffin hydrocarbons. Only one correlation -- the work of Lenoir and Hipkin [42] -- has found much success in predicting the equilibrium ratios of hydrogen in hydrogen-hydrocarbon mixtures.

The convergence pressure of a system for a given temperature is the pressure at which the equilibrium ratios of all components of the system appear to approach unity. The convergence pressure

of a binary system is the critical pressure of the system at the temperature in question. For ternary and multicomponent systems the convergence pressure must be estimated from information about one or more of the equilibrium phase compositions.

Hadden [33], in an earlier work, prepared three nomograms for ideal equilibrium vaporization ratios from -200°F to 1000°F at pressures from 10 psia to 2000 psia. Also included were correlations for obtaining the deviation of the equilibrium ratios from the ideal values as the convergence pressure is approached. In a later work [34], Hadden postulates that convergence pressure is a function of the operating temperature and the liquid phase composition exclusive of the lightest component concentration.

Organick and Brown [56] [57] employ an empirical relationship based on critical pressures for methane binary systems to obtain a "correlating pressure" for any binary or complex mixture of hydrocarbons. The correlating pressure is a function of the equilibrium pressure, the molal average boiling point of the vapor phase, and the weight average equivalent molecular weight of the liquid phase. The equivalent molecular weight of a component is a function of its boiling point for paraffinic and olefinic compounds, and also a function of the characterization factor for naphthenics, aromatics, and other non-paraffins of high molecular weight.

A convergence pressure parameter is also used by Winn[80] along with a solvent character parameter to correlate vapor-liquid equilibria in the light hydrocarbon systems. This correlation consists of a nomogram which is applicable from 40°F to 800°F and

from 10 psia to 5000 psia.

Rzasa, Glass, and Opfell [64] have investigated the use of convergence pressure to correlate complex hydrocarbon systems containing heptanes and heavier. The correlation is based on the relationship of the critical pressure of the system to the product of the molecular weight and specific gravity of the heptanes-plus fraction.

Lenoir and co-workers [42] [43] favor the use of the concept of hypothetical binaries to compute convergence pressures of ternary and multicomponent mixtures. This is accomplished by identifying the hypothetical components by means of effective boiling points. The normal boiling points of the individual components are used to compute the effective boiling points of the lighter and heavier components.

While convergence pressure has been used successfully for the correlation of vapor-liquid equilibrium data in the hydrocarbon systems [53], it has failed, thus far, to predict equilibrium data in the hydrogen-light hydrocarbon systems with an equal degree of accuracy. Benham [13] reports the inability of convergence pressure to satisfactorily correlate data on the hydrogen-methane-propane ternary system and data on a complex system containing hydrogen, methane, ethylene, ethane, propylene and propane. Using the concept of effective boiling points of the heavy equivalent component and the light equivalent component, Lenoir and Hipkin [42] have correlated the equilibrium ratios of hydrogen in the hydrogen-light hydrocarbon systems with a statistical

deviation of 11.3% for a total of 375 comparisons with measured values of hydrogen equilibrium ratios.

Equations of State

Still another approach to the problem of correlating vapor-liquid equilibrium data has been through the use of equations of state. A prime requisite for this approach is that an equation of state be found that will adequately describe both the vapor and liquid states.

There are many equations of state available in the literature, such as the well-known Van der Waals, Berthelot, Dieterici, Keyes, and Beattie-Bridgeman equations [35] [72]. However, all of these equations have the disadvantage of being inapplicable to the liquid state. These equations adequately represent the gaseous state with varying degrees of accuracy over various temperature and pressure ranges, however, at densities greater than the critical density and temperatures below the critical temperature, these equations are all seriously in error.

Only two equations are now known that may be used to adequately represent P-V-T relationships at densities above the critical density. These are the equations of Martin and Hou [50] and Benedict, Webb, and Rubin [7] [8] [9] [10]. Martin and Hou[50] state that their equation has been applied to seven different gases for densities up to about 1.5 times the critical density. Above 1.5 times the critical density the equation predicts too much curvature of the isometrics. The Benedict-Webb-Rubin equation has been stated to be fairly satisfactory to about twice the

critical density and down to temperatures well below the critical [7] [35] [72].

Since the Benedict-Webb-Rubin equation has the ability to cover a greater range of densities above the critical density, it should be the most useful equation of state for predicting vapor-liquid equilibria. It has been used in correlating experimental vapor-liquid equilibrium data in binary and ternary systems of the light hydrocarbons [10], in the carbon monoxide-nitrogen binary system [66], in the carbon dioxide-propane binary system [24], in the nitrogen-methane binary system [70], and, most recently, in the methane-ethane-propane ternary system [60]. Good agreement between the predicted values and experimental data was obtained in the binary and ternary systems of the light hydrocarbons [10], and, after an adjustment of one of the parameters in the equation of state, satisfactory agreement was also obtained in the correlation of the nitrogen-methane binary system [70]. In testing the use of the equation of state for the correlation of vapor-liquid equilibria in the carbon monoxide-nitrogen system, the experimental data of Torocheshnikov [73] were used and a correlation was obtained which was satisfactory within the degree of uncertainty of the experimental measurements [66]. It is possible that many of the deviations observed in the correlation of the carbon monoxide-nitrogen system resulted from discrepancies between some of the vapor pressures for the pure components as reported by Torocheshnikov and those used in fitting the constants in the equation of state [66].

In the correlation of the carbon dioxide-propane binary system by means of the Benedict-Webb-Rubin equation of state, Cullen and Kobe [24] obtained values of the equilibrium ratio for carbon dioxide which were in error by as much as 100 percent at the lowest temperatures for which the correlation was attempted (40°F). This error could possibly be overcome by an adjustment of one or more of the mixture parameters in the equation of state, such as was done by Stotler and Benedict [70] in the correlation of the nitrogen-methane system. However, the value of the equation of state for the prediction of vapor-liquid equilibrium data is greatly reduced unless a general method can be used in combining the constants for the pure components to obtain the constants which will give satisfactory results for various mixtures of the components.

The methane-ethane-propane ternary system was also correlated by Price and co-workers [60] using the Benedict-Webb-Rubin equation. A comparison between the experimental data taken by Price and the predicted vapor-liquid equilibrium data showed that the equilibrium ratios predicted by the equation were greatly in error at the lower temperatures where the density of the liquid phase was greatest. This was probably due to the fact that the limits of the equation were being exceeded (density of the liquid phase was greater than twice the critical density.)

The manner in which an equation of state, specifically the Benedict-Webb-Rubin equation of state, can be utilized for the prediction of vapor-liquid equilibria will now be illustrated.

The Benedict-Webb-Rubin equation of state can be stated in the following form:

$$P = RTd + (B_oRT - A_o - \frac{C_o}{T^2})d^2 + (bRT - a)d^3$$

$$+ a\alpha d^6 + \frac{cd^3}{T^2}\left[(1 + \gamma d^2)e^{-\gamma d^2}\right] \qquad (28)$$

where P is the absolute pressure, T is the absolute temperature, d is the molal density, and R is the universal gas constant, in consistent units. The eight parameters A_o, B_o, C_o, a, b, c, α and γ are numerical constants for pure substances and functions of composition for mixtures. Benedict and co-workers[9] suggest that the dependence of these eight parameters on mole fractions, z_i, be represented as follows:

$$B_o = \left[\sum_i z_i B_{o_i}\right] \qquad (29)$$

$$A_o = \left[\sum_i (z_i A_{o_i}^{1/2})\right]^2 \qquad (30)$$

$$C_o = \left[\sum_i (z_i C_{o_i}^{1/2})\right]^2 \qquad (31)$$

$$b = \left[\sum_i (z_i b_i^{1/3})\right]^3 \qquad (32)$$

$$a = \left[\sum_i (z_i a_i^{1/3})\right]^3 \qquad (33)$$

$$c = \left[\sum_i (z_i c_i^{1/3})\right]^3 \tag{34}$$

$$\alpha = \left[\sum_i (z_i \alpha_i^{1/3})\right]^3 \tag{35}$$

$$\gamma = \left[\sum_i (z_i \gamma_i^{1/2})\right]^2 \tag{36}$$

With the use of these equations, the equation of state for mixtures may be derived from data on pure components without the need for supplementary data on mixtures.

With considerable mathematical manipulation, relations for the thermodynamic properties corresponding to the Benedict-Webb-Rubin equation of state can be derived. Specifically, the fugacity relationship is:

$$\begin{aligned} RT\ell n\left(\frac{f_i}{z_i}\right) = RT\ell ndRT &+ \left[(B_o - B_{oi})RT - 2(A_o A_{oi})^{1/2} - \frac{2(C_o C_{oi})^{1/2}}{T^2}\right] d \\ &+ \frac{3}{2}\left[RT(b^2 b_i)^{1/3} - (a^2 a_i)^{1/3}\right] d^2 \\ &+ \frac{3}{5}\left[a(\alpha^2 \alpha_i)^{1/3} + \alpha(a^2 a_i)^{1/3}\right] d^5 \\ &+ \frac{3d^2(c^2 c_i)^{1/3}}{T^2}\left[\left(\frac{1-e^{-\gamma d^2}}{\gamma d^2}\right) - \left(\frac{e^{-\gamma d^2}}{2}\right)\right] \\ &- \frac{2d^2 c}{T^2}\left(\frac{\gamma_i}{\gamma}\right)^{1/2}\left[\left(\frac{1-e^{-\gamma d^2}}{\gamma d^2}\right) - \left(e^{-\gamma d^2}\right) - \left(\frac{\gamma d^2 e^{-\gamma d^2}}{2}\right)\right] \end{aligned} \tag{37}$$

where the parameters with the subscript "i" refer to the parameters for the pure component "i" and the parameters without subscript refer to the mixture parameters. The value of z_i refers to the mole fraction of component "i" in either the liquid or vapor phase depending upon the phase for which the fugacity is being calculated.

It should be noted that this equation for fugacity contains only the pure component parameters, the mixture parameters, temperature, and phase density. A knowledge of these variables leads to the evaluation of the ratio of fugacity in the liquid phase to mole fraction in the liquid phase and to the evaluation of the ratio of fugacity in the vapor phase to mole fraction in the vapor phase.

$$RT\ell n \left(\frac{f_{i_L}}{x_i}\right) = \varphi_1 \left(T, d_L, A_o, B_o, \ldots\right) \tag{38}$$

$$RT\ell n \left(\frac{f_{i_V}}{y_i}\right) = \varphi_2 \left(T, d_V, A_o, B_o, \ldots\right) \tag{39}$$

Since the fugacity in the liquid phase is equal to the fugacity in the vapor phase at equilibrium:

$$f_{i_L} = f_{i_V} \tag{40}$$

$$\frac{\left(\frac{f_{i_L}}{x_i}\right)}{\left(\frac{f_{i_V}}{y_i}\right)} = \frac{y_i\, f_{i_L}}{x_i\, f_{i_V}} = \frac{y_i}{x_i} = K_i \qquad (41)$$

Assuming a knowledge of the pure component parameters, constant temperature and pressure, and a knowledge of the liquid phase composition, the composition of the vapor phase could be calculated from the equation of state as follows:

1. Assume a logical set of K values for all components.

2. Using these assumed K values and liquid phase composition, calculate an assumed vapor phase composition.

3. Using Equations (29) to (36), calculate the mixture parameters for both the liquid and the assumed vapor phase composition.

4. Using the pressure, temperature, and the mixture parameters, calculate the liquid phase density and the density of the assumed vapor phase. This can be done by solving Equation (28) by trial-and-error.

5. Using temperature, pure component and mixture parameters, and the phase densities, calculate the values of

   $\frac{f_{i_L}}{x_i}$ and $\frac{f_{i_V}}{y_i}$ from Equation (37).

6. Using Equation (41), calculate new K values for each component of the mixture.

7. Check these calculated K values with the values assumed in Step 1.

8. If the K values do not check, assume these new K values and proceed again from Step 2 to Step 7.

9. Repeat the procedure until the assumed K values and the calculated K values are identical.

The above procedure for the calculation of vapor-liquid equilibria is an involved and tedious one. The use of a digital computer is almost a necessity if many calculations are to be made employing this procedure. In order to shorten the procedure and simplify engineering design calculations, Benedict and co-workers (11) (12) developed charts for representing the fugacities and vapor-liquid equilibrium ratios in mixtures of light hydrocarbons as functions of pressure, temperature, and the molal average boiling point of the liquid and vapor phases. These charts (Kellogg Charts) (47) (48) cover a temperature range from -100°F to +400°F and a range of molal average boiling points from -255°F to + 180°F. For pressures between 14.7 psia and 1000 psia the charts show the dependence of the equilibrium ratio on the temperature and the molal average boiling point of the vapor and liquid phases, while for pressures between 1000 psia, and 3600 psia, the charts show the dependence of the ratio of fugacity to mole fraction (f_i/z_i) on temperature and the molal average boiling points. The set of 324 charts covers 12 hydrocarbons from methane to n-heptane.

The molal average boiling point has also been employed by DePriester (26) in his correlation for equilibrium ratios in mixtures of light hydrocarbons. The variables used in this correlation are again: pressure, temperature, and molal average boiling point of the liquid and vapor phases. The equilibrium ratios are obtained as the product of vapor-phase and liquid-phase fugacity functions. Briefly, the correlation can be stated:

$$K_i = A_i B_i = (y_i/x_i) \qquad (42)$$

$$A_i = \varphi_1 \left(T, P, MABP_L \right) \tag{43}$$

$$B_i = \varphi_2 \left(T, P, MABP_V \right) \tag{44}$$

where:

A_i = liquid-phase fugacity function for component "i",

B_i = vapor-phase fugacity function for component "i",

$MABP_j$ = molal average boiling point of phase "j",

φ_1 and φ_2 = graphically correlated functions of the variables T, P, and $MABP_j$.

A method similar to DePriester's was used by Price [59] in correlating his data on the methane-ethane-propane ternary system. However, Benham [13] found that the use of molal average boiling point as a variable would not satisfactorily correlate his data on hydrogen-light hydrocarbon systems.

Kinetic Theory

A basic approach to the problem of correlating and predicting vapor-liquid equilibrium data is through a consideration of the kinetic theory of liquids. Frenkel [30] is one of the early investigators who considered the problem from the standpoint of kinetic theory. A far more comprehensive treatment of the subject is available in the work of Hirschfelder, Curtiss, and Bird [35].

Hirschfelder and co-workers discuss the use of the quantum mechanical partition function and the pair distribution function in the development of an equation of state for dense gases and liquids.

They show that the use of either of these functions leads to an expression for the compressibility factor as a power series in terms of the density.

In applying the partition function method to the liquid state, Hirschfelder makes various approximations to account for liquid structure, such as the "lattice theories" and the "free volume theories." The lattice theories fall into two general categories: the "cell theories," in which each molecule is confined to its own cell and no account is taken of the fact that some of these cells are empty, and the "hole theories" which attempt to account for these vacant cells. The "free volume" theories are based on the concept of an "exact" free volume , which has an extremely complicated geometrical shape, and a "smeared" free volume, which replaces the angle-dependency of the exact free volume by an approximately-equivalent spherically-symmetric function. The smeared free volume is essentially the largest sphere which can fit inside the exact free volume.

Using the Lennard-Jones 6-12 potential (41) to represent the intermolecular potential energy function for non-polar molecules, and the Stockmayer potential (69) to represent the intermolecular potential energy function for polar molecules, Hirschfelder (35) develops his kinetic theory of dense gases and liquids, and proceeds to compare calculated properties with the experimentally determined values. In most cases the calculated values are qualitatively good but quantitatively unsatisfactory.

One possibility which is discussed by Hirschfelder, and which is satisfactorily employed by Hobson and Weber[36] for the correlation of binary hydrocarbon systems, is the principle of corresponding states. Hobson and Weber have shown that the production of a generalized saturation curve depends on the ability of the theorem of corresponding states to correlate the reduced temperature as a function of reduced pressure and the critical compressibility factor. The critical compressibility factors for most substances fall within the range of approximately 0.2 to 0.33, although the theorem of corresponding states requires that this ratio be a constant. Hobson and Weber have correlated the compressibility factors of the saturated liquid and saturated vapor phases as functions of the reduced pressure and reduced temperature at a constant average critical compressibility factor of 0.270. Since most of the hydrocarbons have critical compressibility factors in this range, the correlation is satisfactory for these hydrocarbon systems. However, for systems containing non-hydrocarbons, the correlation may lead to serious errors. (The critical compressibility factor for hydrogen is 0.304, nitrogen is 0.292, and methane is 0.290)[35].

Although a great deal has been learned in recent years during the development of these various theories, much more theoretical and numerical work will have to be done before an adequate description of the properties of dense gases and liquids is achieved. Until this time, the development of a generalized method for the prediction of vapor-liquid equilibrium data by means of the kinetic theory of liquids appears doubtful.

APPENDIX B

OPERATIONAL PROCEDURE

This work would not be complete without a description of the methods employed in preparing the equipment for operation and in operating the equipment during the runs. These methods will be reviewed, and the time intervals required to attain equilibrium will be discussed. The method employed in sampling the liquid and vapor phases will be illustrated.

Preparation for the Run

Since the process of cooling the air bath to the desired temperature required from four to eight hours, the first step in preparing for a run was to begin cooling the constant temperature bath by inserting crushed dry ice. Regardless of the final temperature desired, the first cooling was always accomplished with dry ice. The cooling was usually begun in the evening and the constant temperature bath was left to cool overnight with the circulating fan running to hasten the cooling process. If a temperature of -200°F was to be reached, liquid nitrogen was added to further cool the bath after a temperature of approximately -100°F had been attained. When the desired temperature was reached, the flow of liquid nitrogen was controlled by the Brown Recorder-Controller to maintain the constant temperature. While the amount of time required for the desired temperature to be reached and for good control to be established was large, some of this time could be used

in evacuating the system and flushing it several times with the hydrocarbons and gases to be used in the following run. After flushing and evacuating the cell, the proper hydrocarbons were admitted to the cell and the system was pressurized by addition of hydrogen or nitrogen from the pressure generation section.

Operation of Equipment During the Run

Since the equilibrium cell used in these investigations was a blind cell, it was impossible to visually locate the liquid level in the cell and determine how much liquid was present at any given time. This was particularly disturbing when several successive runs were to be made without recharging the cell with fresh liquid hydrocarbons. On several occasions the analyses of the samples withdrawn from the liquid and vapor sample lines proved that little or no liquid remained in the equilibrium cell after a series of runs. The amount of hydrocarbon which was initially placed in the cell was extremely critical in cases where the hydrocarbon was very volatile such as in the hydrogen-nitrogen-methane system. Therefore, it was necessary to make some preliminary assumptions as to the solubilities and volatilities of the various constituents before a run was made in order that the proper amount of the constituents could be charged. Too great an amount of liquid in the equilibrium cell resulted in non-representative, unreproducible vapor samples, while too great an amount of vapor resulted in extremely good, reproducible vapor samples, but very poor, non-representative liquid samples. The unreproducible vapor

samples were probably caused by entrainment of the liquid in the vapor stream and by poor, and possibly sporadic, pumping rates caused by the large head of liquid through which the vapor stream returning to the cell must pass. Unreproducible liquid samples containing large amounts of the very volatile constituents were the unmistakeable indications that an insufficient quantity of liquid phase was present in the equilibrium cell. In order to avoid most of these difficulties it was extremely important to know the amount of hydrocarbon originally charged to the system.

Two methods were used to measure the quantity of hydrocarbons charged to the cell. When charging a hydrocarbon such as ethane to the cell, the method used was to maintain the cell at some temperature less that room temperature, where condensation of the hydrocarbon occured at some moderate pressure, and to introduce the hydrocarbon until the pressure in the system exceeded that of the hydrocarbon vapor pressure at the cell temperature. The cell was then assumed to be completely full of the liquid hydrocarbon. A wet test meter was then used to measure the amount of hydrocarbon bled off from the system until a predetermined amount of the hydrocarbon remained.

The second method used to determine the amount of a hydrocarbon charged to the cell involved measuring the hydrocarbon as a gas in the pressure generation section. The oil reservoir (F in Figure 2) was calibrated in cubic centimeters, so that, by filling the cylinder (C in Figure 2) with gas, carrying out the

compression process, and injecting the compressed gas into the system, the amount of hydrocarbon charged could be calculated from the known room temperature, original and final pressure in the compression cylinder, and the volume of oil pumped into the compression system. In this manner the quantity of any of the gases added to the system through the pressure generation section could be determined. (As shown on Figure 2, the ethane was added to the system in a different manner than the more volatile gases since the ethane would have liquified in the pressure generation system if it were compressed to its vapor pressure at room temperature.)

After the measured amount of hydrocarbon had been charged to the cell, hydrogen or nitrogen were added until a pressure slightly greater than the desired pressure was obtained. The magnetic circulating pump was then started so that the contacting of vapor and liquid phases might begin. As the circulation of the vapor through the liquid phase proceeded, the pressure generally dropped and more of the volatile constituents would have to be added to the system in order to maintain the pressure at a desired level.

Approach to Equilibrium

The vapor recirculation was continued for several hours after constancy of pressure was attained since it was determined that constancy of pressure is not a good criterion of ternary or quaternary vapor-liquid equilibrium. In order to assure true

equilibrium between the phases, it was found necessary to withdraw samples of both phases at successive intervals of time and obtain analyses of them. When successive analyses of both phases showed identical liquid and vapor phase compositions within the analytical accuracy of the mass spectrometer, it was assumed that equilibrium had been attained. The time intervals between successive samplings were usually one or two hours, but never less than one hour. In one instance the time interval between two samplings was eight hours, with the agreement between the samples of both phases well within the analytical accuracy of the mass spectrometer. The amount of time required to reach equilibrium varied greatly, depending upon the system being studied, as well as upon the pressure, temperature, and pumping rate in the vapor recirculation system.

Sampling of the Liquid and Vapor Phases

The sample of the liquid phase was always removed before sampling of the vapor phase was attempted since the pressure decrease accompanying the removal of the liquid phase sample was much less than that accompanying the removal of the vapor phase sample. Thus, it was much easier to hold the pressure constant while removing a liquid sample and, as a result, the vapor sample, which was taken immediately after removal of the liquid sample, was uneffected by the removal of the first sample. Had the vapor samples been taken first, the liquid samples would possibly have suffered severe composition changes due to the pressure fluctuations

resulting from the greater difficulty in holding the pressure constant while sampling the vapor phase.

The following procedure was found to yield representative, reproducible liquid samples:

1. The sampling system, including the sample bulb, was evacuated to less than 1 mm of mercury pressure.

2. The mercury in the pressure generation system was compressed to a pressure 300-500 psi greater than the pressure in the equilibrium cell so that the mercury would be available at a pressure considerably greater than the cell pressure.

3. The valve leading to the evacuated sample bulb was closed as was the valve leading to the vacuum pump.

4. The liquid sample valve (Q in Figure 2) was opened slightly until the evacuated sampling system was filled to one atmosphere pressure with the liquid phase sample. (The valve leading to the high pressure mercury supply was opened slightly at the same time as the liquid sample valve so that mercury could enter the variable-volume cell (M in Figure 2) and decrease the volume of the system to compensate for the volume occupied by the liquid phase sample being withdrawn.)

5. As soon as the pressure in the sampling system reached one atmosphere, the valve to the wet test meter (V in Figure 2) was opened so that the liquid phase sample being withdrawn could be measured and vented. Meanwhile, the amount of mercury entering the system was carefully being regulated so

that the system pressure would remain constant during the sampling operation.

6. When 0.150 cubic feet of the sample (at room temperature and atmospheric pressure) had been bled from the liquid sample line, the valve leading to the evacuated sample bulb was opened and a sample of the flowing stream was obtained. The valve on the sample bulb was then closed. The liquid sample valve and the valve to the high pressure mercury supply were then closed as was the valve to the wet test meter.

7. The sample bulb was then removed and properly marked, and the sampling system was again evacuated in preparation for the removal of a vapor phase sample.

The procedure for obtaining representative, reproducible vapor phase samples was the same as the procedure for taking the liquid phase sample except that only 0.015 cubic feet of the flowing vapor phase sample (at room temperature and atmospheric pressure) had to be bled from the lines before the sample was withdrawn for analysis.

The amount of sample which had to be bled from the sample lines in order to completely flush the lines was determined by withdrawing vapor and liquid phase samples after varying amounts of the sample had been bled from the lines. It was then determined how much sample had to be removed before a reproducible sample of either phase could be obtained. The results of these tests are shown in Figure 51. While the amount of bleed required from the sample lines is a function of the pressure and temperature under

investigation, severe conditions were imposed during these tests so that the maximum values would be obtained. Safe values were found to be: 0.150 cubic feet of bleed volume for the liquid phase sample line, and 0.015 cubic feet of bleed volume for the vapor phase sample line (both at atmospheric pressure and room temperature).

After sampling, all samples were analyzed using the CEC 21-103B analytical mass spectrometer.

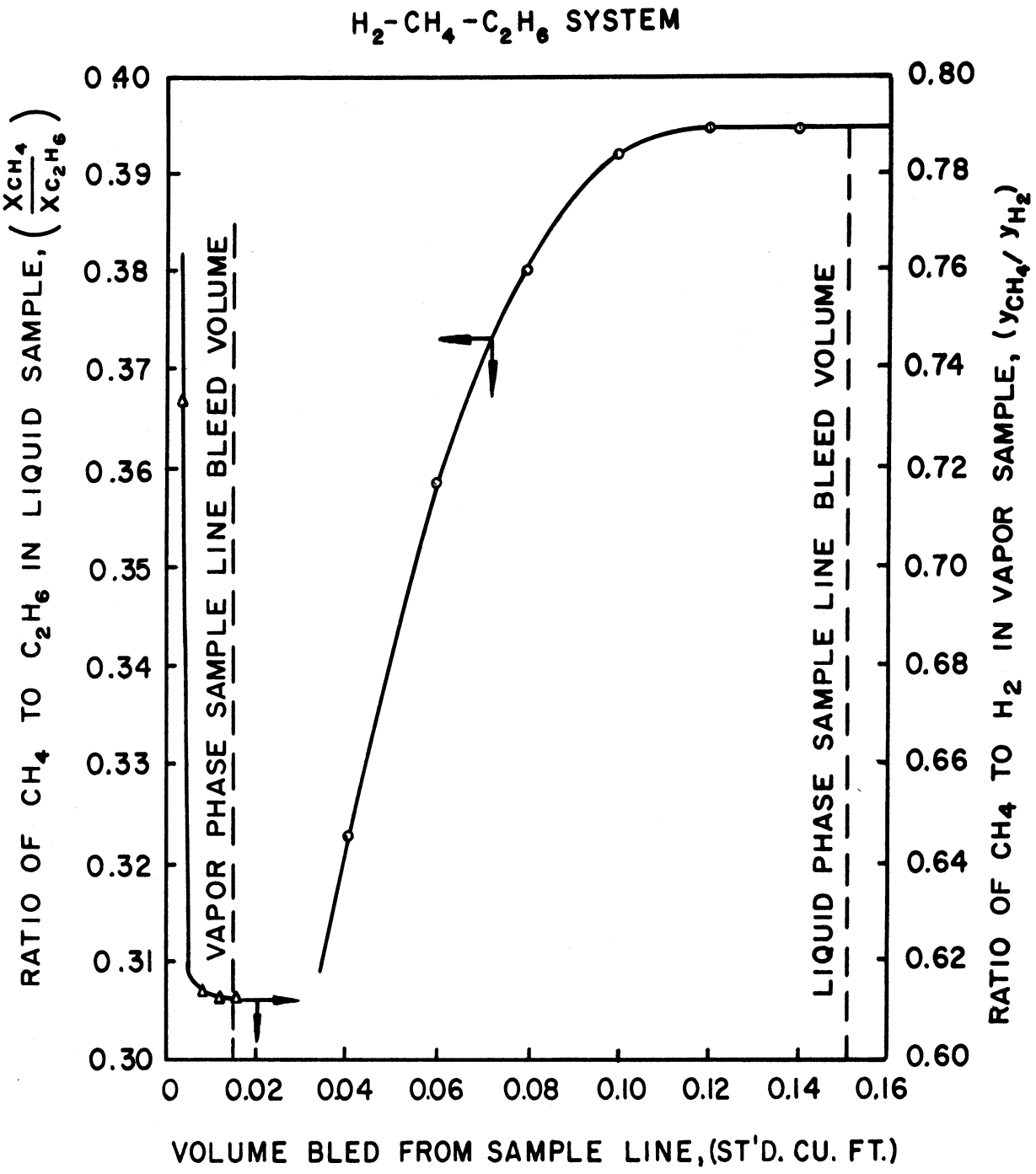

Figure 51. Reproducibility of Liquid and Vapor Phase Samples as a Function of the Volume Bled from Sample Lines

APPENDIX C

CALIBRATION OF PRESSURE GAGES AND THERMOCOUPLES

The pressure gages and thermocouples used in this study were calibrated before any experimental data were obtained. The three junction thermopile used to determine the temperature in the thermowell of the equilibrium cell was calibrated twice during the course of the investigations.

The calibration data for the three pressure gages in the Equilibrium Cell and Circulation Section (O in Figure 2) are given in Table XII. These data were obtained using an American Multipar dead weight gage tester.

Three temperatures were used in the calibration of the thermocouples. These temperatures were: the freezing point of water, the sublimation temperature of solid carbon dioxide, and the boiling point of liquid nitrogen.

The voltage difference, ΔE, between the measured emf of thermopile No. 6 and the standard value as quoted in the literature [3], is plotted in Figure 52 as a function of the standard emf value, E. This plot was used to obtain the emf for intermediate temperatures.

The potentiometer which was used to measure the emf of the thermocouples was also calibrated. This potentiometer was calibrated against a Leeds-Northrup K-2 potentiometer which previously had been calibrated by the Bureau of Standards.

No measurable error could be detected in the readings of the potentiometer used in these studies.

TABLE XII

CALIBRATION OF PRESSURE GAGES

Date: February 15, 1956

Actual Pressure (psi)	Gage Reading (psi)	
	Up	Down
Gage No. C2-470		
300	307	308
400	405	407
450	455	458
475	480	482
500	504	507
550	555	556
650	658	658
750	758	758
Gage No. C2-444		
250	250	250
500	495	495
750	745	745
1000	1000	1000
1250	1250	1250
1500	1500	1500
1750	1755	1755
2000	2005	2005
2250	2255	2255
2500	2500	2500
2750	2750	2750
Gage No. C2-529		
250	260	290
500	560	600
750	795	805
1000	1000	1010
1500	1500	1550
2000	2010	2030
2500	2500	2510
3000	3000	3020
3500	3490	3490
4000	4000	4010
4500	4485	4490
5000	5005	5005

Gages recalibrated: 2/7/58 (no measureable change in calibration at pressures less than 1500 psi)

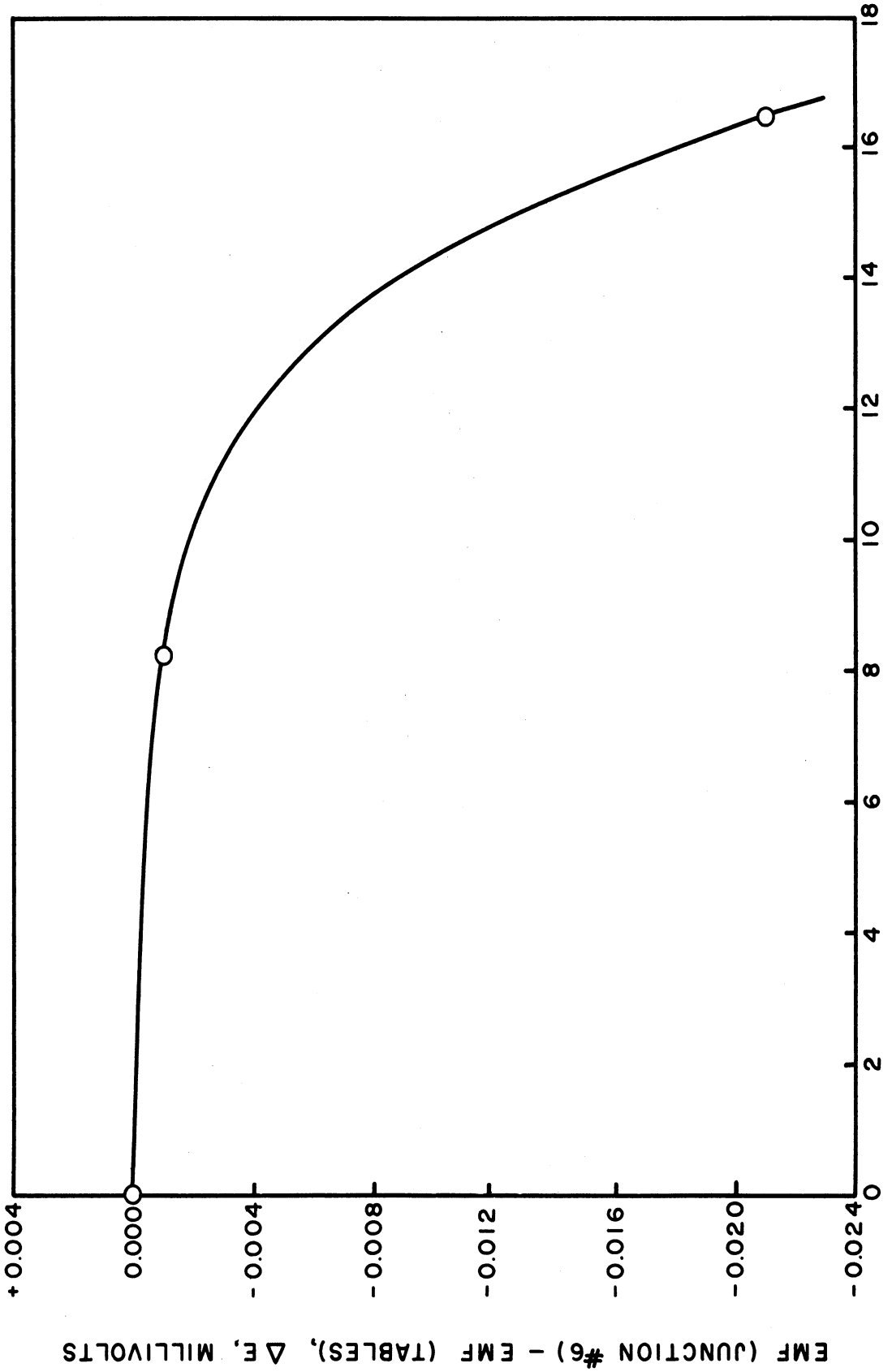

Figure 52. Calibration Chart for Thermopile Number Six

APPENDIX D

ANALYSIS USING THE MASS SPECTROMETER

In order to understand the limiting accuracy of the procedures employed in the analysis of the liquid and vapor phase samples, the theory of operation of the mass spectrometer will be discussed and the CEC 21-103B, the instrument on which all of the analyses for this work were made, will be described briefly. The errors involved in the analysis and the methods employed to minimize these errors will be discussed. Sample calculations for a vapor phase sample and a liquid phase sample will be presented.

Theory of Operation of the Mass Spectrometer

An analytical mass spectrometer is an instrument in which gaseous molecules, admitted at low pressures to the analyzer section from an inlet sample volume, are fragmented and ionized by a stream of electrons. These ions are then sorted into groups according to their mass to charge ratios (m/e), and measured according to their relative abundance.

The fragmented and ionized molecules are sorted in the following manner: The ions formed are accelerated by an adjustable voltage (Ion Accelerating Voltage), and are passed through a magnetic field where they are deflected in a circular path, the radius of which is dependent upon the mass to charge ratio of the ion, the magnetic field strength, and the ion accelerating voltage.

If the magnetic field strength is held constant, it is possible to focus the ions of a given mass to charge ratio on a collector plate at the far end of a semi-circular analyzer tube by adjusting the ion accelerating voltage to the proper value for the given ion. For each mass to charge ratio, at constant magnetic field strength, there is only one ion accelerating voltage which allows the ions of given mass to charge ratio to reach the collector plate. All other ions will be grounded on the sides of the analyzer tube. The ions striking the collector plate give up their charge which is amplified and recorded. The current produced from the collector plate is a measure of the abundance of the ions of the particular mass to charge ratio for which the instrument is focused at the time of collection.

If the conditions under which the ionization takes place can be held constant, the molecules of a given compound will fragment and ionize in a fixed pattern, called the "mass spectrum" of the compound. A whole spectrum of the ions may be obtained by slowly and systematically varying the ion accelerating voltage from a high value to a low one, maintaining a constant magnetic field. The largest peak in the spectrum of a pure compound is called the "major peak" of the compound, and the peak at the mass to charge ratio corresponding to the molecular weight of the compound is called the "parent peak". The relative heights of the peaks compared to any one of the peaks selected as a reference peak (usually the major peak) is called the "cracking pattern" for the compound. The reference peak used in calculating a cracking

pattern for a compound is known as the "base peak". The important peaks in the cracking patterns for hydrogen, nitrogen, methane and ethane are given in Table XIII, and the mass spectrum of a typical analysis is shown in Figure 53.

The height of any peak in a mass spectrum of a compound is directly proportional to the pressure of that compound in the inlet system of the mass spectrometer. If the partial pressure of a compound in the inlet system of an instrument were doubled, each of the peak heights resulting from the fragmentation and ionization of that compound would also be exactly doubled. Since the cracking pattern for a compound is the ratio of the peak heights, the cracking patterns for all compounds are independent of the sample inlet pressure.

The relationship between the height of any peak in the spectrum of a pure compound and the pressure of the compound in the inlet system of the instrument is expressed as the "sensitivity" of the instrument for that particular compound at the particular mass to charge ratio in question. Thus:

$$\text{Sensitivity} = \frac{\text{Peak height in scale units (at a specific m/e)}}{\text{Microns pressure in the inlet system}}$$

Using this sensitivity referred to some base peak and the cracking pattern for each compound, the mole percentages of each compound in a mixture of gases can be computed. The mass spectrometer is constructed and operated in such a way that the sensitivity and cracking pattern for a certain molecular species does not change from that obtained by running a calibration standard

for the pure compound even though that compound exists in a mixture with many other compounds. The spectrum of a mixture is the linear superposition, or simple summation, of the individual spectra of all the components. Given the spectrum of a mixture and the sensitivities and cracking patterns of all the components of the mixture, the composition of the mixture can be determined.

Analysis Using the CEC 21-103B

The CEC 21-103B mass spectrometer, which was used for all of the analyses in this study, requires less than 0.2 cc of gas at standard conditions for analysis. The gas is transferred to a three liter volume from which it passes into the analyzer assembly through a small leak. An electronic, extremely-sensitive micromanometer is used to determine the pressure of the gas sample in the inlet sample volume. The inlet pressure is commonly from 10 to 40 microns. Using sensitive light-beam galvanometers and high amplification, a photographic record of the relative abundance of the ions with certain mass to charge ratios is obtained from the CEC 21-103B mass spectrometer. The cracking pattern coefficients given in Table XIII and the mass spectrum shown in Figure 53 were obtained on this instrument.

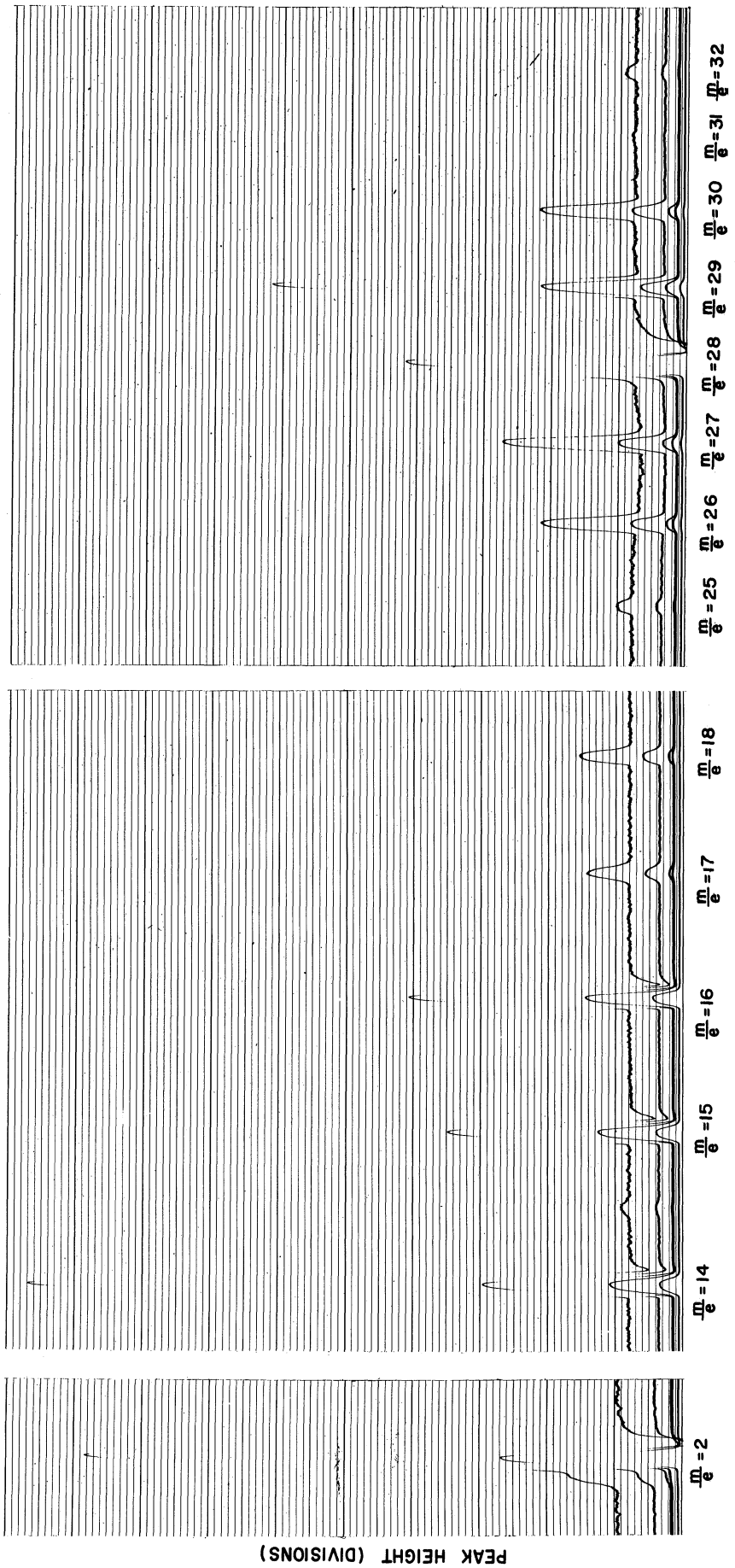

Figure 53. Mass Spectrum of a Mixture Containing Hydrogen, Nitrogen, Methane, and Ethane

Errors Involved in the Analysis

When analyzing a mixture in which all of the components are present in the mixture in substantial amounts, the mixture peaks are large compared with any instrument background. By background is meant those peaks which are present in the instrument when no sample is passing through. In the high vacuum system of the mass spectrometer there is always a small m/e = 18 background peak due to traces of water, and there is usually a m/e = 28 background due to traces of CO in the system. Also, the time required to pump various samples out of the inlet vacuum system and the exhaust vacuum system varies from compound to compound so that the background may change slightly because of traces of preceding samples remaining in the instrument. Some substances adhere to the walls of the analyzer tube and/or to the glass walls of the sample inlet system even though the instrument is thoroughly pumped out. In the case of gases adhering to the walls of the instrument, the background run (m/e scan with no sample in the instrument) will show no peaks, yet when a new material is admitted, it drives from the walls compounds formerly run. This substitution or driving off of one material from the walls by another material is called elution. There is a very small amount of elution with most substances. Elution is known to vary with the pressure; hence the background may be somewhat different at a high sample pressure from that at a low pressure. These effects all become serious when the sample is to be analyzed for minute amounts of one of the constituents. When the problem is to find a trace amount of one material in another or in a mixture of several others,

peaks of a few tenths of a division become significant, and the background must be closely controlled and known to 0.1 or 0.2 divisions.

Minimizing the Analytical Errors

Since most of the analyses in this work involved the determination of very small amounts of ethane in the vapor phase(0.050 to 0.50% in many cases), and very small amounts of hydrogen in the liquid phase (0.50 to 1.00% in many cases) , background runs were taken before every analysis, and the peak heights obtained on the background runs were subtracted from the mass spectra obtained for the mixtures. This eliminated most of the errors involving the small background at m/e = 28 due to the traces of CO or N_2 in the vacuum system, and greatly helped to reduce the errors involved in the excessive length of time required to pump the ethane out of the inlet and exhaust vacuum systems after a liquid sample containing a large percentage of ethane had been run through the instrument. In order to minimize the errors due to elution, the sample inlet system was flushed before each run with a small portion of the sample to be analyzed next, and only after flushing with sample at least once was a sample admitted to the inlet system for analysis. Using these precautions, the errors in the analytical technique were minimized, although not completely eliminated. For all components present in excess of 10 mole percent the reproducibility of the analysis was usually about 0.2 percent of the component composition, which is, theoretically, the limiting accuracy of the instrument. For components present in quantities from 1.0 to 10 mole percent, the reproducibility of the analysis was

usually within 0.03 to 0.05 percent. For the components present in quantities ranging from 0.1 to 1.0 mole percent, the reproducibility of analysis was usually within 0.008 percent (especially for the percent hydrogen in the liquid phase), although values range as high as 0.03 percent for the reproducibility of the percent ethane in the vapor phase in some instances. This is probably due to elution of ethane from previous liquid phase samples.

Sample Calculations

As examples of the calculation of a mixture analysis, consider the computation of the analyses for liquid phase sample No. 58-1 and vapor phase sample No. 58-5. These samples contain hydrogen, nitrogen, methane, and ethane. The cracking patterns and base peak sensitivities for these components are given in Table XIII.

TABLE XIII

CRACKING PATTERN COEFFICIENTS AND SENSITIVITIES FOR HYDROGEN, NITROGEN, METHANE, AND ETHANE

m/e	Hydrogen	Nitrogen	Methane	Ethane
2	1.0000	0.0000	0.0069	0.0325
16	0.0000	0.0000	1.0000	0.0024
28	0.0000	1.0000	0.0000	4.4000
30	0.0000	0.0000	0.0000	1.0000
base peak sens.	$\left(241.9\frac{\text{div}}{\mu}\right)$	$\left(533.3\frac{\text{div}}{\mu}\right)$	$\left(427.1\frac{\text{div}}{\mu}\right)$	$\left(163.8\ \frac{\text{div}}{\mu}\right)$

The mixture spectra of samples No. 58-1 and No. 58-5 gave the following results:

Liquid Phase Sample No. 58-1		Vapor Phase Sample No. 58-5	
m/e	Peak Height	m/e	Peak Height
2	104.7	2	4057
16	558.0	16	436.6
28	9774	28	6286
30	2105	30	21.5

Calculating liquid phase sample No. 58-1:

Let p_{H_2} = partial pressure of H_2 in the mixture (in microns)

p_{N_2} = partial pressure of N_2 in the mixture (in microns)

p_{C_1} = partial pressure of CH_4 in the mixture (in microns)

p_{C_2} = partial pressure of C_2H_6 in the mixture (in microns)

s_{H_2} = base peak sensitivity for H_2 (base peak: m/e = 2)

s_{N_2} = base peak sensitivity for N_2 (base peak: m/e = 28)

s_{C_1} = base peak sensitivity for CH_4 (base peak: m/e = 16)

s_{C_2} = base peak sensitivity for C_2H_6 (base peak: m/e = 30)

For peak height at m/e = 30:

$$\underline{2105 \text{ divisions}} = \left(p_{C_2} s_{C_2}\right)(1.000) = p_{C_2} s_{C_2}$$

For peak height at m/e = 28:

$$9774 \text{ divisions} = \left(p_{C_2} s_{C_2}\right)(4.400) + \left(p_{N_2} s_{N_2}\right)(1.000)$$

$$[9774 - (2105)(4.400)] \text{ divisions} = p_{N_2} s_{N_2} = \underline{512 \text{ divisions}}$$

For peak height at m/e = 16:

$$558.0 \text{ divisions} = \left(p_{C_2} s_{C_2}\right)(0.0024) + \left(p_{C_1} s_{C_1}\right)(1.000)$$

$$[558.0 - (2105)(0.0024)] \text{ divisions} = p_{C_1} s_{C_1} = \underline{553.0 \text{ divisions}}$$

For peak height at m/e = 2:

$$104.7 \text{ divisions} = \left(p_{C_2} s_{C_2}\right)(0.0325) + \left(p_{C_1} s_{C_1}\right)(0.0069) + \left(p_{H_2} s_{H_2}\right)(1.000)$$

$$[104.7 - (2105)(0.0325) - (553.0)(0.0069)] \text{ divisions} = p_{H_2} s_{H_2} = \underline{32.6 \text{ div.}}$$

Dividing by the base peak sensitivities, (s_i), adding the partial pressures of all the components, and dividing the partial pressure of each of the components by the sum of the partial pressures of all the components, the mole percentages of each component in the mixture are obtained:

Component	$p_i s_i$ (in divisions)	s_i (in div/μ)	p_i (in microns)	Mole Percentage
hydrogen	32.6	241.9	0.135	0.886%
nitrogen	512	533.3	0.960	6.30 %
methane	553.0	427.1	1.295	8.50 %
ethane	2105	163.8	12.85	84.32 %
TOTAL			15.24	100.006%

Observed sample inlet pressure (micromanometer reading) = 15.24 microns

Using the same nomenclature as above and calculating the analysis of vapor phase sample No. 58-5, one finds:

For peak height at m/e = 30:

$$\underline{21.5 \text{ divisions}} = \left(p_{C_2} s_{C_2}\right)(1.000) = p_{C_2} s_{C_2}$$

For peak height at m/e = 28:

$$6286 \text{ divisions} = \left(p_{C_2}s_{C_2}\right)(4.400) + \left(p_{N_2}s_{N_2}\right)(1.000)$$

$$[6286 - (21.5)(4.400)] \text{ divisions} = p_{N_2}s_{N_2} = \underline{6191 \text{ divisions}}$$

For peak height at m/e = 16:

$$436.6 \text{ divisions} = \left(p_{C_2}s_{C_2}\right)(0.0024) + \left(p_{C_1}s_{C_1}\right)(1.000)$$

$$[436.6 - (21.5)(0.0024)] \text{ divisions} = p_{C_1}s_{C_1} = \underline{436.6 \text{ divisions}}$$

For peak height at m/e = 2:

$$4057 \text{ divisions} = \left(p_{C_2}s_{C_2}\right)(0.0325) + \left(p_{C_1}s_{C_1}\right)(0.0069) + \left(p_{H_2}s_{H_2}\right)(1.000)$$

$$[4057 - (21.5)(0.0325) - (436.6)(0.0069)] \text{ divisions} = p_{H_2}s_{H_2} = \underline{4053 \text{ div.}}$$

Performing the same operations as before, the mole percentages of each of the components are obtained:

Component	$p_i s_i$ (in divisions)	s_i (in div/μ)	p_i (in microns)	Mole %
hydrogen	4053	241.9	16.75	56.75%
nitrogen	6191	533.3	11.61	39.34%
methane	436.6	427.1	1.022	3.46%
ethane	21.5	163.8	0.131	0.444%
TOTAL			29.513	99.994%

Observed sample inlet pressure (micromanometer reading) = 29.62 microns

In the preceding liquid and vapor phase sample calculations it may be noted that the accuracy and stability required of the cracking patterns was far less in the case of the vapor phase sample than in the case of the liquid phase sample. Due to the slight amount of ethane

in the vapor phase, the contributions to the 2, 16, and 28 peaks from the cracking pattern of ethane are very small In most cases only 2 or 3 divisions must be subtracted from the peak at m/e = 2 in order to correct for the contributions of both methane and ethane to the 2 peak. This amounts to a correction of approximately 0.1 percent. The correction for the ethane contribution to the peak at m/e = 16 is completely negligible, and the correction for the ethane contribution at m/e = 28 is normally about 1.5 percent of the height of the 28 peak. Thus, the accuracy of the cracking patterns affects the vapor phase analysis only slightly, and extremely-good, completely-stable cracking patterns are not required for an analysis of this phase.

However, due to the large amount of ethane present in the liquid phase, the contributions to all of the peaks from the cracking pattern of ethane become very significant. In the case of the liquid phase sample No. 58-1, the ethane contributes approximately 94.9 percent of the peak height at m/e = 28, and yet, the nitrogen must be calculated by a difference method. This is also true of the amount of hydrogen present in the liquid phase. The total contribution of methane and ethane to the peak at m/e = 2 is approximately 69.0 percent of the 2 peak, and yet, the amount of hydrogen present in the mixture must also be calculated by difference. These difference calculations, required in the analysis of a liquid phase sample, necessitate the operation of the mass spectrometer under conditions which will provide accurate, stable cracking patterns. Fortunately, the cracking pattern of ethane on the 28 and 30 peaks was found to be extremely stable over

long periods of time. Over a period of several months the largest variation in the cracking pattern of ethane on the 28 and 30 peaks was found to be 0.23 percent, while the day to day variation was always less than 0.10 percent. Since the pure component sensitivities changed considerably over a period of a few days and had to be determined each time a set of mixture spectra were obtained, new cracking patterns were also obtained from these pure component spectra. In this manner, slight changes in the cracking patterns, as well as the changes in the sensitivities, could be incorporated in the computations, although day to day changes in the cracking pattern on the m/e = 28 peak were never significant. Day to day changes in both the methane and the ethane cracking pattern on the peak at m/e = 2 were often noticed. Over a period of several months the cracking patterns of the hydrocarbons on the 2 peak were found to fluctuate approximately $\pm$ 3 percent from the values quoted in Table XIII although the day to day variations were usually much less. It was, therefore, beneficial to check the cracking patterns every time that the pure component spectra were obtained in order to keep a close check on the hydrocarbon cracking patterns at the m/e = 2 peak. Using these precautions, it is thought that the reproducibility of the analysis is approximately as quoted in the section "Minimizing the Analytical Errors". The results of a few typical analyses are given in Table XIV.

In order to check the accuracy of the analytical technique as well as the reproducibility, several standard mixtures of the gases were prepared and analyzed. Table XV gives the prepared compositions for three

of these mixtures and compares them with the analyses obtained from the mass spectrometer. It is believed that these results are representative of the accuracy obtained in the analysis of the phase samples using the mass spectrometer.

TABLE XIV

RESULTS OF TYPICAL ANALYSES

Liquid Phase Sample No. 58-1	
Component	Mole Percent
hydrogen	0.886
nitrogen	6.30
methane	8.50
ethane	84.32
TOTAL	100.008%

Liquid Phase Sample No. 58-3	
Component	Mole Percent
hydrogen	0.878
nitrogen	6.36
methane	8.47
ethane	84.29
TOTAL	99.998%

Vapor Phase Sample No. 58-4	
Component	Mole Percent
hydrogen	56.77
nitrogen	39.29
methane	3.47
ethane	0.469
TOTAL	99.999%

Vapor Phase Sample No. 58-5	
Component	Mole Percent
hydrogen	56.75
nitrogen	39.34
methane	3.46
ethane	0.444
TOTAL	99.994%

Liquid Phase Sample No. 45-3	
Component	Mole Percent
hydrogen	0.300
nitrogen	41.71
methane	57.99
TOTAL	100.00%

Liquid Phase Sample No. 45-5	
Component	Mole Percent
hydrogen	0.304
nitrogen	41.81
methane	57.88
TOTAL	99.994%

TABLE XIV (cont'd)

RESULTS OF TYPICAL ANALYSES

Vapor Phase Sample No. 45-6		Vapor Phase Sample No. 45-7	
Component	Mole Percent	Component	Mole Percent
hydrogen	2.37	hydrogen	2.36
nitrogen	67.98	nitrogen	67.87
methane	29.65	methane	29.77
TOTAL	100.00%	TOTAL	100.00%

TABLE XV

ANALYSES OF STANDARD MIXTURES ON THE MASS SPECTROMETER

Component	Prepared Composition (Mole Percent)	Composition From Analysis on the Mass Spectrometer (Mole Percent)
Mixture No. 1		
Hydrogen	47.80	47.89
Methane	47.01	46.90
Ethane	5.19	5.21
Mixture No. 2		
Nitrogen	21.10	21.19
Methane	22.47	22.43
Ethane	56.43	56.38
Mixture No. 3		
Hydrogen	1.63	1.60
Nitrogen	11.98	12.07
Methane	10.51	10.37
Ethane	75.88	75.96

NOMENCLATURE

A_i	Liquid-phase fugacity function in DePriester correlation
A_{i-j}	Binary constants in Margules equation
A_o, B_o, C_o, a, b, c, α and γ	Parameters in the Benedict-Webb-Rubin equation of state (constants are characteristic of a pure substance and are functions of composition for a mixture)
B_i	Vapor-phase fugacity function in DePriester correlation
C	Number of components (Phase Rule)
C*	Ternary constant in the three-suffix Margules equation
d	Density
F	Degrees of freedom (Phase Rule)
f_i	Fugacity of component "i"
f_{i_L}	Fugacity of component "i" in the liquid phase
f_{i_V}	Fugacity of component "i" in the vapor phase
$f^{\circ}_{L_i}$	Fugacity of pure component "i" as liquid at same temperature and total pressure
$f^{\circ}_{V_i}$	Fugacity of pure component "i" as vapor at same temperature and total pressure
H_i	Henry's Law constant for component "i," ($x_i = H_i p_i$)
K_i	Equilibrium ratio for component "i," ($K_i = y_i/x_i$)
M_i	Molecular weight of component "i"
MABP	Molal average boiling point, $(\sum_i z_i (nBP_i))$
MW	Molal average molecular weight, $(\sum_i z_i M_i)$
m/e	Mass to charge ratio of an ion
nBP_i	Normal boiling point for component "i"
P	Number of phases (Phase Rule)
P	Pressure
P_{c_i}	Critical pressure of component "i"

NOMENCLATURE (Cont'd)

P_{pc_i}	Pseudocritical pressure of phase "i"
P_{R_i}	Pseudoreduced pressure of phase "i," ($P_{R_i} = P/P_{pc_i}$)
p_i	Partial pressure of component "i"
p_i°	Vapor pressure of component "i" at temperature, T
R	Gas constant
r	Volatility ratio in Smith-Watson correlation
s_i	Sensitivity of mass spectrometer for component "i"
T	Temperature
T_{c_i}	Critical temperature of component "i"
T_{pc_i}	Pseudocritical temperature of phase "i"
T_{R_i}	Pseudoreduced temperature of phase "i," ($T_{R_i} = T/T_{pc_i}$)
x_i	Mole fraction of component "i" in the liquid phase
y_i	Mole fraction of component "i" in the vapor phase
z_i	Mole fraction of component "i" in either the liquid or vapor phase
γ_i	Activity coefficient ($y_i f^\circ_{V_i} = \gamma_i f^\circ_{L_i} x_i$)
θ	Derived concentration variable
$\phi(x,y,P,T)$	A function of the variables x, y, P and T
ϕ_{L_i}	Liquid-phase activity coefficient in the Smith-Watson correlation
ϕ_{V_i}	Vapor-phase activity coefficient in the Smith-Watson correlation

BIBLIOGRAPHY

1. Akers, W. W., Attwell, L. L., and Robinson, J. A., Ind. Eng. Chem., 46, 2539-40, (1954).

2. Akers, W. W., Kehn, D. M., and Kilgore, C. H., Ind. Eng. Chem., 46, 2536-9, (1954).

3. American Institute of Physics, "Temperature, Its Measurement and Control in Science and Industry," Reinhold Publishing Corp., New York, (1941).

4. Aroyan, H. J., "Low Temperature Vapor-Liquid Equilibria in the Hydrogen - n-Butane System," Ph.D. Thesis, University of Michigan, (1949).

5. Aroyan, H. J. and Katz, D. L., Ind. Eng. Chem., 43, 185-9, (1951).

6. Benedict, M., Johnson, C. A., Solomon, E., and Rubin, L. C., Trans. Am. Inst. Chem. Eng., 41, 371-92, (1945).

7. Benedict, M., Webb, G. B., and Rubin, L. C., J. Chem. Phys., 8, 334-45, (1940).

8. Benedict, M., Webb, G. B., and Rubin, L. C., J. Chem. Phys., 10, 747-58, (1942).

9. Benedict, M., Webb, G. B., and Rubin, L. C., Chem. Eng. Prog., 47, 419-22, (1951).

10. Benedict, M., Webb, G. B., and Rubin, L. C., Chem. Eng. Prog., 47, 449-54, (1951).

11. Benedict, M., Webb, G. B., Rubin, L. C., and Friend, L., Chem. Eng. Prog., 47, 571-8, (1951).

12. Benedict, M., Webb, G. B., Rubin, L. C., and Friend, L., Chem. Eng. Prog., 47, 609-20, (1951).

13. Benham, A. L., "Vapor-Liquid Equilibria of Light Hydrocarbon Systems Containing Hydrogen at Low Temperature," Ph.D. Thesis, University of Michigan, (1956).

14. Benham, A. L. and Katz, D. L., A.I.Ch.E. Journal, 3, 33-36, (1957).

15. Benham, A. L., Katz, D. L., and Williams, R. B., A.I.Ch.E. Journal, 3, 236-41, (1957).

16. Bloomer, O. T., Gami, D. C., and Parent, J. D., Inst. Gas Tech. Res. Bulletin No. 22, 1-39, (1953).

17. Bloomer, O. T. and Parent, J. D., Chem. Eng. Prog. Symposium Series No. 6, 49, 11-24, (1953).

BIBLIOGRAPHY (Cont'd)

18. Boomer, E. H., Johnson, C. A., and Piercey, A. G. A., Can. J. Research, 16B, 319-27, (1938).

19. Boomer, E. H. and Johnson, C. A., Can.J. Research, 16B, 328-35, (1938).

20. Boomer, E. H., Johnson, C. A., and Piercey, A. G. A., Can.J. Research, 16B, 396-410, (1938).

21. Burris, W. L., Hsu, N. T., Reamer, H. H., and Sage, B. H., Ind. Eng. Chem., 45, 210-3, (1953).

22. Case, L. O., "Elements of the Phase Rule," Edwards Letter Shop, Ann Arbor, Michigan, Copyright 1939.

23. Cines, M. R., Roach, J. T., Hogan, R. J., and Roland, C. H., Chem. Eng. Prog. Symposium Series No. 6, 49, 1-10, (1953).

24. Cullen, E. J. and Kobe, K. A., A.I.Ch.E. Journal, 1, 452-5, (1955).

25. Dean, M. R. and Tooke, J. W., Ind. Eng. Chem., 38, 389-93, (1946).

26. DePriester, C. L., Chem. Eng. Prog. Symposium Series No. 7, 49, 1-43, (1953).

27. Dodge, B. F. and Dunbar, A. K., J. Am. Chem. Soc., 49, 591-610, (1927).

28. Fastowsky, V. G. and Gonikberg, M. G., J. Phys. Chem. (USSR), 14, 427-8, (1940).

29. Freeth, F. A. and Verschoyle, T. T. H., Proc. Roy. Soc. (London), 130A, 453-63, (1931).

30. Frenkel, J., "Kinetic Theory of Liquids," Dover Publications, Inc., New York, (1955).

31. Gilliland, E. R. and Scheeline, H. W., Ind. Eng. Chem., 32, 48-54, (1940).

32. Gonikberg, M. G., Fastowsky, V. G., and Gurwitsch, I. G., Acta Physicochimica (USSR), 11, 865-82, (1939).

33. Hadden, S. T., Chem. Eng. Prog., 44, 37-54 and 135-56, (1948).

34. Hadden, S. T., Chem. Eng. Prog. Symposium Series No. 7, 49, 53-66, (1953).

35. Hirschfelder, J. O., Curtiss, C. F. and Bird, R. B., "Molecular Theory of Gases and Liquids," John Wiley and Sons, Inc., New York, (1954).

BIBLIOGRAPHY (Cont'd)

36. Hobson, M. and Weber, J. H., A.I.Ch.E. Journal, 2, 354-9, (1956).

37. Joffe, J., Ind. Eng. Chem., 39, 837-8, (1947).

38. Katz, D. L. and Hackmuth, K. H., Ind. Eng. Chem., 29, 1072-7, (1937).

39. Katz, D. L. and Kurata, F., Ind. Eng. Chem., 32, 817-27, (1940).

40. Kay, W. B., Chem. Reviews, 29, 501-7, (1941).

41. Lennard-Jones, J. E. and Devonshire, A. F., Proc. Roy. Soc. (London), A163, 53-70, (1937).

42. Lenoir, J. M. and Hipkin, H. G., A.I.Ch.E. Journal, 3, 318-20, (1957).

43. Lenoir, J. M. and White, G. A., Petroleum Refiner, 32, No. 10, 121-3, and No. 12, 115-9, (1953).

44. Levitskaya, E. P., J. Tech. Phys. (USSR), 11, 197-204, (1941).

45. Levitskaya, E. P. and Pryannikov, K., J. Tech. Phys. (USSR), 9, 1849-53, (1939).

46. Likhter, A. I. and Tikhonovich, N. P., J. Tech. Phys. (USSR), 10, 1201-6, (1940).

47. "Liquid-Vapor Equilibrium in Mixtures of Light Hydrocarbons - M. W. Kellogg Equilibrium Constants," M. W. Kellogg Company, New York, (1950).

48. "Liquid-Vapor Equilibrium in Mixtures of Light Hydrocarbons - M. W. Kellogg Fugacity Charts," M. W. Kellogg Company, New York, (1950).

49. Margules, M., Sitzungsberichte der Mathematisch-Naturwissenschaftlichen Classe der Kaiserlichen Akademie der Wissenschaften (Vienna), 104, 1243-78, (1895).

50. Martin, J. J. and Hou, Y., A.I.Ch.E. Journal, 1, 142-51, (1955).

51. McTaggart, H. A. and Edwards, E., Trans. Roy. Soc. Can., 13, Sect. iii, 57-66, (1919).

52. Napier, J. W., Trans. Inst. of Chem. Eng. (London), 23, 20-31, (1945).

53. Natural Gasoline Association of America, "Equilibrium Ratio Data Book," Tulsa, (1955).

54. Nelson, E. E. and Bonnell, W. S., Ind. Eng. Chem., 35, 204-6, (1943).

55. Nichols, W. B., Reamer, H. H., and Sage, B. H., A.I.Ch.E. Journal, 3, 262-7, (1957).

BIBLIOGRAPHY (Cont'd)

56. Organick, E. I., "Prediction of Hydrocarbon Vapor-Liquid Equilibria," Ph.D. Thesis, University of Michigan, (1950).

57. Organick, E. I. and Brown, G. G., Chem. Eng. Prog. Symposium Series No. 2, 48, 97-111, (1952).

58. Palazzo, D. F., Schreiner, W. C., and Skaperdas, G. T., Ind. Eng. Chem., 49, 685-8, (1957).

59. Price, A. R., Ph.D. Thesis, Rice Institute, Houston, Texas, (1957).

60. Price, A. R., Leland, T. W., and Kobayashi, R., "Evaluation of the Benedict-Webb-Rubin Equation for Prediction of Phase Equilibrium of Light Hydrocarbon Mixtures at Low Temperatures," Dept. of Chemical Engineering Report, Rice Institute, Houston, Texas, (1957).

61. Redlich, O. and Kister, A. T., Ind. Eng. Chem., 40, 345-8, (1948).

62. Ruhemann, M., Proc. Roy. Soc. (London), A171, 121-36, (1939).

63. Ruhemann, M. and Zinn, N. M., Physik. Zeit. der Sowjetunion, 12, 389-403, (1937).

64. Rzasa, M. J., Glass, E. D., and Opfell, J. B., Chem. Eng. Prog. Symposium Series No. 2, 48, 28-35, (1952).

65. Scatchard, G. and Hamer, W. J., J. Am. Chem. Soc., 57, 1805-9, (1935).

66. Schiller, F. C. and Canjar, L. N., Chem. Eng. Prog. Symposium Series No. 7, 49, 67-72, (1953).

67. Smith, K. A. and Watson, K. M., Chem. Eng. Prog., 45, 494-507, (1949).

67A Souders, M., Selheimer, C. W., and Brown, G. G., Ind. Eng. Chem., 24, 517-9, (1932).

68 Steckel, F. A. and Zinn, N. M., J. Chem. Ind. (USSR), 16, 24-8, (1939).

69. Stockmayer, W. H., J. Chem. Phys., 9, 398-402, (1941).

70. Stotler, H. H. and Benedict, M., Chem. Eng. Prog. Symposium Series No. 6, 49, 25-36, (1953).

71. Stutzman, L. F. and Brown, G. M., Chem. Eng. Prog., 45, 139-42, (1949).

72. Taylor, H. S. and Glasstone, S., "A Treatise on Physical Chemistry," Vol. 2, (States of Matter), D. Van Nostrand Company, New York, (1951).

73. Torocheshnikov, N. S., Tech. Phys. (USSR), 4, 365, (1937).

BIBLIOGRAPHY (Cont'd)

74. Torocheshnikov, N. S. and Levius, L. A., J. Chem. Ind. (USSR), 16, 19-22, (1939).

75. Tsiklis, D. S., J. Phys. Chem. (USSR), 21, 355-9, (1947).

76. Van Laar, J. J., Z. Physik. Chem., 72, 723-51, (1910).

77. Verschoyle, T. T. H., Phil. Trans. Roy. Soc. (London), 230A, 189-220, (1931).

78. Williams, R. B., "Vapor-Liquid Equilibria in the Hydrogen-Light Hydrocarbon Systems," Ph.D. Thesis, University of Michigan, (written but not submitted).

79. Williams, R. B. and Katz, D. L., Ind. Eng. Chem., 46, 2512-20, (1954).

80. Winn, F. W., Chem. Eng. Prog. Symposium Series No. 2, 48, 121-34, (1952).

81. Wohl, K., Trans. Am. Inst. Chem. Eng., 42, 215-49, (1946).